

THERMAL METAMORPHIC SCHISTS
ADJACENT TO THE WALCHA ROAD ADAMELLITE,
NEW ENGLAND, NEW SOUTH WALES

By

Graham S. Teale

Thesis submitted for the Honours
Degree of Bachelor of Arts,
Macquarie University, N.S.W.
1974

ACKNOWLEDGEMENTS

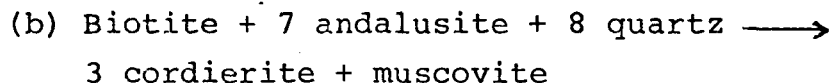
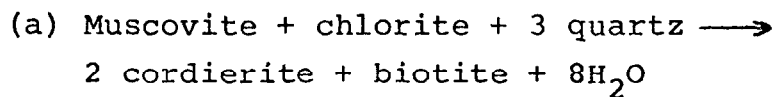
The author wishes to gratefully acknowledge the advice and encouragement given by his supervisor, Dr. R.H. Flood. Dr. S.E. Shaw and Mr. J. Bedford gave advice and assistance on wet chemical XRF and XRD techniques. Their help in these matters is appreciated. Thanks are also due to Mr. S. Dobos and Mr. D. Gray, who gave valuable assistance throughout the year, and to all students and members of staff who offered advice and assistance.

The author also wishes to thank Miss Beverley Venteman for the capable assistance given in the typing of this thesis. The co-operation of Mr. J. Gilfillan of Falconbridge (Australia) Pty. Limited is also appreciated. Finally, I wish to thank my parents for the support they have given me throughout the year.

ABSTRACT

The forceful intrusion of the Walcha Road Adamellite has resulted in the development of a schistose fabric in the intruded sediments. As the contact is approached the regional structure is altered so as to concordantly wrap the Walcha Road Pluton, and at the immediate contact, a "migmatitic" zone is developed. This "migmatitic" zone represents the highest metamorphic grade reached in the Walcha Road aureole, with the development of cordierite-K-feldspar bearing schists and "gneisses". Further from the contact another four distinct metamorphic zones are present. The first indication of aureole conditions is the formation of biotite at approximately 3.0km from the contact, the incoming of biotite representing the commencement of the biotite zone. With increasing metamorphic grade the andalusite zone is entered followed by the cordierite and cordierite-almandine zones. The varying dimensions of the cordierite zone are attributed to the presence of graphitic sediments, the graphite in these sediments lowering PH_2O and allowing the cordierite forming reaction to proceed at a lower temperature.

A thorough geochemical and petrological investigation of the metamorphic zones of the Walcha Road aureole has resulted in the delineation of three metamorphic reactions, namely:



(c) 5 K-feldspar + 2 chlorite \longrightarrow

4 biotite + muscovite + andalusite + 13 quartz + 4H₂O

Using all available data it has been estimated that the aureole of the Walcha Road Adamellite formed at 420°C - 605°C at 1.5 - 2.0Kb.

C O N T E N T S

PART ONE: THERMAL METAMORPHIC SCHISTS ADJACENT TO THE WALCHA ROAD ADAMELLITE

	Page
1. INTRODUCTION	1
(a) Preamble	1
(b) Previous Work	2
2. REGIONAL GEOLOGY	5
3. THE SEDIMENTS	11
(a) Woolomin Type	11
(b) Sandon Type	13
(c) Comparison with Meta-Pelites from Cooma, NSW	14
4. CONTACT METAMORPHISM OF MINOR ACID AND BASIC INTRUSIVES	23
(a) Acid Intrusives	23
(b) Basic Intrusives	23
(c) Description of Minerals from the Basic Hornfelses	27
5. METAMORPHISM OF IMPURE CALCAREOUS SEDIMENTS	32
(a) Description	32
(b) Contact Metamorphism	33
(c) Mineralogy	36
6. MINERALS FROM THE METAMORPHIC ZONAL SEQUENCE	38
7. THE METAMORPHIC ZONES	66
(a) Cordierite-K-Feldspar Zone	66
(b) Cordierite-Almandine Zone	70
(c) Cordierite Zone	82
(d) Andalusite Zone	86
(e) Biotite Zone	87
8. DISCUSSION	89
9. BIBLIOGRAPHY	97

PART TWO: CORDIERITE FORMING REACTIONS IN THE
AUREOLE OF THE WALCHA ROAD ADAMELLITE

	Page
1. INTRODUCTION	103
2. PREVIOUS WORK	108
3. SUGGESTED REACTIONS	115
(a) Cordierite	115
(b) Biotite	126
4. DISCUSSION	130
5. BIBLIOGRAPHY	134

PART THREE: APPENDICES

1. Structural Aspects at Walcha Road	139
2. The Geology and Metamorphic Zonation Adjacent to the Yarrahapinni (Way-Way) Adamellite Intrusions	146
3. Analytical Procedure	160
4. Mapping and Sampling Techniques	163
5. Trace Element Analyses	164
6. Location and Mineralogy of Thin Sectioned Samples	167
7. Calculation of Compositional Diagram Values	175
8. Analyses of Meta-Pelites from Adjacent the Bathurst Granite and Uralla Granodiorite	177
9. Location and Opaque Mineralogy of Polished Sectioned Samples	178
10. (a) Map showing metamorphic zonation adjacent to the Walcha Road Adamellite	Back cover
(b) Map showing metamorphic zonation adjacent to the Yarrahapinni Intrusives	Back cover
11. Bibliography	179

LIST OF PLATES

	Page
<u>PART ONE</u>	
Plate 1: Relict clinopyroxene in dolerite dyke x65	26
Plate 2: Radiating sub-aluminous amphibole x104	28
Plate 3: Biotite rimming blue/green hornblende x104	28
Plate 4: Cummingtonite in basic hornfels x104	29
Plate 5: Hypersthene-biotite-augite-andesine hornfels x260	30
Plate 6: Calcareous concretion	32
Plate 7: Decussate aggregate of biotite from cordierite-K-feldspar zone x104	42
Plate 8: Biotite associated with quartz vein x65	42
Plate 9: Cyclic twinning in cordierite from the cordierite-K-feldspar zone x520	47
Plate 10: Twin lamellae in cordierite from the cordierite-K-feldspar zone x520	47
Plate 11: Biotite-cordierite schist x25	48
Plate 12: Pinitisation of cordierite x260	49
Plate 13: Chlorite replacing cordierite x520	50
Plate 14: Replacement of cordierite by muscovite x104	51
Plate 15: Garnet from cordierite-K-feldspar zone x104	52
Plate 16: Inclusions of biotite in quartz from cordierite-K-feldspar zone x520	53
Plate 17: Muscovite replacing biotite and K-feldspar x520	58
Plate 18: Porphyroblastic muscovite from andal- usite zone x415	59

	Page
Plate 19: Banded appearance of schists from Macdonald River	67
Plate 20: Biotite-cordierite-almandine schist x104	73
Plate 21: Almandine nucleating in cordierite x104	74
Plate 22: Biotite folia wrapping cordierite porphyroblast x104	84
Plate 23: Preferred orientation of biotite x260	84
Plate 24: Cordierite from outer cordierite zone x65	85
Plate 25: Cordierite from outer cordierite zone x25	85

PART TWO

Plate 26: Incipient development of cordierite in mica rich knots of the inner andalusite zone x65	117
Plate 27: Relict outline of andalusite in cordierite x65	119
Plate 28: Andalusite from Walcha Road aureole x135	119
Plate 29: Biotite, inner cordierite zone x104	121
Plate 30: Biotite, cordierite-almandine zone x104	121
Plate 31: Biotite, cordierite-K-feldspar zone x104	122

PART THREE

Plate 32: Crenulation cleavage x65	140
Plate 33: Ptygmatic quartz vein x25	140
Plates 34-38: Structures associated with intrusion of adamellite	142-145
Plate 39: Crenulation cleavage preserved in cordierite porphyroblast x65	149
Plate 40: S ₄ crenulation cleavage x65	150
Plate 41: Cordierite from the cordierite zone at Yarrahapinni x104	153
Plate 42: Biotite from the biotite zone at Yarrahapinni x415	156

LIST OF FIGURES

Page

PART ONE

Figure 1:	Subdivisions of the New England Batholith	4
Figure 2:	Major blocks of the southern part of the New England Fold Belt	6
Figure 3:	Cordierite and biotite isograds adjacent to the Walcha Road Adamellite	10
Figure 4:	Primary arenite triangle of Folk	12
Figure 5:	Cu-Pb-Zn plots of meta-sediments	12
Figure 6:	Alkali-lime diagram	16
Figure 7:	Metamorphic zoning (southern section)	65
Figure 8:	Mineral compositions plotted on Thompson projection	75
Figure 9:	fO_2 -T diagram	80
Figure 10:	Maximum temperature thermal gradient curve for the Walcha Road aureole	91
Figure 11:	Maximum temperature thermal gradient curve for the Shalimar aureole	93

PART TWO

Figure 12:	AFK compositional diagram for Walcha Road schists	104
Figure 13:	AFM projection of Walcha Road schists	105
Figure 14:	SiO_2 -(MgO+FeO)- Al_2O_3 diagram	106
Figure 15:	ACF compositional diagram for Walcha Road schists	107
Figure 16:	Petrogenetic grid	132

PART THREE

Figure 17:	Orientation diagram of fold axes	143
Figure 18:	Metamorphic zonation adjacent the Yarrahapinni intrusives	148
Figure 19:	AMF plot of carbonaceous meta- pelites from Yarrahapinni	153
Figure 20:	AFK and SiO_2 -(MgO+FeO)- Al_2O_3 plots of meta-pelites from Yarrahapinni	157

LIST OF TABLES

Page

PART ONE

Table 1:	Chemical and modal analysis of the Walcha Road Adamellite	8
Table 2:	Chemical Analysis of a meta-greywacke	15
Table 3:	Chemical analyses of carbonaceous meta-pelites	17
Table 4:	Chemical analyses of high potassium carbonaceous meta-pelites	19
Table 5:	Chemical analyses of non carbonaceous meta-pelites	20
Table 6:	Chemical analyses of high potassium non carbonaceous meta-pelites	22
Table 7:	Chemical analyses of acid intrusives	24
Table 8:	Modal analyses of contact metamorphosed basic dykes	26
Table 9:	Chemical analyses of silica poor calcareous meta-sediments	35
Table 10:	Biotite analyses	40
Table 11:	Cordierite analyses	45
Table 12:	Chlorite analyses	55
Table 13:	White mica analyses	57
Table 14:	Plagioclase analyses	60
Table 15:	Ilmenite analysis	63
Table 16:	Mineral development in the Walcha Road aureole	69
Table 17:	Garnet analyses	71
Table 18:	Comparison of garnet, biotite and cordierite analyses	76

PART TWO

Table 19:	Modal analyses of meta-pelites from the Walcha Road area	111
Table 20:	Zonal distribution of minerals in the Walcha Road aureole	116
Table 21:	C.I.P.W. Norms of pelitic rocks	123

PART THREE

Table 22:	Chemical analyses of carbonaceous meta-pelites from Yarrahapinni	147
Table 23:	C.I.P.W. Norms of Yarrahapinni meta-pelites	158
Table 24:	Yarrahapinni trace element analyses	159

1. INTRODUCTION

(a) Preamble

The study of a contact metamorphic aureole has distinct advantages over regional metamorphic studies when considering the delineation of metamorphic zones and reactions, for in a contact aureole there is always an increasing metamorphic grade as the actual contact is approached. In a regionally metamorphosed terrain the "upgrade" and "downgrade" sequence is not always clear. In the Walcha Road aureole, increasing metamorphic grade has resulted in the development of prograde metamorphic zones, each zone being represented by a particular prograde assemblage. Therefore, when studying metamorphic reactions the contact aureole offers obvious advantages.

A detailed mineralogical and geochemical study defined certain cordierite forming reactions in the Walcha Road aureole, the cordierite so formed occurring up to 1.2km from the contact. The width of the cordierite isograd and the actual width of the aureole (3km) suggests that the adamellite was intruded as a single pulse of magma at a depth of 5-6 kilometres. The metamorphic assemblages present in the aureole give a definite indication as to the pressures that existed at the time of intrusion. Studies of contact metamorphism associated with intrusions of the New England Batholith should, therefore, help delineate important parameters such as level of emplacement and amount of H_2O present in the melt at pressures that existed during intrusion. The study of the aureole of the Walcha Road Adamellite has successfully answered many questions as to the method and depth of emplacement of this particular intrusion.

(b) Previous Work

The classic investigations of the Great Serpentine belt of NSW by Benson (1913, 1914a, 1914b, 1915, 1917, 1918) did include some petrological descriptions of some contact metamorphic rocks adjacent to the Moonbi Adamellite and Inlet Monzonite. In the Horse Arm Creek area, north of the Inlet Monzonite, Benson (1917) briefly described calcite-grossularite-diopside-wollastonite assemblages derived from metamorphosed calcareous sediments, and also cordierite-biotite assemblages in the associated pelitic rocks. In 1915 he (Benson) reported that basic volcanics adjacent to the Moonbi Adamellite in the Kootingal area had been converted to actinolite-albite assemblages. Binns (1965) suggested that these assemblages may be due to abnormal rock chemistry rather than grade of metamorphism.

At Tilbuster, north of Armidale, contact metamorphism and metasomatism of basic rocks adjacent to an adamellite-monzonite intrusion has been described by Spry (1955). It has been reported by Spry that extensive introduction of material, accompanied in places by shearing, has taken place in the hornfels zone leading to the formation of grossularite, scapolite, diopside, calcite and epidote in the metamorphosed basic rocks. Spry (1953) also investigated contact metamorphism in the Puddledock area, which also lies to the north of Armidale. A further investigation of contact metamorphic effects in the Tilbuster area was carried out by Binns (1965). Binns investigated the contact metamorphic effects on the basic rocks, with special emphasis on the generation and the chemistry of metamorphic hornblende. He found that with increasing grade the hornblende changed from

a pale blue-green variety with a ragged actinolitic habit to a deeply coloured brownish type with a granular habit. He attributed this colour change to a progressive increase in the amount of alkalis and titanium held by the hornblende as metamorphic grade increased.

In the Uralla area, some 21km south of Armidale, Palaeozoic sediments have been contact metamorphosed by the Uralla granodiorite and have been described by Vernon (1961). Close to the contact Vernon describes biotite-cordierite-K-feldspar (\pm almandine) hornfels and andalusite hornfels. Farther from the contact former argillites carry porphyroblastic chiastolite. Similar assemblages have been described briefly by Flood (1964) in the Woolbrook-Walcha Road area.

Howarth (1973) examined the thermal metamorphic rocks between the Walcha Road Adamellite, Bendemeer Adamellite, Moonbi Adamellite and Limbri leucoadamellite. He noted that close to the contact the assemblage biotite-cordierite \pm K-feldspar was common in the pelitic rocks whilst plagioclase-amphibole was the dominant assemblage in the metamorphosed volcanic rocks. He also located the cordierite isograd adjacent to the abovementioned plutons.

Although assemblages from many localities in the New England region have been described petrologically, very little detailed work (e.g. delineating isograds) has been carried out. The absence of appropriate geochemical studies is also noteworthy.

The present study differs markedly from previous work in the New England region in that metamorphic zones have been mapped, and metamorphic reactions in these zones have been attempted, only after thorough geochemical and petrological investigations.

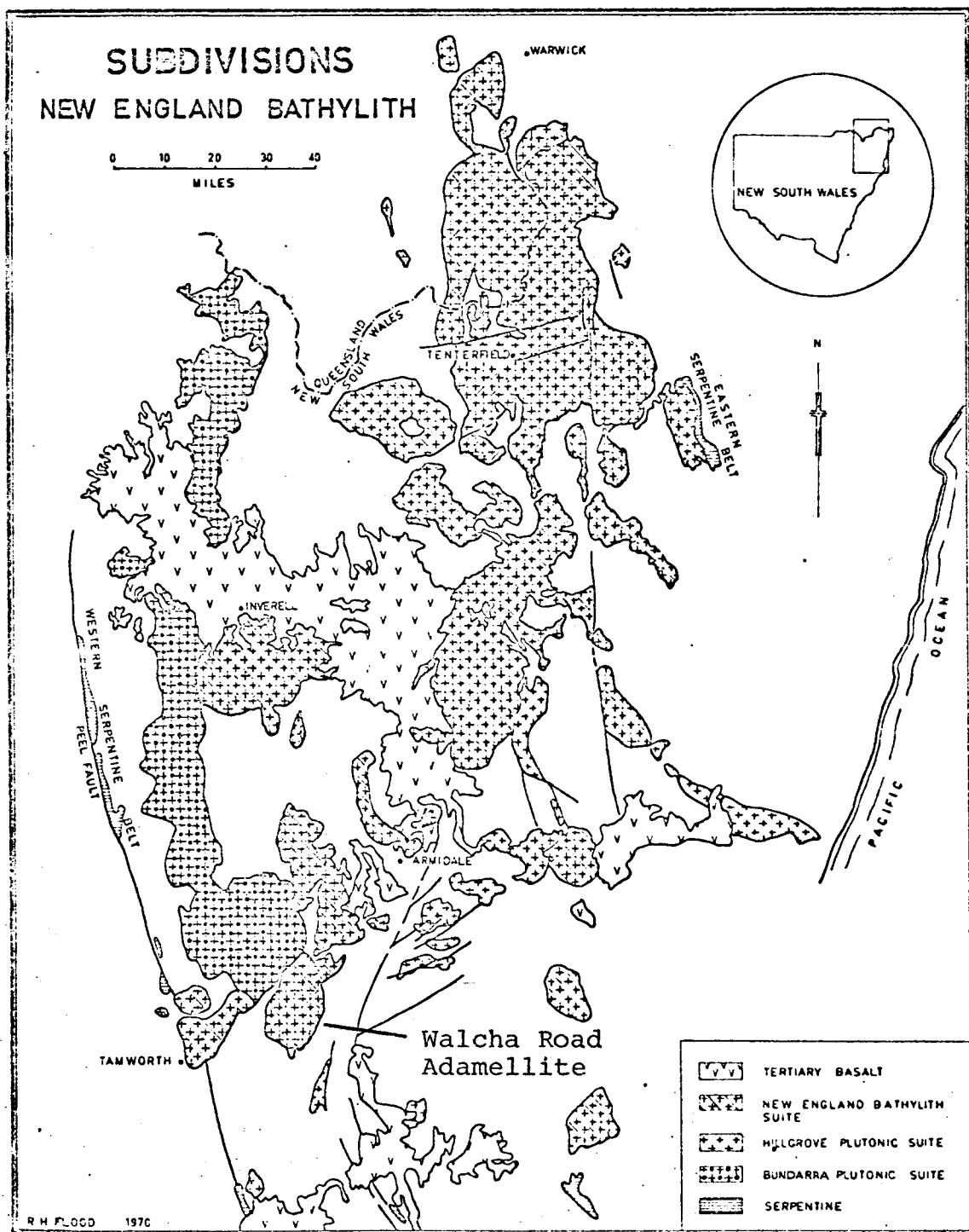


Fig. 1

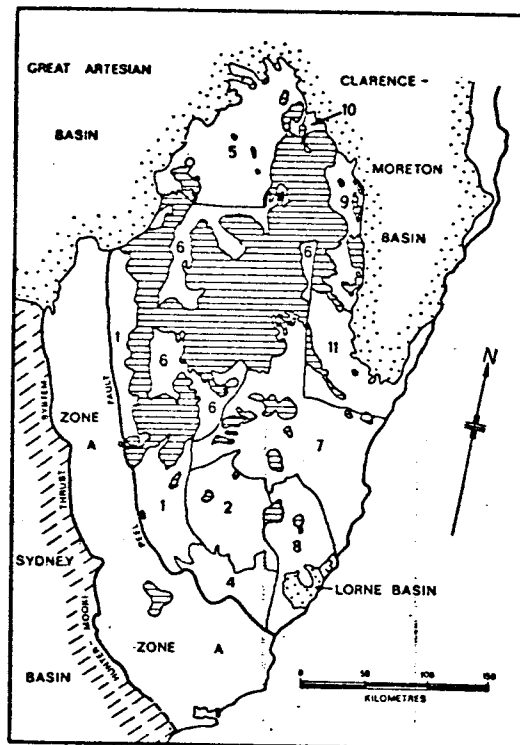
2. REGIONAL GEOLOGY

The Walcha Road Adamellite forms part of the New England Batholith which is a large, composite, mainly discordant, upper Palaeozoic batholith extending from about Tamworth, in southern New England, to Warwick in Queensland, a distance of some 340 kilometres (Figure 1). The batholith is intruded into a largely undifferentiated, moderately deformed sequence of marine sediments which have been usefully grouped by Voisey (1959) as the New England Central Complex. The Central Complex is separated from the western belt of folds and thrusts by the Peel Thrust, which is a major fault marked over much of its length by elongate masses of alpine serpentinite.

A re-investigation of the New England fold belt by Leitch (1974) led him to subdivide the Central Complex (Voisey, op. cit.) into seven major blocks (Figure 2), the study area lying in the central eastern section of the Macdonald Block.

The typical sediments of the Macdonald Block are that of the Palaeozoic Woolomin type. The Woolomin Beds were first described by Benson (1913-1918), and have since been described in part only, this work being summarised by Packham (1969). Complex folding and faulting, lack of marker units, and scarcity of fossils have made it difficult to subdivide the Woolomin type beds stratigraphically.

The only attempt at subdividing the Woolomins was carried out by Lewington (1973) who described the regional burial metamorphism and structure of these sediments to the south



Major blocks of the southern part of the New England Fold Belt. Key to blocks of Zone B: (1) Macdonald, (2) Yarrawitch, (3) Port Macquarie, (4) Manning, (5) Bonshaw, (6) Armidale, (7) Nambucca, (8) Hastings, (9) Tabulam, (10) Warwick, (11) Coffs Harbour. Horizontal lines — granitic rocks and Upper Permian acid volcanics.

Figure 2: After E.C. Leitch, 1974

of the study area. Lewington subdivided these sediments into meta-greywackes, meta-lutites and massive and rhythmic cherts, complete gradations occurring between the meta-lutites and the cherty sediments. He suggests that the chert nearest the contact of the Walcha Road Adamellite (in his area) is the oldest unit, giving way to meta-lutites and then rhythmically bedded cherts. At this point he suggests a marked environmental change occurs with the introduction of volcanism. An attempt to correlate these beds with the sediments from the study area was not successful as Woolomin type sediments in the study area, adjacent to the eastern contact of the

Walcha Road Adamellite are dominantly pelites (Lewington's op. cit. meta-lutites) no cherts (or quartzites) being present. Woolomin type beds comprise approximately 60% of the study area, the other 40% belonging to the younger (carboniferous), less deformed Sandon beds (Voisey, 1959). A description of the sediments of both the Woolomin and the Sandon type is given in chapter three.

Two regions within the so called Central Complex (Voisey op. cit.) have been regionally metamorphosed to almandine-amphibolite grade, forming sillimanite, cordierite and almandine bearing schists. Binns (1966) describes one of these areas, termed the Wongwibinda complex, situated to the west of the township of Wongwibinda, while the other area, the Tia complex, is found south of the village of Tia, and has been described by Gunthorpe (1970). The lack of sillimanite in the Walcha Road thermal schists suggests that the abovementioned areas (containing sillimanite) were subjected to a higher total pressure.

According to Leitch (1973) most of the Woolomin beds have undergone prehnite-pumpellyite burial metamorphism, however, rocks adjacent to the Walcha Road Adamellite that have not been effected by the intrusion, are of a regional greenschist grade.

Papers on the "Geology of New South Wales" by Wilkinson, Shaw, Chappell, Bofinger and Phillips (1969), and a review of Permian plutonism in NSW by Leitch (1969) had covered most of the previous work done on the New England Batholith prior to the study of Flood (1971). Binns (1967) had originally divided the New England Batholith into two suites, namely (a) the New England Batholith suite, consisting of the main body of post kinematic "granites" (248-220 m.y.) and, (b) the Hillgrove suite (269-250 m.y.)

a smaller group of pre and synkinematic "granites" which can be distinguished chemically by lower CaO , Al_2O_3 and Fe_2O_3 compared with rocks of similar acidity in the Batholith suite. Flood (1971) suggests a three field division of the New England Batholith, the additional division being the Bundarra suite.

The Walcha Road Adamellite belongs to the New England Batholith suite and is a coarse grained hornblende-biotite adamellite with an areal extent of some 190 square kilometres. The intrusion is elliptical in shape with the long axis oriented north/south parallel to the general structural grain of New England.

TABLE 1

SiO_2	69.13	Quartz	27.3
TiO_2	0.48	Orthoclase	23.7
Al_2O_3	14.04	Plagioclase	37.9
Fe_2O_3	0.87		
FeO	1.62	Biotite	6.8
MnO	0.07	Hornblende	6.8
MgO	1.72	Sphene	0.5
CaO	2.73	Opagues	0.3
Na_2O	3.55	Apatite	0.3
K_2O	3.93		
P_2O_5	0.16		
H_2O^+	0.60		
H_2O^-	0.14		
Total	<u>98.99</u>		

Chemical and Modal Analysis of
Walcha Road Adamellite (WRL, from Flood, 1971)

The Walcha Road Adamellite shows signs of forceful emplacement and strongly alters the structures of the contact rocks (Appendix One). The steeply dipping contacts of the adamellite and vertical foliation of the associated sediments suggests that the Walcha Road Adamellite has a near vertical contact with the intruded sediments. The forceful emplacement has resulted in the sediments "wrapping around" the adamellite, and there has been a development of a schistose fabric in the sediments of the aureole region, the actual aureole being 3km wide (Figure 3). It is suggested that similar aureole conditions are associated with intrusions having the same composition and areal extent as the Walcha Road Adamellite. Binns (1965) states that the Moonbi aureole is 1km wide, however, Howarth (1973) noted the development of biotite at approximately 3km from the contact, suggesting an aureole width similar to that at Walcha Road.

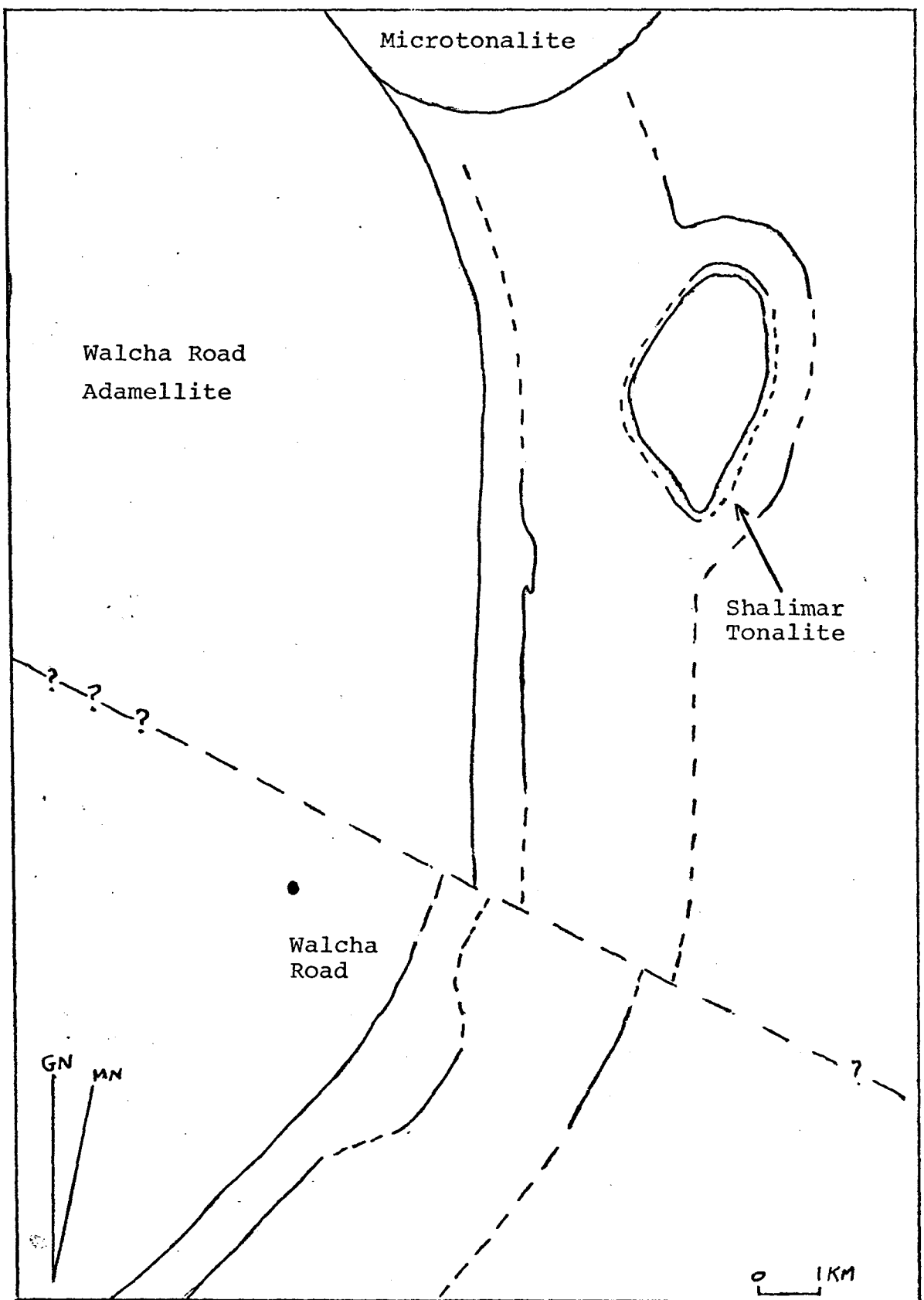


Figure 3: Cordierite and biotite isograds adjacent to Walcha Road Adamellite

3. THE SEDIMENTS

(a) Woolomin Type Beds

The Woolomin beds in the study area include what were originally carbonaceous and non-carbonaceous siltstones, very fine grained sub-feldsarenites, and minor calcareous and cherty units. The relative proportions of the major rocks are siltstones (60%), sub-feldsarenites (30%) and impure calcareous rocks, cherts (10%). Tables 3, 4, 5 and 6 show chemical analyses for carbonaceous and non-carbonaceous contact metamorphosed siltstones, which, from now on, will be referred to as meta-pelites. The meta-pelites rich in carbonaceous material are easily identified in the field by their dark appearance. Meta-pelites with only minor carbonaceous material can be recognised by three other methods:

- (i) Digestion in HF acid, leaving a dark carbonaceous residue .
- (ii) Trace element analyses, showing that carbonaceous meta-pelites are generally richer in copper (Figure 5) and,
- (iii) Polished section studies can be used to aid in the identification of carbonaceous material.

The latter method is quite useful for the higher grade rocks where well formed euhedral graphite grains are easily detected in reflected light.

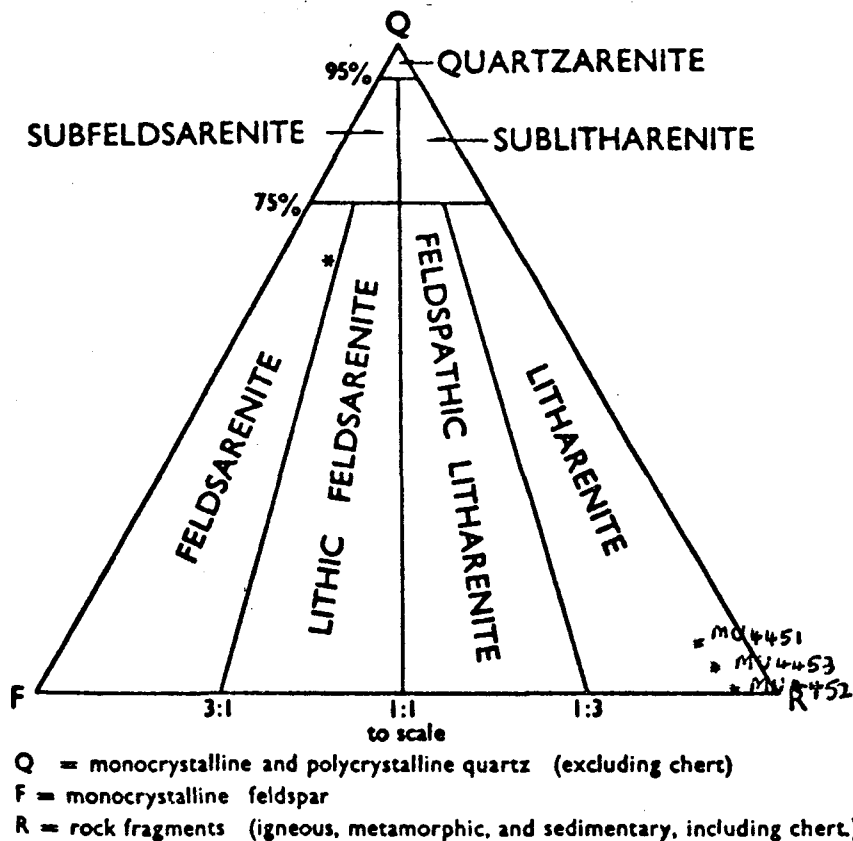


Figure 4: Primary arenite triangle of Folk (1972) showing the locations of three litharenites from the Sandon Beds.

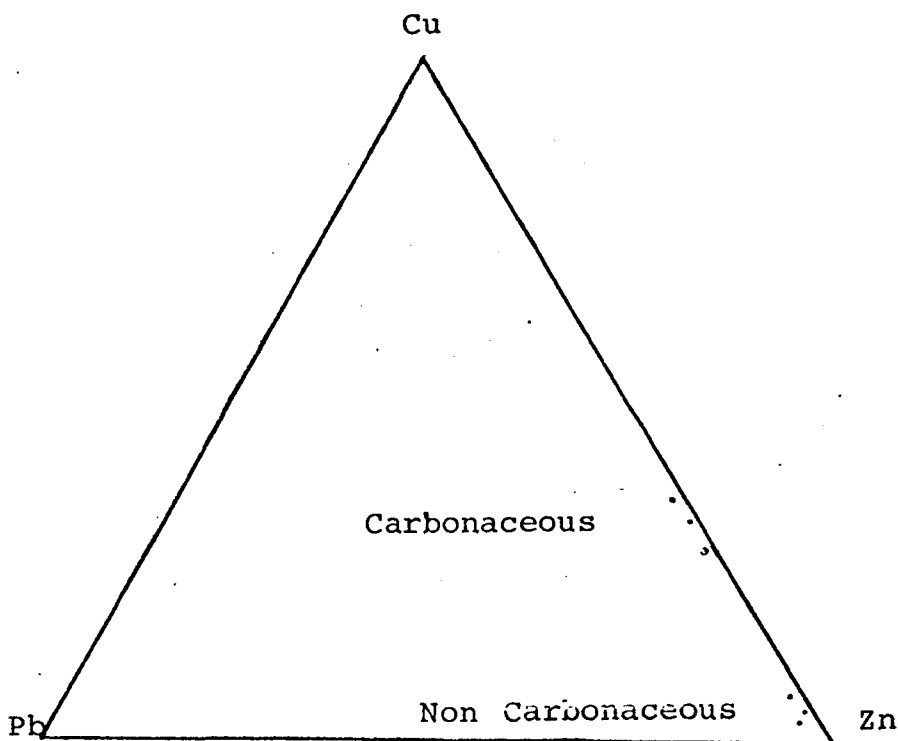


Figure 5: Cu-Pb-Zn diagram showing positions of some Walcha Road sediments.

Associated non-carbonaceous meta-pelites are slightly coarser grained, and there is a predominance of these non-carbonaceous meta-pelites in the southern sections of the area. Throughout the whole area (Woolomins and Sandons) there are minor lenses and concretions of what was originally a limy mud material. The thermal metamorphism of these calcareous rocks is discussed in a later section. Quartz arenites and conglomerates are absent from the Woolomin type beds of the area.

(b) Sandon Beds

In the area studied, the Sandon Beds are located to the north of the Oxley Highway. These sediments differ markedly from the Woolomin type beds to the south of the highway, in that fine to coarse grained feldsarenites and litharenites (Folk, 1972) predominate. The relative proportions of the major rocks are lith and feldsarenites (70%), meta-pelites (20%) and rhyolitic flows, conglomerates, radiolarian chert and impure calcareous rocks (10%).

The meta-pelites themselves differ slightly in chemical composition to the Woolomin type meta-pelites having higher K_2O and/or Na_2O values.

Radiolarian cherts are found throughout the area and generally form small but distinct ridges. Close to the intrusives (mainly the Shalimar Tonalite) these radiolarian cherts are completely recrystallised to a fine grained, granular mosaic of quartz. Minor conglomerates in the area contain angular fragments of volcanic material and minor radiolarian chert.

The litharenites of the area are immature and contain angular volcanic rock fragments and minor sub-rounded radiolarian chert fragments. The litharenites exhibit poor sorting. Fragments are grain supported and matrix plays a minor role. The feldsarenites are more predominant in the western section of the study area. The relict feldspars are slightly rounded, and in general, matrix supported.

A sub-feldsarenite (meta-greywacke, MU4436) was analysed (Table 2) and compared with Chappell's (1968) average for analyses of Baldwin greywackes and Lewington's (op. cit.) average of analyses of greywackes from Woolomin type sediments south of the study area. The noticeable difference between MU4436 and Lewington's average is the amount of CaO, MU4436 being some 2% richer in CaO.

(c) Comparison of Sediments from the Walcha Road Aureole
with Sediments from the Cooma Area, NSW

When comparing the Walcha Road pelites with pelites from the Cooma area (Joplin, 1942) the following points can be recognised:

- (i) The pelites from Cooma are 12-15% corundum normative whilst the Walcha Road pelites are approximately 5-6% corundum normative.
- (ii) The Cooma pelites are low in Na_2O and high in K_2O (Figure 6) compared to the Walcha Road pelites.
- (iii) The pelites contain an average of 55% SiO_2 compared to an average 65% SiO_2 in the Walcha Road pelites.

TABLE 2

CHEMICAL ANALYSIS OF A META-GREYWACKE
ADJACENT TO EASTERN CONTACT OF THE
SHALIMAR GRANODIORITE

	MU4436	Lewingtons Average	Chappell's Average
SiO ₂	60.97	62.68	54.63
TiO ₂	0.85	0.88	1.11
Al ₂ O ₃	16.94	15.23	15.69
Fe ₂ O ₃	1.86	1.36	1.65
FeO	5.35	4.93	7.30
MnO	0.17	0.11	0.16
MgO	3.84	3.04	3.70
CaO	5.47	3.18	5.01
K ₂ O	1.24	1.49	0.66
Na ₂ O	4.00	4.66	4.79
P ₂ O ₅	0.25	0.19	0.23
Total	100.94	97.75	94.93

- (iv) Cooma pelites have a higher $\text{Al}_2\text{O}_3/\text{FeO}+\text{MgO}$ ratio compared to the Walcha Road pelites.

The outstanding and critical difference between the Cooma and Walcha Road pelites is the percentage of Al_2O_3 that is available in the rock. The extra Al_2O_3 in the Cooma pelites allows andalusite (and sillimanite) to form and remain stable in the higher grade zones, whereas at Walcha Road, as grade is increased the andalusite reacts to form cordierite (see Part II).

The chemistry of the sediments of the Cooma area is not unique in the Lachlan Fold Belt, in that most documented cases of metamorphism (Guy 1968, Vallance, 1953, Browne 1943) occur in sediments with similar chemistry. Analyses of rocks from the Bathurst area can be found in Appendix Eight. These rocks have very high $\text{K}_2\text{O}/\text{Na}_2\text{O}$ ratios, similar to the pelites from Cooma.

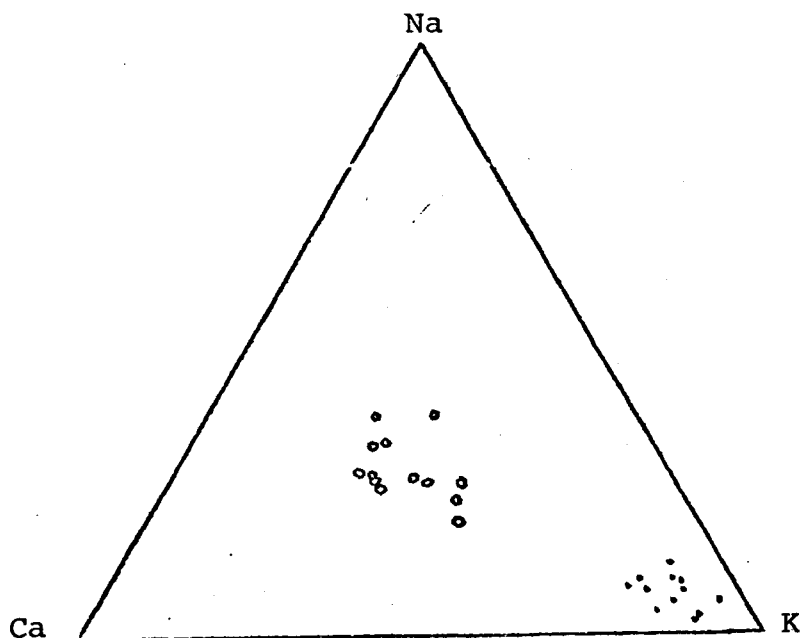


Figure 6; Alkali/lime diagram for pelites from Walcha Road (o) and from Cooma (.), NSW.

TABLE 3.

CHEMICAL ANALYSES OF CARBONACEOUS
META-PELITES ADJACENT TO THE
WALCHA ROAD ADAMELLITE

	MU4423	MU4474	MU4368	MU4397
SiO ₂	82.53	61.87	66.93	67.73
TiO ₂	0.24	0.80	0.72	0.64
Al ₂ O ₃	5.56	16.74	15.15	15.58
Fe ₂ O ₃	1.62	1.95	1.37	1.01
FeO	0.72	4.48	4.13	3.76
MnO	0.05	0.08	0.08	0.09
MgO	0.85	2.27	2.23	1.85
CaO	0.26	2.66	2.87	2.19
K ₂ O	1.26	2.86	2.61	2.99
Na ₂ O	0.75	4.29	2.33	3.18
P ₂ O ₅	0.02	0.23	0.15	0.12
Total	93.86	98.23	98.57	95.14

	R	CK	C	B
MgO/MgO + FeO	67.85	47.43	49.02	46.74

	MU4395	MU4405	MU4435	MU4409
SiO ₂	68.49	64.53	66.05	64.16
TiO ₂	0.74	0.77	0.79	0.86
Al ₂ O ₃	16.05	16.94	15.66	17.39
Fe ₂ O ₃	2.62	1.35	0.56	1.14
FeO	2.34	4.17	5.70	5.06
MnO	0.08	0.10	0.11	0.13
MgO	1.62	1.67	2.38	2.30
CaO	1.14	1.79	2.74	2.62
K ₂ O	2.74	3.06	1.79	2.24
Na ₂ O	2.09	2.26	2.89	3.45
P ₂ O ₅	0.09	0.19	0.21	0.28
Total	98.00	96.83	98.88	99.63

	B	C	CA	C
MgO/MgO + FeO	41.11	41.65	42.66	44.74

Analyst: G.S. Teale

CA = Cordierite-Almandine zone
C = Cordierite zone
B = Biotite zone
R = Regional greenschist (biotite)
RC = Regional greenschist (chlorite)

Chemical Analyses of Carbonaceous Meta-Pelites (cont.)

	MU4418	MU4374	MU4465	MU4466
SiO ₂	63.25	75.87	65.64	66.84
TiO ₂	0.76	0.39	0.76	0.76
Al ₂ O ₃	16.69	11.56	16.02	15.92
Fe ₂ O ₃	0.91	0.72	0.89	1.34
FeO	4.47	3.28	4.28	3.88
MnO	0.17	0.12	0.05	0.06
MgO	2.03	2.16	1.79	2.14
CaO	2.32	0.64	2.12	1.67
K ₂ O	2.75	3.07	2.76	1.95
Na ₂ O	4.38	1.41	3.80	2.77
P ₂ O ₅	0.20	0.06	0.16	0.16
Total	97.93	99.28	98.27	97.49
	B	B	B	C
MgO/MgO + FeO	44.71	53.98	42.69	49.58

	MU4408	MU4481	MU4403
SiO ₂	64.85	65.97	64.30
TiO ₂	0.82	0.72	0.75
Al ₂ O ₃	16.71	15.25	17.28
Fe ₂ O ₃	2.17	0.74	0.76
FeO	3.84	5.31	4.66
MnO	0.04	0.07	0.07
MgO	1.71	2.21	1.83
CaO	1.04	2.21	2.06
K ₂ O	3.20	1.97	3.09
Na ₂ O	1.75	2.70	3.00
P ₂ O ₅	0.17	0.22	0.19
Total	96.30	97.37	97.99
	C	RC	C
MgO/MgO + FeO	44.26	42.58	41.16

Analyst: G.S. Teale

TABLE 4

CHEMICAL ANALYSES OF HIGH POTASSIUM
CARBONACEOUS META-PELITES

	MU4366	MU4462	MU4393
SiO ₂	68.92	70.15	64.88
TiO ₂	0.62	0.77	0.72
Al ₂ O ₃	14.94	16.06	17.02
Fe ₂ O ₃	2.98	1.52	1.70
FeO	2.37	1.26	3.27
MnO	0.13	0.06	0.06
MgO	2.06	1.31	1.76
CaO	1.06	0.20	1.49
K ₂ O	3.68	4.48	3.67
Na ₂ O	1.63	0.81	2.24
P ₂ O ₅	0.21	0.06	0.17
Total	98.60	96.68	96.98

	B	B	B
MgO/MgO + FeO	60.76	65.00	48.99

	MU4490	MU4492	MU4464
SiO ₂	67.00	65.26	65.68
TiO ₂	0.52	0.74	0.75
Al ₂ O ₃	15.67	15.93	15.87
Fe ₂ O ₃	0.93	0.63	3.90
FeO	2.25	4.50	2.07
MnO	0.04	0.06	0.06
MgO	1.32	1.98	1.84
CaO	1.72	1.95	0.94
K ₂ O	3.62	3.66	3.92
Na ₂ O	3.66	2.81	1.34
P ₂ O ₅	0.13	0.23	0.16
Total	96.86	97.75	96.53

	R	B	B
MgO/MgO + FeO	51.09	43.96	61.29

Analyst: G.S. Teale

B = Biotite zone

R = Regional greenschist (chlorite)

TABLE 5

CHEMICAL ANALYSES OF NON CARBONACEOUS
META-PELITES ADJACENT TO THE
WALCHA ROAD ADAMELLITE

	MU4413	MU4383	MU4437
SiO ₂	63.80	54.18	75.43
TiO ₂	0.88	1.05	0.46
Al ₂ O ₃	15.77	22.98	11.47
Fe ₂ O ₃	0.94	1.03	0.70
FeO	4.53	8.95	3.25
MnO	0.11	0.16	0.10
MgO	2.25	3.70	1.44
CaO	2.80	1.57	1.31
K ₂ O	2.40	2.80	2.26
Na ₂ O	3.92	1.79	1.88
P ₂ O ₅	0.18	0.14	0.10
Total	97.58	98.35	98.40
	B	CK	C
MgO/MgO + FeO	46.97	42.42	44.13
	MU4438	MU4400	MU4439
SiO ₂	72.89	75.43	62.63
TiO ₂	0.57	0.45	0.83
Al ₂ O ₃	13.70	11.53	16.80
Fe ₂ O ₃	0.93	0.80	1.06
FeO	3.69	3.06	5.05
MnO	0.11	0.11	0.14
MgO	1.76	1.64	3.23
CaO	1.27	0.99	3.05
K ₂ O	3.46	3.37	3.02
Na ₂ O	2.17	0.81	3.76
P ₂ O ₅	0.13	0.08	0.20
Total	100.68	98.27	99.77
	C	C	C
MgO/MgO + FeO	45.95	48.86	53.26

Analyst: G.S. Teale

CA = Cordierite-Almandine zone
 CK = Cordierite-K-feldspar zone
 C = Cordierite zone
 B = Biotite zone
 R = Regional greenschist (chlorite)

Chemical Analyses of Non Carbonaceous Meta-Pelites (cont.)

	MU4491	MU4471	MU4417
SiO ₂	62.16	77.54	64.93
TiO ₂	1.01	0.42	0.66
Al ₂ O ₃	15.59	10.55	15.68
Fe ₂ O ₃	2.28	0.43	0.67
FeO	5.24	3.70	5.16
MnO	0.13	0.15	0.07
MgO	2.61	1.90	2.30
CaO	3.73	0.97	1.91
K ₂ O	0.74	1.79	3.33
Na ₂ O	2.15	0.90	3.55
P ₂ O ₅	0.22	0.09	0.14
Total	95.86	98.44	98.40

	R	CK	B
MgO/MgO + FeO	47.02	47.77	26.98

	MU4472	MU4450
SiO ₂	78.78	60.44
TiO ₂	0.42	0.87
Al ₂ O ₃	9.68	18.19
Fe ₂ O ₃	0.47	0.54
FeO	3.37	5.81
MnO	0.12	0.08
MgO	1.70	2.41
CaO	0.56	2.61
K ₂ O	2.14	2.63
Na ₂ O	0.64	4.36
P ₂ O ₅	0.06	0.25
Total	97.94	98.19

	CK	CA
MgO/MgO + FeO	44.80	40.23

Analyst: G.S. Teale

TABLE 6

CHEMICAL ANALYSES OF HIGH POTASSIUM
NON CARBONACEOUS META-PELITES

	MU4356	MU4382	MU4431	MU4354
SiO ₂	60.52	53.99	71.40	70.76
TiO ₂	1.01	1.00	0.61	0.69
Al ₂ O ₃	20.47	22.60	13.84	15.10
Fe ₂ O ₃	0.47	0.96	0.88	0.36
FeO	3.19	7.80	3.76	2.70
MnO	0.11	0.13	0.11	0.11
MgO	2.30	3.15	1.87	1.91
CaO	2.56	1.00	2.04	1.23
K ₂ O	5.97	5.58	3.82	5.05
Na ₂ O	2.30	1.59	0.81	1.41
P ₂ O ₅	0.42	0.16	0.12	0.22
Total	99.32	97.96	99.26	99.54
	CK	CK	C	CK
MgO/MgO + FeO	56.21	41.83	47.01	55.76
	MU4353	MU4359	MU4358	MU4414
SiO ₂	77.20	78.28	61.19	63.10
TiO ₂	0.50	0.21	0.76	0.73
Al ₂ O ₃	11.24	11.25	19.68	18.90
Fe ₂ O ₃	0.32	0.14	0.41	3.56
FeO	2.85	1.46	5.35	1.62
MnO	0.08	0.01	0.03	0.07
MgO	1.40	1.12	2.22	1.63
CaO	0.92	1.08	1.66	0.39
K ₂ O	3.92	3.85	5.66	5.25
Na ₂ O	1.05	1.28	1.58	1.07
P ₂ O ₅	0.11	0.08	0.16	0.16
Total	99.59	98.76	98.70	96.48
	CK	CK	CK	C
MgO/MgO + FeO	46.64	57.80	42.52	64.23

Analyst: G.S. Teale

CK = Cordierite-K-feldspar zone
C = Cordierite zone

4. MINOR ACIDIC AND BASIC INTRUSIONS IN THE WALCHA ROAD AREA

(a) Minor Acidic Intrusions

Two small silica rich intrusions occur in the area. Dyke like, quartz porphyry intrusions, which in hand specimen look similar to a porphyritic rhyolite, are exposed in Congi Creek in the central section of the area. The intrusives have been contact metamorphosed and foliated by the Walcha Road Adamellite. A chemical analysis of this variety of intrusion can be found in Table 7 (MU4486). In thin section the rock consists of relict quartz phenocrysts which have been marginally resorbed, and which sit in a matrix of polygonal quartz grains. Metamorphic biotite occurs as ragged red-brown grains often altering to chlorite. The second intrusion is a stock like granodioritic body which is located approximately 0.8km south of the Oxley Highway. The minor intrusion has not effected the surrounding sediments, but has been contact metamorphosed itself by the Walcha Road Adamellite (analysis in Table 7 , MU4476). Quartz in this intrusion has been recrystallised into granular aggregates due to this contact metamorphism.

(b) Minor Basic Intrusions

Many sub-ophitic dolerite dykes are found throughout the area. The larger dykes are easily recognised in the field by their cross cutting nature, dark colour and texture. In hand specimen individual plagioclase grains are easily identified and can be up to 5mm in length. All basic dykes investigated were intruded prior to the intrusion of the Walcha Road Adamellite. Metamorphic assemblages (from lowest to highest grade) are as follows:

TABLE 7

CHEMICAL ANALYSES OF CONTACT METAMORPHOSED
ACID INTRUSIVES ADJACENT TO THE
WALCHA ROAD ADAMELLITE

	MU4486	MU4476
SiO ₂	74.75	68.05
TiO ₂	0.02	0.38
Al ₂ O ₃	14.37	13.85
Fe ₂ O ₃	0.48	1.34
FeO	0.28	1.77
MnO	0.01	0.13
MgO	0.16	1.94
CaO	0.10	2.50
K ₂ O	4.31	4.24
Na ₂ O	4.33	4.50
P ₂ O ₅	0.03	0.28
Total	98.84	98.98

Blue-green amphibole-plagioclase-minor calcite-minor epidote-minor biotite (MU4489).

Blue-green hornblende-plagioclase-biotite(MU4365).

Green-blue hornblende-plagioclase-biotite(MU4534).

Green hornblende-plagioclase (MU4441).

Tan hornblende-plagioclase (Flood, 1964).

The presence of biotite at lower grades is compositionally controlled and not due to metamorphic grade. Relict clinopyroxene (Plate 1) can be found at the lower metamorphic grades, and blastophitic textures are common. Modal analyses for MU4365 and MU4534 are shown in Table 8.

Rare porphyritic basic dykes (or basaltic flows?) are also present (MU4398). These rocks are much finer grained than their doleritic counterparts and are always conformable with the surrounding sediments. Ovoid patches of ragged hornblende, in these rocks, are thought to have been clinopyroxene phenocrysts which have been broken down to form hornblende during the contact metamorphism. Binns (1965) suggests that ovoid patches of ragged amphibole found in the basic hornfels of the Tilbuster area have been derived from original pyroxene phenocrysts.

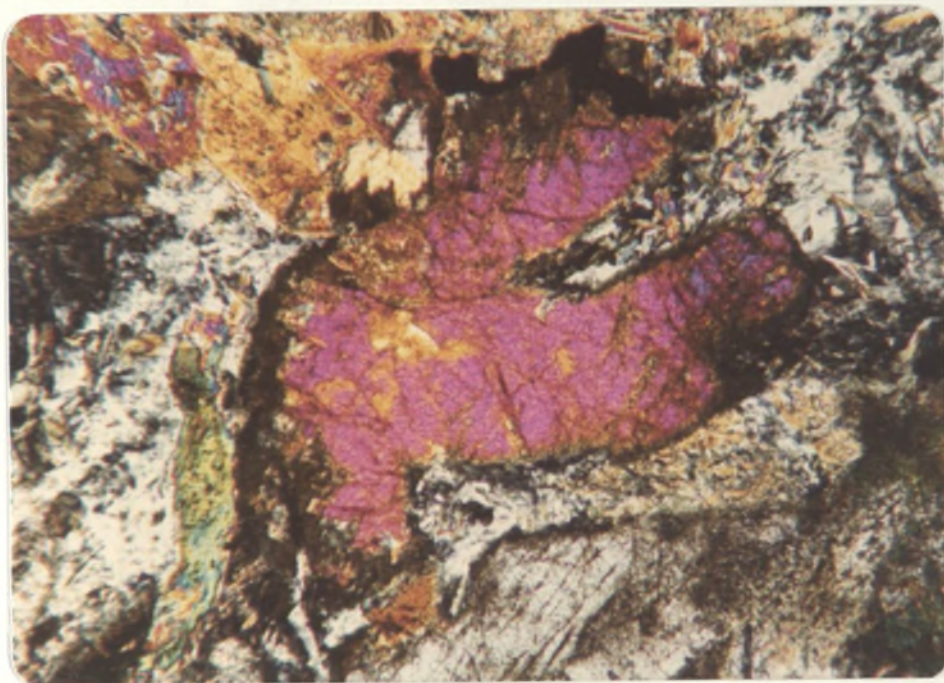


Plate 1: MU4365, Relict Clinopyroxene in Doleritic Dyke (note blastophitic texture)
x 65 (crossed Nicols)

TABLE 8

Modal Analyses of Contact
Metamorphosed Basic Dykes

	MU4365	MU4534
Blue-green hornblende	53.43	46.15
Plagioclase	30.46	35.98
Clinopyroxene	6.13	3.85
Biotite	4.41	6.33
Opagues	4.18	5.45
Quartz	1.39	2.24

MU4365: located 2.1km from the contact in the biotite zone

MU4534: located 1.2km from the contact in the andalusite zone.

(c) Description of Metamorphic Minerals from the Basic
Hornfelses

(i) Hornblende

Hornblende in contact metamorphosed basic igneous rocks generally forms xenoblastic, ragged and fibrous grains which become subidioblastic to idioblastic as the contact is approached. Table 20 indicates the changes in colour of the hornblende as the contact is approached. This agrees with the work of Binns (1965) who investigated hornblendes from the Moonbi and Tilbuster areas. In brief, the hornblende changes from blue-green in colour in the biotite zone, through green-blue, green, brown-green and finally tan in colour within 10-20 metres of the contact. Similar observations were made adjacent to the Bannalasta Adamellite, with tan hornblende being found in hornfelses that occurred as large included blocks within the actual adamellite (Teale, 1972). Hornblendes found in impure calcareous rocks, however, are usually a bright green colour regardless of metamorphic grade (within 10 metres of the contact they do take on a slight brown colouration). Colourless sub-aluminous hornblendes(?) occur as fibrous and acicular radiating aggregates (Plate 2) in Ca rich sediments.

The contact metamorphosed dolerite dykes of the area provide excellent samples for the study of the hornblendes. In these rocks hornblende replaces clinopyroxene (Plate 1) and also plagioclase, the plagioclase being marginally altered to hornblende. Biotite can be found rimming and replacing hornblende in these rocks (Plate 3) and can represent 6% by volume of the rock (Table 8).

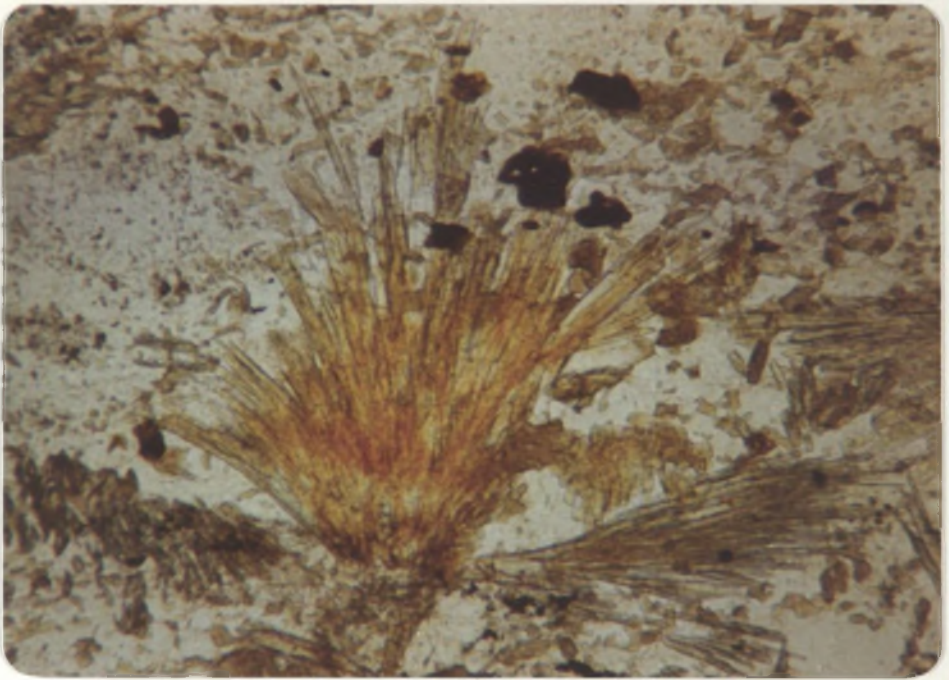


Plate 2: MU4411, Radiating sub-aluminous hornblende(?)
x 104

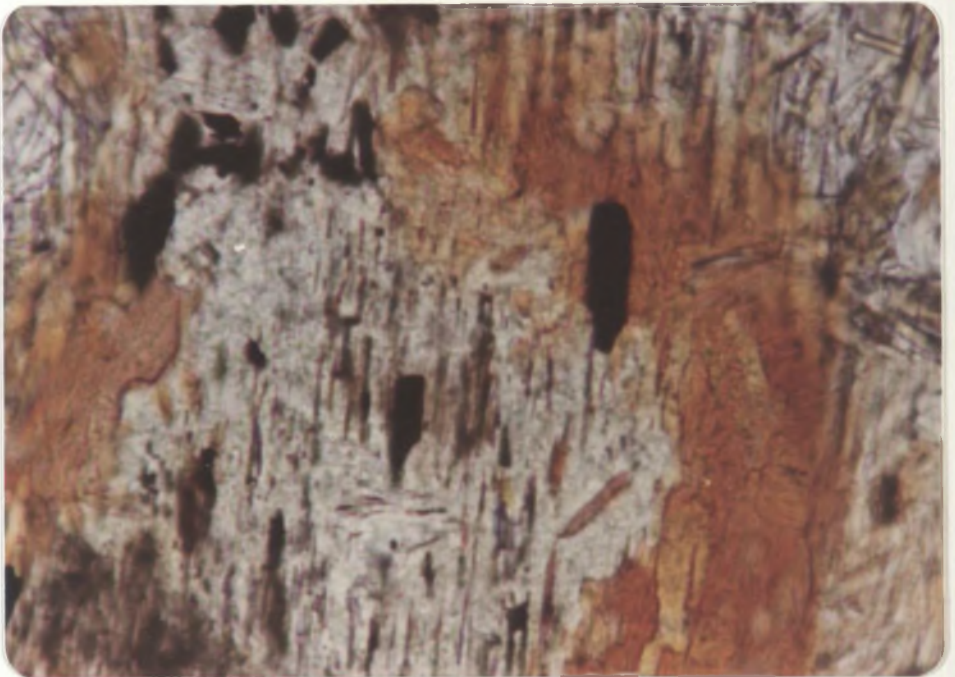


Plate 3: MU4406, Biotite rimming a blue-green hornblende grain. Note the ilmenite(?) grains formed by the replacement of titanaugite by hornblende.
x 104

(ii) Cummingtonite

Cummingtonite, with characteristic twinning, is only found in the inner zones of the aureole. It is associated with plagioclase, quartz and minor hornblende and opaques. In thin section, the sieve textured cummingtonite occurs in a granoblastic groundmass of quartz and plagioclase with minor brown-green subidioblastic hornblende. Inclusions within the cummingtonite are usually quartz with minor opaques and plagioclase.

In hand specimen the rock is lighter in colour than the normal hornblende bearing rock. A large outcrop of cummingtonite-hornblende hornfels (fabric differs from the pelitic schists) can be found in Surveyors Creek, directly north of the Surveyors Creek Homestead.

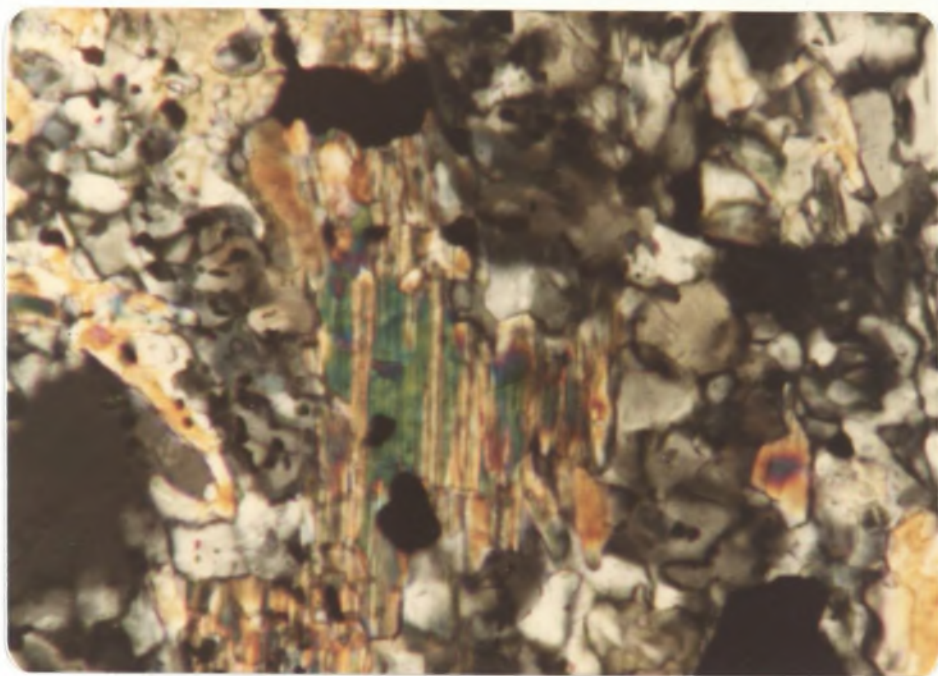


Plate 4: MU4384, Cummingtonite showing characteristic twinning
x 104 (crossed nicols)

(iii) Hypersthene

Hypersthene bearing pyroxene hornfels occur as included blocks (xenoliths) contained in the Kentucky Diorite (Flood, 1971) a few kilometres to the north of the study area. The granoblastic texture of the quartz and andesine, and the euhedral to subhedral grain shapes of the biotite and hypersthene are shown in Plate 5. The hypersthene-biotite-augite-andesine hornfels are distinguished in the field by their fine grain size and light colour compared to the coarser grain size and darker (green) colour of their diorite host.

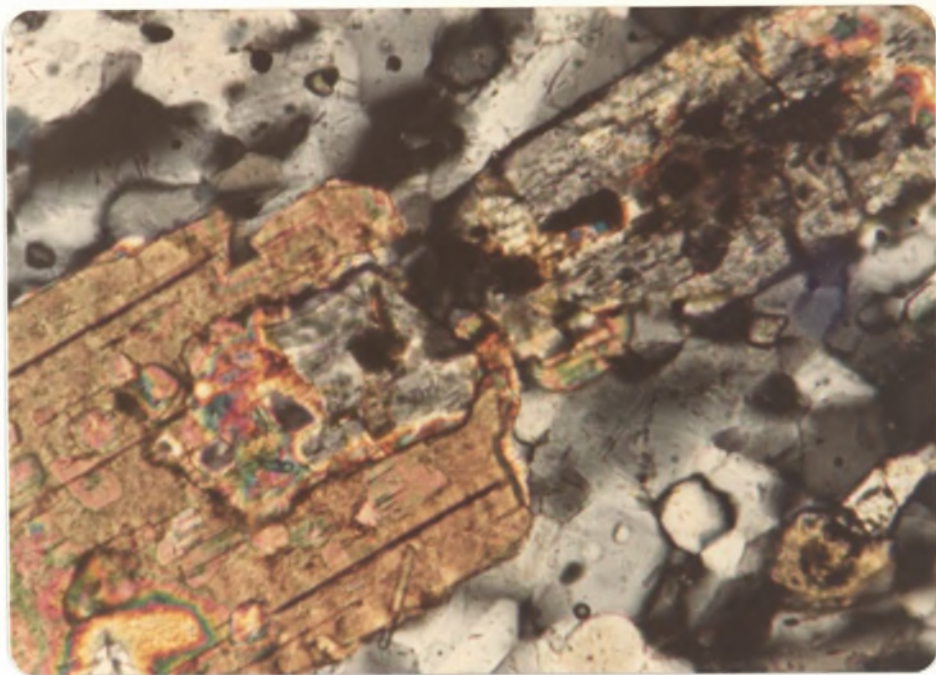


Plate 5: MU4458, Hypersthene-biotite-augite-andesine hornfels contained within the Kentucky Diorite x 260 (crossed Nicols)

There are no orthopyroxene bearing hornfels (pyroxene hornfels) adjacent to the eastern contact of the Walcha Road Adamellite. However, Flood (1971) has described pyroxene hornfels that occur as discontinuous lenses between the eastern contact of the Bannalasta Adamellite and the western contact of the Walcha Road Adamellite. These rocks contain hypersthene-augite-andesine and hypersthene-augite-biotite-andesine assemblages, and have a granoblastic microstructure.

Flood (1971) states that the anomalous occurrence of pyroxene hornfels facies rocks in this area is not clear, however, he does suggest that two factors could be of importance, namely (a) that the lenses of higher metamorphic grade may have been forced up with the adamellites from greater depths and/or (b) the formation of pyroxene may have resulted from the overprinting of the contact metamorphism of the Bannalasta Adamellite by the Walcha Road Adamellite, the first intrusion causing considerable dehydration allowing for the conversion of hornblende to pyroxene at lower temperatures during the subsequent intrusion of the Walcha Road Adamellite.

5. CONTACT METAMORPHISM OF IMPURE CALCAREOUS SEDIMENTS

(a) Subdivisions of Sediment Types

Two types of impure calcareous sediment occur in the Walcha Road area:

- (i) Silica rich calcareous concretions can be found throughout the area. They are buff coloured in hand specimen, and have diameters of up to 0.5 metres. These concretions are considered to be original calcareous "pockets" that formed within the siltstones.



Plate 6: Calcareous concretion from cordierite
K-feldspar zone, MacDonald River area.

- (ii) Silica poor calcareous sediments differ from the above sediments, in that they occur as thin beds and lenses and not as concretions. They are a red and/or green colour in hand specimen, and it is thought that they were originally clay rich limy "marls". Chemical analyses of this variety are shown in Table 9.

(b) Contact Metamorphism

(i) Silica Rich Concretion Type

The concretions close to the contact, (in the cordierite-K-feldspar zone) contain the assemblage:

Quartz-diopside-hornblende-K-feldspar(?)-scapolite, with minor magnetite(?), grossularite and calcite (MU4455).

A feature of these rocks when found in the cordierite-K-feldspar zone is the well developed poikiloblastic green-brown hornblende, twinned in some cases, and up to 0.8mm in length. The hornblende includes quartz and diopside. A lack of plagioclase feldspar is noted.

It is the concretions that show a metamorphic zoning. In the cordierite zone, the following assemblages have been noted:

Centre of Concretion:	Quartz-diopside-epidote-plagioclase and minor calcite and hornblende.
Rim of Concretion:	Plagioclase-calcite-hornblende-quartz.
Reaction Jacket in Pelite:	Biotite-hornblende-plagioclase-quartz.

Pelite: Cordierite-biotite-quartz-plagioclase.

Minor grossularite and opaques can occur within the centre and rim of the concretions.

Binns (1966) discussed similar calcareous nodules and noted the metamorphic zoning. He considered the zoning to have been caused by some diffusion process by which K_2O and H_2O passed into the concretion from the adjacent schists and Ca passed out from the concretion. Binns (op. cit.) was uncertain whether the silica impurities were original or derived from the enclosing schist. At Walcha Road, relict detrital quartz can be observed in the concretions of the outer zone.

Similar zoning around calcareous nodules and concretions has been documented by Loomis (1966) and Suzuki (1934), whilst Crawford (1972) has discussed metamorphic reactions that take place in rocks of similar mineralogy. Suzuki (op. cit.) considered the concretions found in rocks of Central Hokkaido, Japan, to be chemically similar to the concretions of the original sediments, with the exception, of course, of the amount of Co_2 withdrawn during the decarbonisation reactions.

(ii) Silica Poor Type

No zoning is present in rocks of this type and their adjacent sediments. At 1000 metres from the contact these sediments develop the assemblage:

Epidote-diopside-calcite-quartz, with minor plagioclase, grossularite, green hornblende(?) and sphene (MU4370).

TABLE 9

CHEMICAL ANALYSES OF SILICA POOR
CALCAREOUS META-SEDIMENTS

	MU4435	MU4370
SiO ₂	46.03	41.59
TiO ₂	0.24	0.24
Al ₂ O ₃	24.84	26.27
Fe ₂ O ₃	2.40	2.87
FeO	4.40	5.42
MnO	0.28	0.25
MgO	0.63	0.53
CaO	18.22	20.69
K ₂ O	0.27	tr.
Na ₂ O	0.50	0.27
P ₂ O ₅	0.09	0.11
Total	97.90	98.24

Closer to the contact the following assemblage is observed (600 metres):

Diopside-epidote, plus minor green hornblende(?), plagioclase and grossularite (MU4434).

From these assemblages it can be deduced that quartz and calcite have been consumed in the formation of Mg poor diopside. The lower modal percent of epidote at higher grades suggests a breakdown of this epidote to form diopside.

(c) Brief Description of Minerals Associated with the Impure Calcareous Rocks

(i) Scapolite

Scapolite is only observed in calcareous rocks found in the cordierite-K-feldspar zone. It occurs as highly bi-refrangent, sieve textured grains (MU4455), which include diopside and quartz grains, and as weakly bi-refrangent, cross cutting veins (MU4440). According to Deer et. al. (1966) the high bi-refrangent variety is Ca rich, whilst the weakly bi-refrangent (cross cutting) variety is Na rich. In both cases the scapolite appears to have been the last phase to form suggesting a "metasomatic" origin.

(ii) Diopside

Diopside occurs in impure calcareous rocks as high relief grains with moderate bi-refrangement, and is found throughout the aureole. No impure calcareous

rocks were encountered in the biotite zone, so it is not known if diopside occurs here. A description of the diopside bearing assemblages has been discussed in parts (a) and (b) of this chapter.

(iii) Calcite

Calcite occurs as a major constituent of the impure calcareous rocks of the outer zones. In these outer zones it can also be observed in mafic rocks, being a by-product of the breakdown of calcic plagioclase. An amphibole appears to nucleate in calcite of rocks from outer zones, this amphibole having an acicular habit and a green colour. Calcite decreases in modal percent as the contact is approached, but still can be found in minor amounts in the diopside-hornblende-scapolite rocks of the cordierite-K-feldspar zone (usually associated with grossular).

(iv) Grossularite

Grossularite forms anhedral flesh pink grains, which are usually associated with calcite. Grossularite can be found up to 800 metres from the contact, but is only a minor phase (less than 3%) in these impure calcareous rocks.

The amphibole that is associated with these rocks is an olive green at lower grades, and a bright green at higher grades, with a brown-green hornblende forming within 20 metres of the contact.

6. MINERALS FROM THE METAMORPHIC ZONAL SEQUENCE (PELITES)

(a) Biotite

Biotite is present, usually in significant amounts, throughout the metamorphic aureole. It first appears approximately 3.5km from the contact in feldspathic and lithic arenites (MU4448, MU4424) and there is often a distinct lag before it develops in the pelites (3.2km; MU4459, MU4456, MU4425). This has been adequately explained by Mather (1970) in terms of the stability of the mineral pair phengite-chlorite in the more pelitic rocks. It should be mentioned that at Walcha Road the pair phengite-chlorite is stable in the cordierite bearing schists of the outer cordierite zone, these schists being originally extremely fine grained carbonaceous shales.

Biotite first appears in these outer zones as minute (0.02mm) green-brown grains, with poorly developed (001) faces. This green-brown biotite does not persist well into the aureole and it gives way to a brown biotite in the outer biotite zone. This brown colouration of the biotites increases with grade and at the contact itself, they are a foxy red-brown in colour. According to Hayama (1959) the change in colour of biotites from greenish-brown and brown to reddish brown is related to a decrease in the ratio $\text{Fe}_2\text{O}_3/\text{Fe}_2\text{O}_3 + \text{FeO}$ and/or an increase in the TiO_2 content caused by an increase in the metamorphic grade. Tilley (1926) also noting similar colour changes in biotites, suggested that the FeO content of biotites from certain metamorphic areas

may increase with increase in metamorphic grade. Whole rock analyses, and electron probe analyses of biotites (Table 10) from the cordierite, cordierite-almandine and cordierite-K-feldspar zones at Walcha Road support Hayama's idea. There is a decrease in the $\text{Fe}_2\text{O}_3/\text{Fe}_2\text{O} + \text{FeO}$ ratio (in whole rock analyses) and there is an increase in the TiO_2 content of the biotites as the metamorphic grade rises.

The suggestion that biotite generally becomes more Mg rich with increasing grade (Engel and Engel, 1958, 1960) is not supported by the data (Table 10) on the biotites of the Walcha Road aureole. The $\text{MgO}/\text{MgO} + \text{FeO}$ ratio of the biotites appears to be a function of the $\text{MgO}/\text{MgO} + \text{FeO}$ ratio of the rocks. This ratio is low (0.09 - 0.50) in these rocks and Fe rich biotites are observed throughout the entire aureole. In the Ardara aureole (Pitcher and Sinha, 1957) biotite composition follows the change in composition of the sediment accurately, and is unrelated to the metamorphic grade.

There is a slight overall increase in the grain size of the biotite as the contact is approached (outer biotite zone 0.02mm; cordierite-almandine zone 0.045mm; cordierite-K-feldspar zone 0.20mm parallel to (001)), the increase in size of the biotite being more dramatic in the cordierite-K-feldspar zone.

TABLE 10

BIOTITE ANALYSES

	1	2
SiO ₂	35.26	35.52
TiO ₂	2.72	2.65
Al ₂ O ₃	18.67	19.11
FeO*	21.92	21.65
MgO	8.60	8.35
K ₂ O	8.30	8.25
CaO	-	-
Na ₂ O	-	0.18
Cr ₂ O ₃	0.23	-
Total	95.70	95.70

Numbers of Ions on the basis of 22(0)

Si	5.3743] 8.0000	5.3971] 8.0000
Al	2.6257		2.6029	
Al	0.7289] 5.8163	0.8198] 5.7628
Ti	0.3119		0.3030	
Fe ²⁺	2.7943		2.7511	
Fe ³⁺	-		-	
Cr	0.0272] 1.6124	-] 1.6510
Mg	1.9540		1.8889	
Ca	-		-	
Na	-		0.0530	
K	1.6124		1.5980	

1. MU4435, Biotite from cordierite-almandine zone, approximately 250 metres from contact
2. MU4435, as for (1)

+ All analyses recalculated to 95.7% dry

* Total iron as FeO

Analyses 1 and 2: R.H. Flood

Analyses 3 and 4: S. Dobos

Biotite Analyses (cont.)

	3	4
SiO ₂	35.65	34.05
TiO ₂	1.48	2.98
Al ₂ O ₃	19.97	20.72
FeO	21.50	21.91
MgO	7.83	5.92
K ₂ O	8.22	8.58
CaO	0.09	-
Na ₂ O	0.17	0.28
Cr ₂ O ₃	-	-
Total	94.91	94.44

Numbers of Ions on the Basis of 22(0)

Si	5.4156] 8.0000	5.2303] 8.0000
Al	2.5844		2.7697	
Al	0.9914] 5.7504	0.9814] 5.6362
Ti	0.1705		0.3444	
Fe ²⁺	2.7320		2.9101	
Fe ³⁺	-		-	
Cr	-] 1.7352	-] 1.8263
Mg	1.8565		1.4003	
Ca	0.0157		-	
Na	0.0511		0.0874	
K	1.6684] 1.7389	1.7389	

3. MU4466, Biotite from outer cordierite zone, approximately 740 metres from contact.
4. MU4383, Biotite from cordierite-K-feldspar zone, approximately 2 metres from the contact.

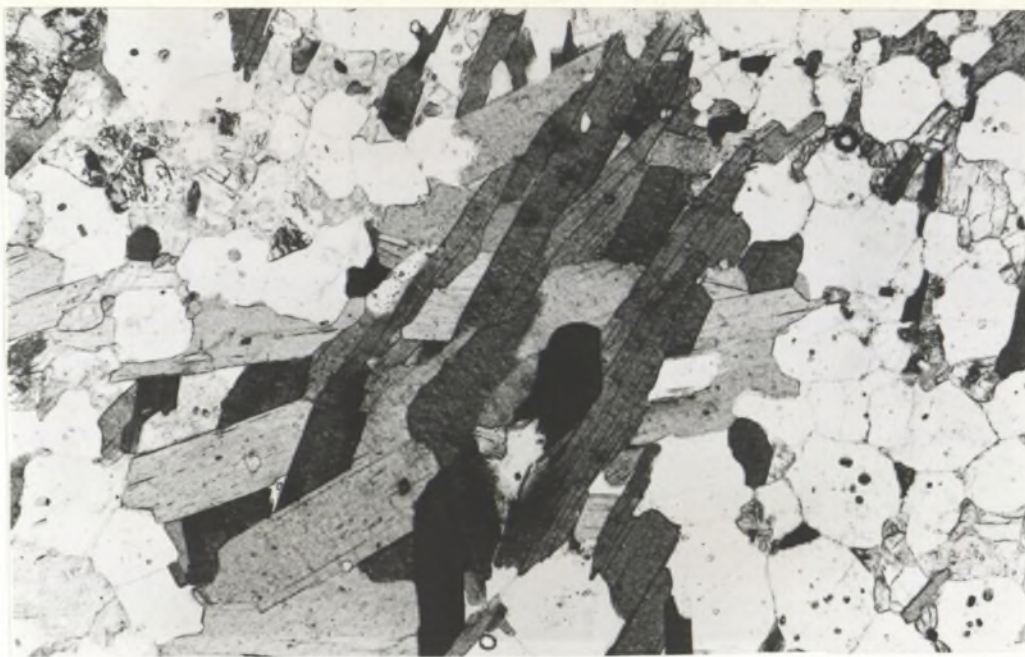


Plate 7: MU4471, Decussate aggregate of biotite from
cordierite-K-feldspar zone
x 104

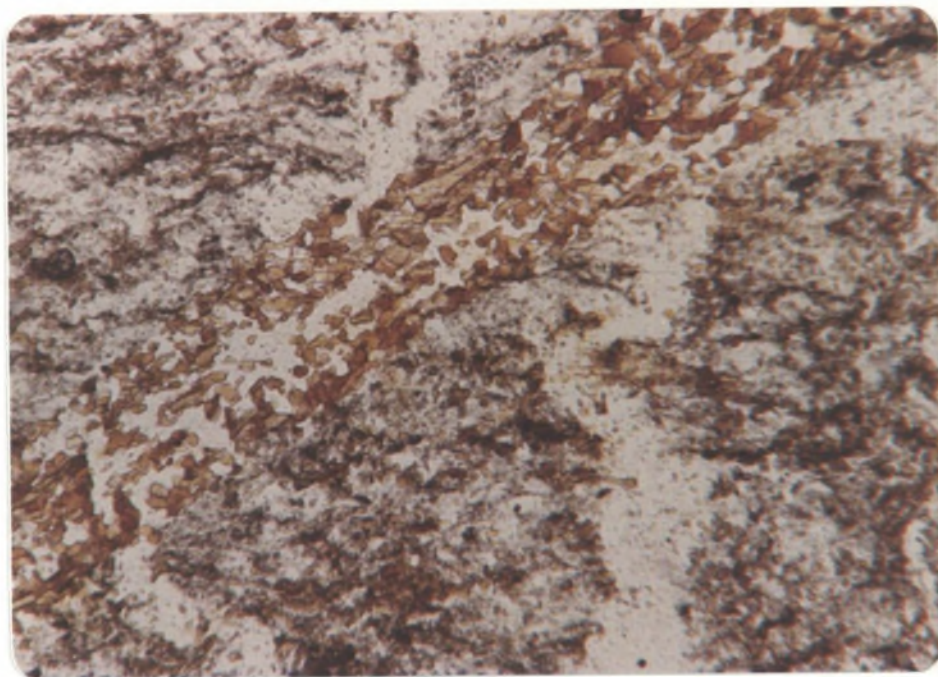


Plate 8: MU4407, Biotite associated with quartz vein
x 65

(b) Cordierite

At Walcha Road cordierite occurs up to 0.8km from the contact in non graphite bearing schists and up to 1.2 km from the contact in graphite bearing rocks. The extension of the cordierite isograd in the graphitic rocks is explained in the following chapter.

In the inner zones (cordierite-almandine and cordierite-K-feldspar zones) cordierite is identified by its poikiloblastic nature, rough lamellar twinning (Plate 10) cyclic twinning in pseudo-hexagonal cross sections (Plate 9) and common alteration products (Plates 12, 13 and 14). In the actual cordierite zone, cordierite occurs as highly poikiloblastic oval porphyroblasts (av. 0.6mm) which developed post the S_1 cleavage and pre the flattening (Appendix One). There is an absence of twinning, and the cordierite is characterised by its highly poikiloblastic nature (Plate 14) and occasional rim of yellow alteration products (pinite). Inclusions in the cordierite are predominantly quartz, biotite and opaque minerals in the inner zones (cordierite-almandine and cordierite-K-feldspar) and quartz, graphite, muscovite, biotite, chlorite and opaque minerals in the cordierite zone. Inclusions in cordierite of higher grade are usually well rounded (Plate 10) whereas inclusions in cordierite of lower grade usually retain their original shapes.

The composition of the cordierite varies slightly in the different zones, composition depending not on metamorphic grade, but on the whole rock $MgO/MgO+FeO$ ratio. For convenience, cordierite analyses were recalculated to

100% dry (Table 11). Before recalculation the totals of the cordierites were consistently lower than 100%, ranging from approximately 96.5% in the outer cordierite zone, 97.3% in the cordierite-almandine zone and 99.2% in the inner cordierite-K-feldspar zone. Since the sum of cations per 18 oxygens is sufficiently close to the theoretical value 11(11.05-11.18), the deficiency in the analyses' totals suggests an amount of approximately 0.8-3.5% H₂O.

The structural location of this H₂O still remains a problem. Iiyama (1960) suggested that (H₄O₄)⁴⁻ replaces (SiO₄)⁴⁻ in tetrahedra, however, it is more likely, zeolite like molecular water, loosely bound in the large channels parallel to the z axis (Newton, 1972; Schreyer and Yoder, 1964). It has been suggested (Weisbrod, 1973; Schreyer and Yoder, 1964) that Mg and Fe cordierites contain the same amount of water, at least at 750°C and between 0-3Kb. Newton (1972) states that Fe cordierite will contain more H₂O (1.7-2.0 moles) than Mg cordierite (0.6 moles) at 700°C and 3.3Kb. It is suggested, that at the lower temperature and pressure conditions of the Walcha Road area more molecular H₂O can be accommodated, along with other molecular impurities (K and Na) which more than likely fill similar sites as the H₂O in the cordierite structure. At Walcha Road, the amounts of H₂O, Na and K held in the cordierite structure, decrease with increasing grade.

In the view of the writer the suggested 3.5% H₂O content of the cordierite from the outer cordierite zone is approximately correct. It should be mentioned that some cordierites from rocks of the Harts Range area, South Australia, also contain in the vicinity of 3.5% H₂O (S. Dobos, pers. comm.).

TABLE 11

CORDIERITE ANALYSES

	1	2	3
SiO ₂	48.95	48.41	49.12
Al ₂ O ₃	33.31	33.13	32.69
FeO*	9.51	10.05	9.78
MnO	0.19	0.28	0.25
MgO	7.60	7.60	7.61
K ₂ O	-	0.05	0.10
Na ₂ O	0.37	0.48	0.45
CaO	0.07	-	-
Total ⁺	100.00	100.00	100.00

Number of Ions on the Basis of 18(0)

Si	4.9876] 6.0000	4.9550] 6.0000	5.0160] 6.0000
Al	1.0124		1.0450		0.9840	
Al	2.9876] 2.9876	2.9513] 2.9513	2.9507] 2.9507
Fe ³⁺	-		-		-	
Mg	1.1540] 2.0611	1.1586] 2.1480	1.1575] 2.1163
Fe ²⁺	0.8104		0.8602		0.8358	
Ca	0.0076		-		-	
K	-		0.0071		0.0136	
Na	0.0729		0.0981		0.0883	
Mn	0.0162		0.0240		0.0216	

Mg/Mg + Fe 58.7

57.4

58.1

1. MU4435, cordierite from cordierite-almandine zone, approximately 250 metres from the contact.
2. MU4435, as for (1)
3. MU4435, as for (1) and (2)

+ All analyses recalculated to 100% dry

* Total iron as FeO

Analysis 1: R.H. Flood

Analyses 2-6: S. Dobos

Cordierite Analyses (cont.)

	4	5	6
SiO ₂	48.07	48.03	48.33
Al ₂ O ₃	33.05	32.64	33.55
FeO	11.81	10.58	9.87
MnO	0.23	0.27	0.36
MgO	6.30	7.19	7.14
K ₂ O	0.08	0.86	-
Na ₂ O	0.46	0.43	0.75
CaO	-	-	-
Total	100.00	100.00	100.00

Number of Ions on the Basis of 18(0)

Si	4.9574	4.9497	4.9456
Al	1.0426	1.0503	1.0544
Al	2.9744	2.9134	2.9921
Fe ³⁺	-	-	-
Mg	0.9695	1.1045	1.0884
Fe ²⁺	1.0181	0.9120	0.8448
Ca	-	-	-
K	0.0110	0.0565	-
Na	0.0923	0.1709	0.1488
Mn	0.0204	0.0246	0.0312

Mg/Mg + Fe 48.8

54.8

56.3

4. MU4383, cordierite from cordierite-K-feldspar zone, approximately 2 metres from contact.
5. MU4466, cordierite from cordierite zone, approximately 740 metres from contact.
6. MU4466, as for (5).

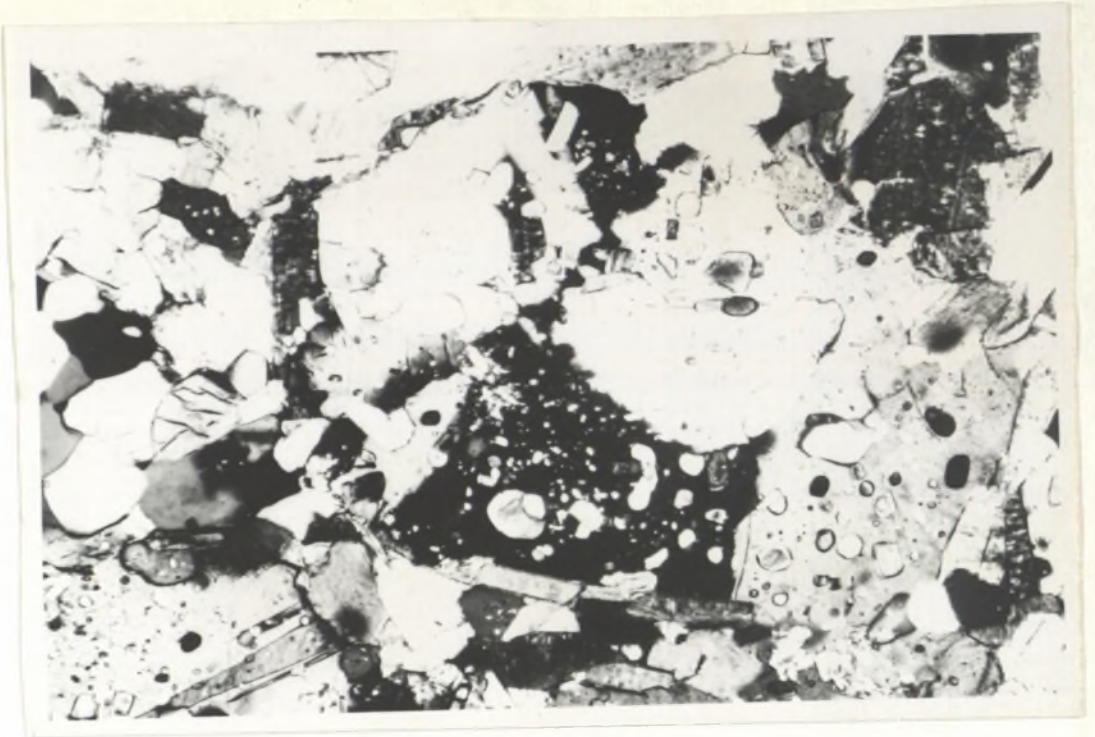


Plate 9: MU4383, Cyclic twinning of cordierite in the cordierite-K-feldspar zone
x 520 (crossed Nicols)

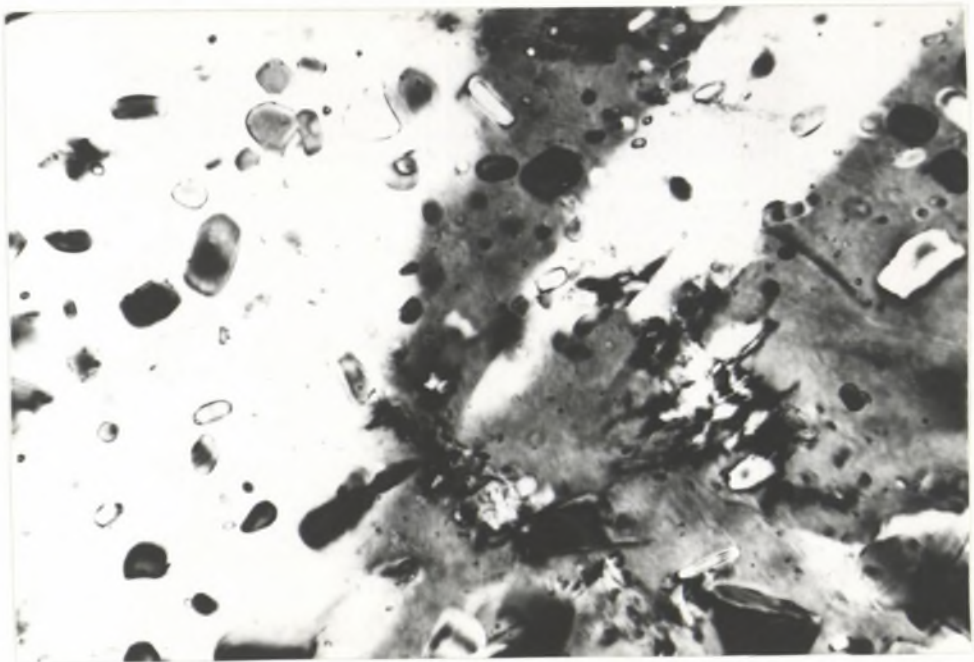


Plate 10: MU4382, twin lamellae in cordierite. Note the rounded nature of inclusions and the chloritic alteration products.
x 520 (crossed Nicols)

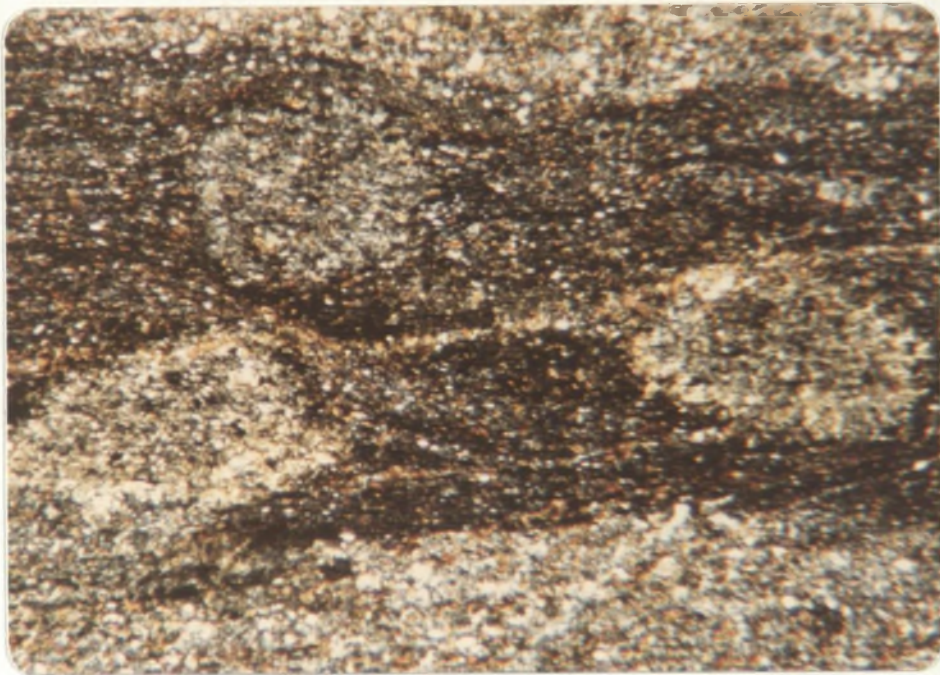


Plate 11: MU4409, Biotite-cordierite schist from the
outer cordierite zone
x 25 (crossed nicols)

Retrogression of Cordierite

The most common alteration product of cordierite is pinite which has been shown to be a fine aggregate of chlorite and muscovite (Michel-Levy, 1960). The pinite alteration can commence at cordierite grain boundaries (Plate 12) growing into and replacing the cordierite. This pinitisation of cordierite is a low temperature alteration phenomenon, although it has been suggested (Loomis, 1972) that similar alteration occurs due to the final release of water during the cordierite-K-feldspar forming reaction.

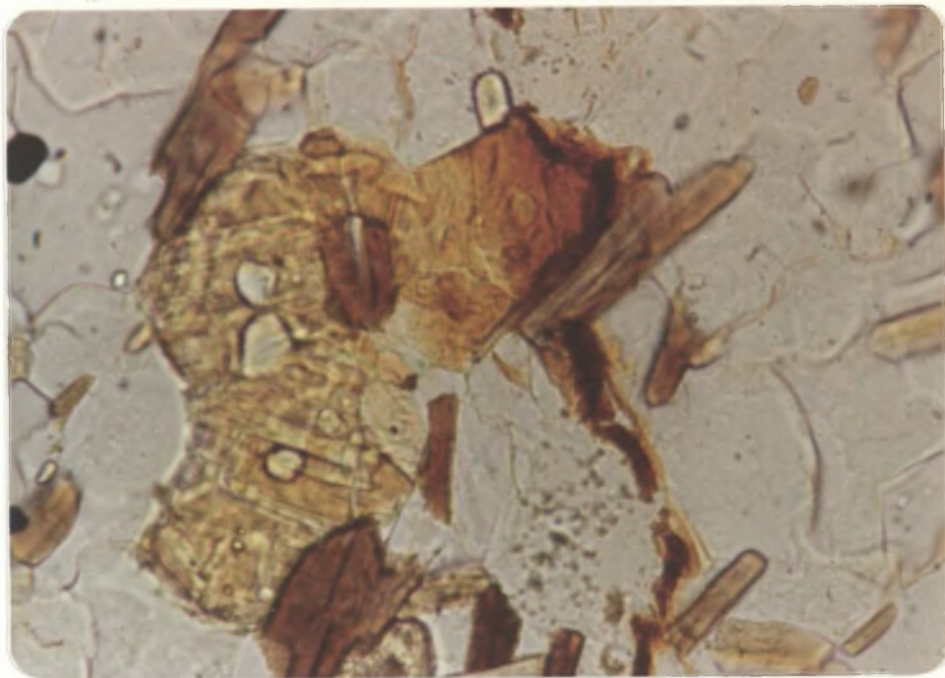


Plate 12; MU4353, Pinitisation of cordierite adjacent to a minor fracture.
x 260

A second type of cordierite alteration is due to ingress of potassium by hydrothermal solutions from the intrusion. It must be noted that this type of

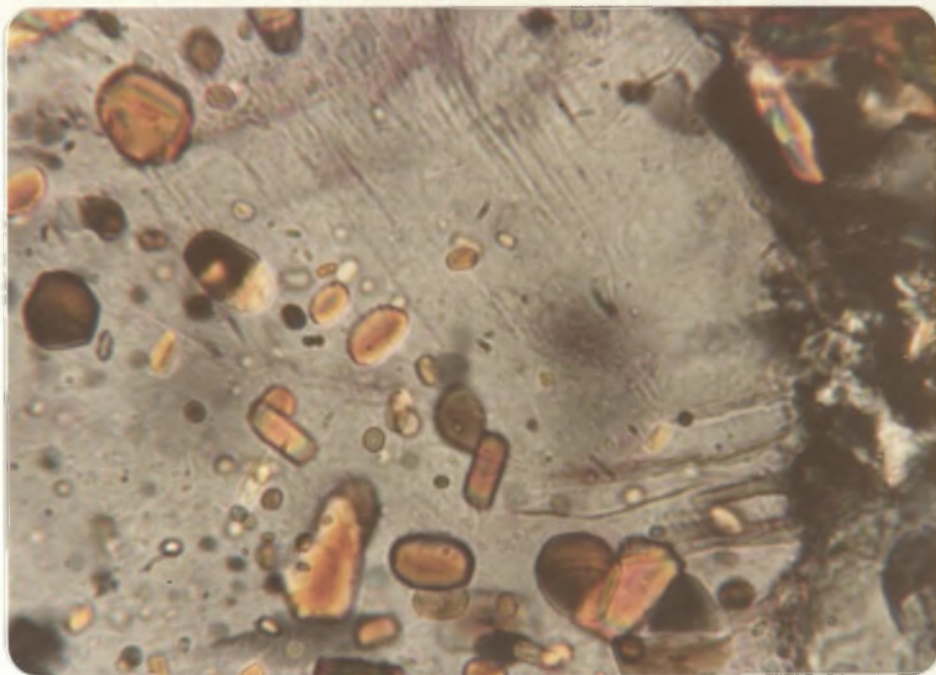


Plate 13: MU4383, Chlorite replacing cordierite.
Note its apparent nucleation at cordierite
grain boundaries.
x 520 (crossed nicols)

alteration is not widespread, and appears to be restricted to within 200-250 metres of the contact. It is suggested that alteration proceeds as potassium bearing solutions move outwards from the intrusion along microscopic fractures, the alteration occurring adjacent to these fractures. Analyses of these altered rocks show a dramatic increase in K_2O and B, and noticeable increases in Rb, Sr and Pb.

An earlier introduction of Si and B is represented by quartz tourmaline veins and pegmatites which have been contorted and buckled subsequent to their injection into the thermal metamorphic schists. This buckling of the veins and pegmatites is most

probably due to the further intrusion of the adamellite. It is thought that this earlier introduction of material had no effect on the cordierite.

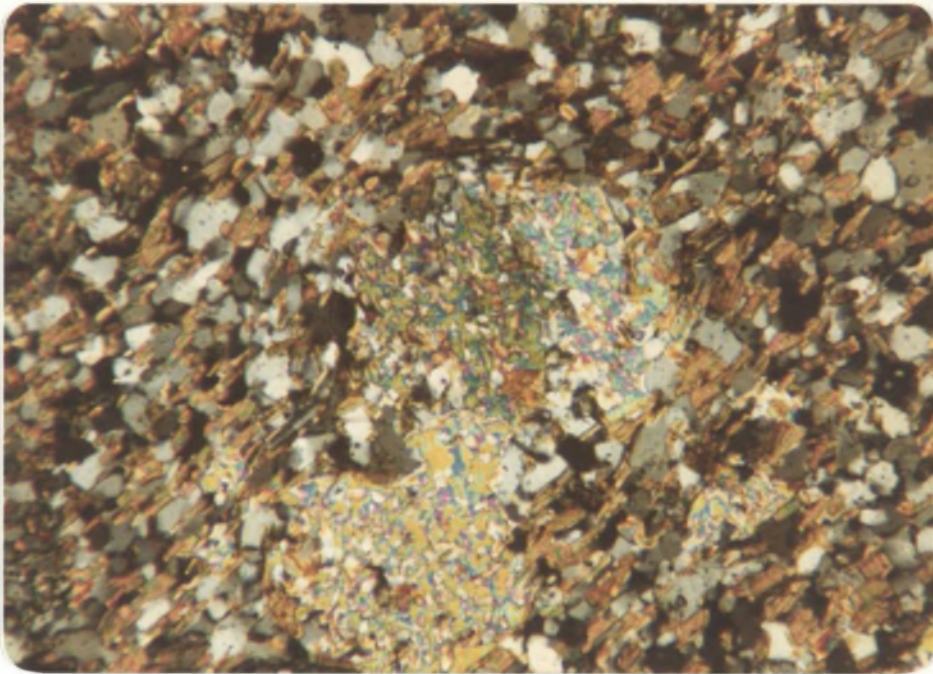


Plate 14: MU4437, Replacement of cordierite by muscovite
x 104 (crossed nicols)

(c) Almandine Garnet

Almandine forms xenoblastic to subidioblastic grains, and occurs up to 250 metres from the contact in graphitic schists. It generally nucleates in close proximity to the Fe rich cordierite that is present, and often it is found replacing this cordierite. Analyses of almandine garnet from sample MU4435 can be found in Table 17. A more detailed description of almandine and the cordierite-almandine zone is presented in the following chapter.

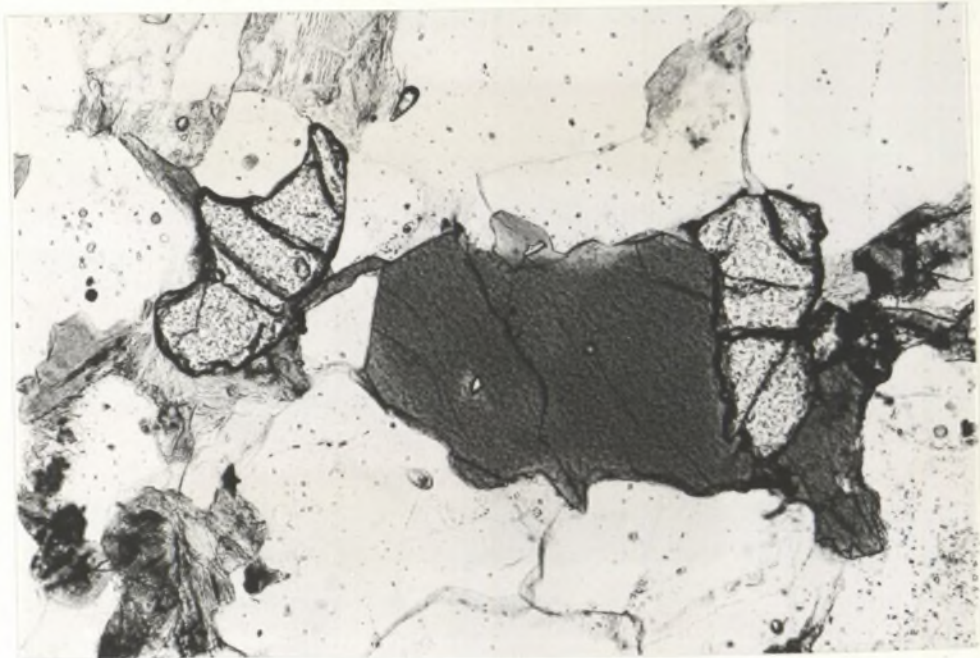


Plate 15: MU4471, Garnet from the cordierite-K-feldspar
zone.
x 104

(d) Quartz

Relict grains of sub-rounded quartz (av. 0.30mm) derived from a volcanic source (Folk, 1968) exhibit straight extinction in the outer zones, except where local shearing has strained the quartz, inducing an undulose extinction (MU4491). In the inner zones, extinction becomes undulose as the contact is approached, and many grains are recrystallised to form strain free aggregates. Metamorphic quartz forms a finely granular mosaic and is commonly oriented along the schistosity. In the cordierite, cordierite-almandine and cordierite-K-feldspar zones the quartz generally carries inclusions of biotite and minor apatite and ilmenite. The biotite is circular in basal sections but longitudinal crystals develop (001) with rounded ends (Vernon, 1968).

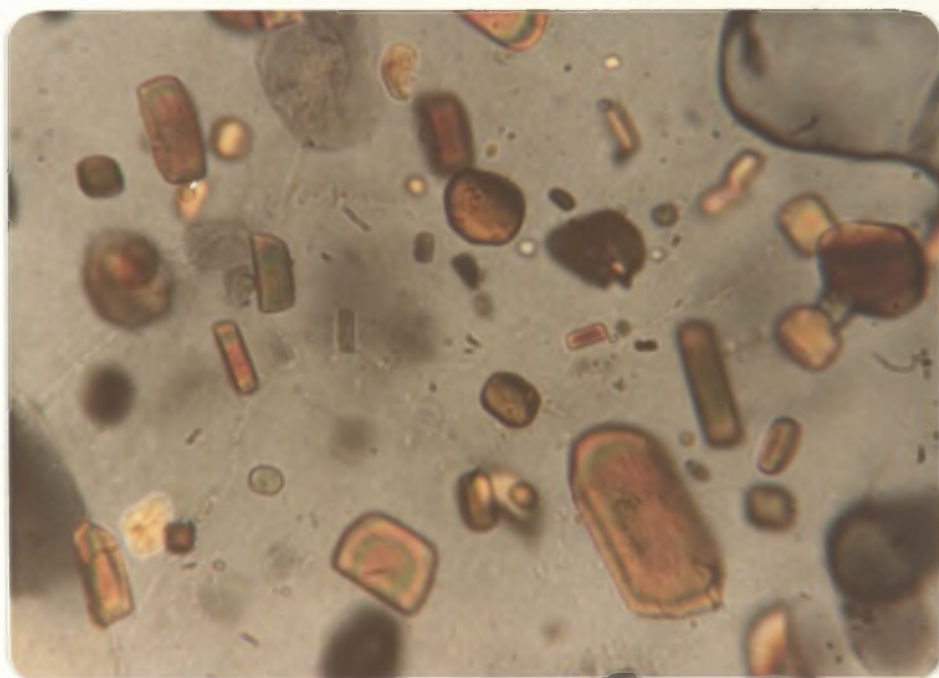


Plate 16: MU4471, Inclusions of biotite and minor apatite(?) in quartz.
x 520 (crossed nicols)

(e) Chlorite

Chlorite occurs in the study area as a primary and as a retrogressive phase. The latter phase occurs as an alteration product of primarily cordierite and biotite. The secondary chlorite, when replacing biotite occurs as ragged, green pleochroic grains with anomalous blue bi-refringence. When replacing cordierite the chlorite is only slightly pleochroic and usually does not exhibit anomalous bi-refringence.

Primary chlorite of the corundophilite-thuringite association is stable in the cordierite and outer zones, and also appears to be stable in the cordierite-almandine zone. The stability of chlorite at higher grades is dependent on the presence of graphite, for primary chlorite is not present in the coarser grained graphite free schists of the cordierite and cordierite-almandine zones.

The primary chlorite occurs as very small pale green flakes in the groundmass of the schists. There is a definite tendency to lower chlorite modal percentages at higher grades (Table 19), but from the limited data available it appears that there is little compositional dependence on grade. As with biotite and cordierite, the composition of the chlorite depends on the whole rock chemistry and the associated mineral phases. Table 12 gives the analyses of two chlorites from the aureole region.

(f) Phengite

Phengite (Table 13) occurs as very small, pale green grains in the groundmass of the fine grained graphite bearing schists. Table 20 shows that phengite co-

TABLE 12

CHEMICAL ANALYSES OF CHLORITES

	1	2
SiO ₂	29.20	23.39
Al ₂ O ₃	21.30	23.28
FeO*	23.58	26.88
MnO	0.16	0.12
MgO	11.67	12.34
CaO	0.13	-
Na ₂ O	0.25	0.30
K ₂ O	0.10	0.07
Total	86.39	86.38

Numbers of Ions on the Basis of 28(O)

Si	6.1129	-8.0000	5.0654	-8.0000
Al	1.8871		2.9346	
Al	3.3684		3.0086	
Fe ²⁺	4.1266		4.8704	
Mn	0.0293		0.0231	
Mg	3.6403	-11.3244	3.9867	-12.0360
Ca	0.0290		-	
Na	0.1037		0.1274	
K	0.0271		0.0198	

* Total iron as FeO

Analyst: S. Dobos

1. Corundophilite-Thuringite from sample MU4466, located approximately 740 metres from the contact.
2. Corundophilite-Thuringite from sample MU4435, located approximately 250 metres from the contact.

exists stably with chlorite well into the cordierite zone, however, it must be remembered that in the Walcha Road area, the pair phengite-chlorite are only stable together (or only occur together) in the fine grained graphitic schists. In the coarser grained graphite free schists and the coarser grained graphite poor schists, phengite does not occur with chlorite.

Detrital K-feldspar is associated with chlorite (e.g. MU4397) in the phengite-free, coarser grained schists, but is not observed in the fine grained phengite bearing graphitic schists. The implications of this, with reference to the genesis of biotite are discussed in Part Two.

(g) Muscovite

Three muscovite types showing different textural relations occur in the Walcha Road area; these are:

- (i) Secondary muscovite which replaced cordierite and K-feldspar (Plate 17) in the cordierite-K-feldspar zone, in the post magmatic retrogressive stage when a transfer of material from the intrusive body, resulted in the muscovitisation of the earlier formed hornfelses and schists. An analysis of this type of muscovite is shown in Table 13 (MU4383). Muscovite also replaces andalusite in the andalusite zone.
- (ii) Fabric forming muscovite occurs as very small flakes in the groundmass of the meta-pelites in the biotite, andalusite and cordierite zones. It takes on the same preferred orientation as the biotite and chlorite.

TABLE 13

CHEMICAL ANALYSES OF WHITE MICAS

	1	2
SiO ₂	45.36	56.81
TiO ₂	-	0.28
Al ₂ O ₃	36.40	26.16
FeO*	1.04	1.37
MgO	0.53	1.12
CaO	-	0.16
Na ₂ O	0.63	0.70
K ₂ O	10.03	6.90
Total	93.99	93.50

Number of Ions on the Basis of 22(0)

Si	6.0942	-8.0000	7.4248	-8.0000
Al	1.9058		0.5752	
Al	3.8587		3.4536	
Ti	-		0.0273	
Fe ²⁺	0.1175	-4.0825	0.1492	-3.8475
Mg	0.1063		0.2174	
Ca	-		0.0220	
Na	0.1630	-1.8815	0.1773	-1.3494
K	1.7185		1.1501	

* Total iron as FeO

Analyst: S. Dobos

1. Muscovite from sample MU4383, located approximately 2 metres from the contact.
2. Phengitic muscovite from sample MU4466, located approximately 740 metres from the contact.

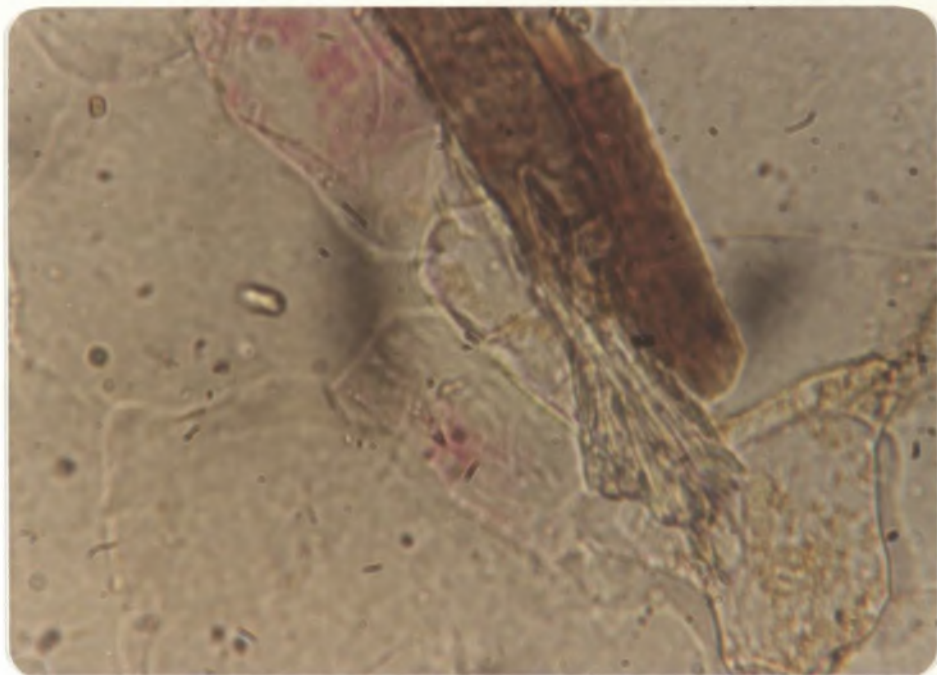


Plate 17: MU4471, Muscovite nucleating in biotite and replacing K-feldspar (stained)
x 520

- (iii) Post tectonic, porphyroblastic muscovite (Plate 18) is found only in the andalusite zone, and is distinct from muscovite that replaces andalusite in that it is poikiloblastic and contains inclusions and "trails" of biotite and graphite. Muscovite that replaces andalusite is free of inclusions and usually retains the shape of the original andalusite.

The modal percent of muscovite increases rapidly as the andalusite zone is entered, and decreases rapidly as the cordierite zone is entered. Table 19 showing modal

analyses of the schists from the different zones verifies this. No muscovite was observed in the rocks of the regional greenschist facies, the only white mica present in these rocks being phengite.

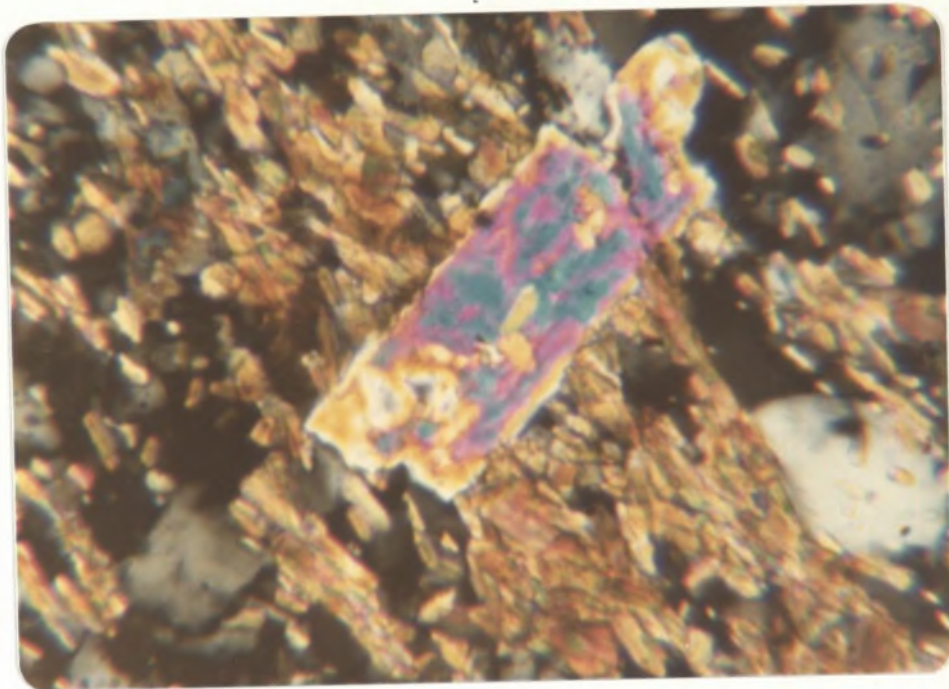


Plate 18: MU4492, Porphyroblastic muscovite from the andalusite zone.
x 415 (crossed nicols)

(h) Plagioclase

Plagioclase in the pelitic schists occurs as part of the groundmass or as rare relict plagioclase grains. The relict grains are recognised by their larger size, usual sub-rounded nature and strongly altered appearance. The groundmass plagioclase decreases modally and becomes more calcic as the contact is approached.

TABLE 14

PLAGIOCLASE FELDSPAR ANALYSES

	1	2
SiO ₂	60.29	63.53
Al ₂ O ₃	25.04	22.93
FeO*	0.15	-
MgO	0.39	0.50
CaO	6.49	3.09
Na ₂ O	7.51	9.24
K ₂ O	0.13	0.44
Total	100.00	99.73

Number of Ions on the Basis of 32(0)

Si	10.7257	11.2386
Al	5.2497	4.7801
Fe ²⁺	0.0220	-
Mg	0.1040	0.1323
Na	2.5905	3.1690
Ca	1.2380	0.5859
K	0.0291	0.0993

MOL % AL - 67.15
AN - 32.09
OR - 0.76

MOL % AL - 83.3
AN - 14.4
OR - 2.3

* FeO = total iron

1. Analyst: R.H. Flood

2. Analyst: S. Dobos

1. MU4435, 250 metres from contact.

2. MU4466, 740 metres from contact.

Outer cordierite zone *	An ₁₄
Inner cordierite zone +	An ₂₃
Cordierite-almandine zone *	An ₃₂
Cordierite-K-feldspar zone +	An ₃₅

* Probe result shown in Table

+ Plagioclase An determined optically.

(i) K-Feldspar

K-feldspar occurs as detrital grains found in the regionally metamorphosed rocks and biotite zone rocks, as a stable mineral phase in the cordierite-K-feldspar zone and as rare myrmekitic intergrowths associated with plagioclase and found in rocks at distances of no greater than ten metres from the contact. It is readily recognised after staining with sodium cobaltinitrite.

In the cordierite-K-feldspar zone it forms xenoblastic grains, which sometimes carry inclusions of quartz. The K-feldspar has formed from the breakdown of biotite at the cordierite-K-feldspar isograd.

(j) Andalusite

Andalusite occurs as idioblastic grains (av. 0.6mm), being found only in rocks of the andalusite zone. Closer to the contact, andalusite reacts with biotite to form cordierite (Part Two). The andalusite usually contains fine graphitic inclusions towards the centre of the porphyroblast, the outer sections being free from inclusions. The andalusite in thin section is easily distinguished from cordierite by its idioblastic shape and high relief.

(k) Graphite

Graphite occurs throughout the aureole region as dispersed opaque matter throughout the lower grade schists, and as euhedral grains in the higher grade schists. As a consequence of the presence of graphite in these schists, the Co_2 partial pressure makes up a considerable portion of the total pressure (Muller and Schneider, 1971). The buffering capacity of graphite with increasing metamorphic grade thus stabilises minerals whose existence depends on a low oxygen fugacity (almandine).

(l) Sulphides

Pyrrhotite is ubiquitous in the graphite bearing schists of the aureole region. It occurs (with minor pyrite) in the biotite and andalusite zones as sub-globular poikiloblastic grains (av. 0.04mm) which show marked anisotropism. Closer to the contact the pyrrhotite occurs as inclusion free, globular grains, that, in most cases have chalcopyrite exsolved from them. The non graphite bearing schists contain rare pyrite, no pyrrhotite being observed.

(m) Oxides

Ilmenite occurs as a minor accessory throughout the entire aureole, and is associated with iron sulphides in the graphite bearing schists, and with rare magnetite in the non graphite bearing schists. The absence of magnetite in the graphite bearing schists of the aureole has been attributed to a low oxygen activity in these rocks, due to the buffering effect on the graphite.

TABLE 15

CHEMICAL ANALYSIS OF AN ILMENITE
FROM OUTER CORDIERITE ZONE (MU4466)

SiO ₂	1.11
TiO ₂	53.04
Al ₂ O ₃	0.69
FeO*	43.24
MnO	1.82
K ₂ O	0.10
Total	100.00

Number of Ions on the Basis of 6(0)

Al	0.0408	
Ti	1.9778	
Fe ²⁺	1.7928] - 1.8754
Mn	0.0766	
K	0.0060	

* Total iron as FeO

Analyst: S. Dobos.

(n) Accessories

Detrital zircon and tourmaline are ubiquitous. It is noted that tourmaline in the outer zones is a blue colour, while tourmaline close to the contact (400 metres) is an olive green in colour. A marked increase in the modal percent of tourmaline is also noted as the contact is approached, and some rocks of the cordierite-K-feldspar zone contain up to 2% by volume of tourmaline. This increase in tourmaline is interpreted as being due to the infiltration of B (and K) bearing fluids into the rocks immediately adjacent to the contact. Further evidence suggesting this introduction of material can be seen both macroscopically (quartz-tourmaline pegmatites) and microscopically (potassium alteration of cordierite to muscovite with associated increases in tourmaline).

The dominant opaque assemblage (in the graphite bearing schists) is graphite-pyrrhotite-ilmenite, and some detrital rutile is present at low grades. Table 15 presents an analyses of an ilmenite from the outer cordierite zone.

-65-

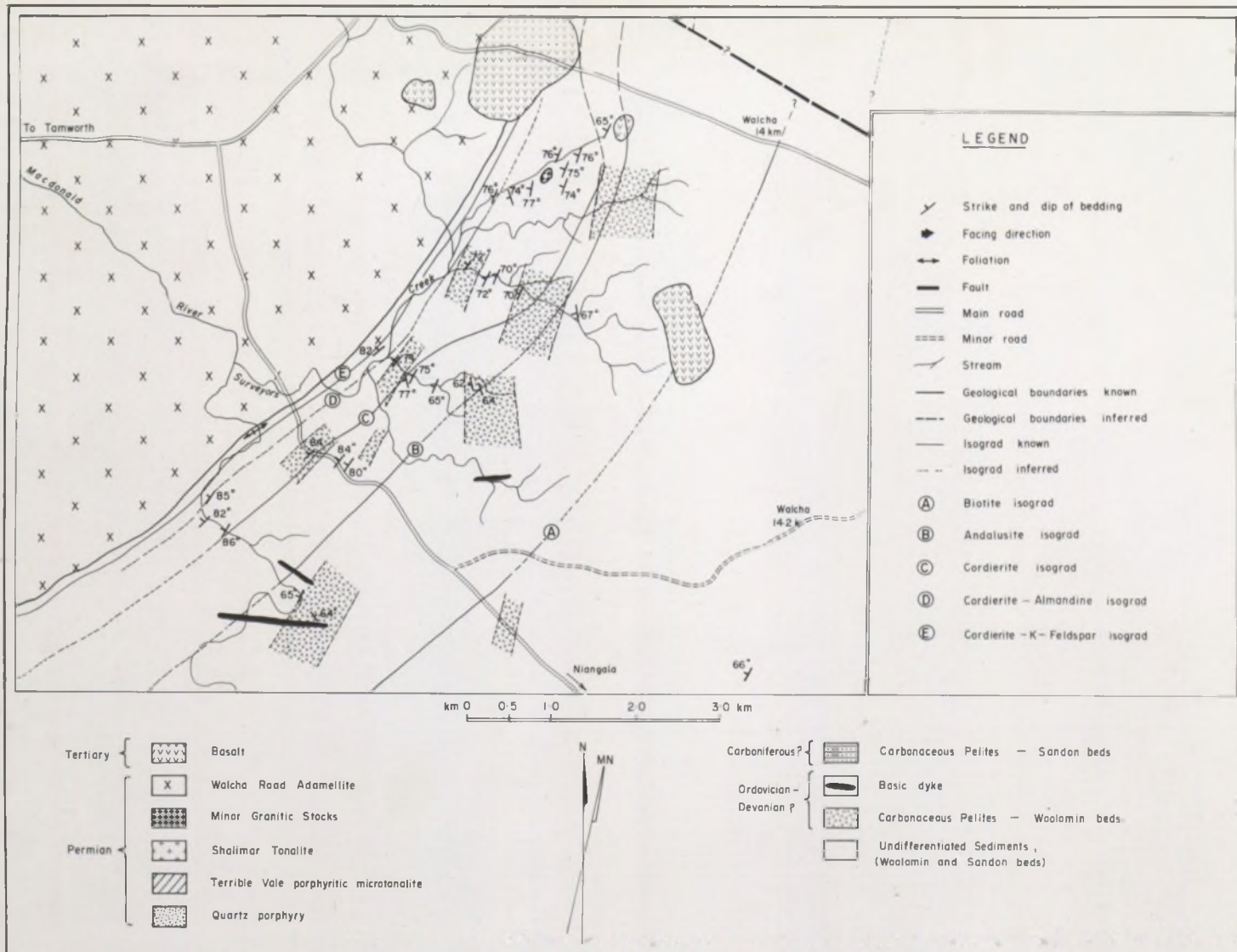


Fig. 1.

7. METAMORPHIC ZONES

Assemblage descriptions used in this chapter will be understood to include quartz and plagioclase.

(a) Cordierite-K-Feldspar Zone

(i) Assemblages

Biotite-cordierite-K-feldspar (MU4358)

Biotite-cordierite-K-feldspar-almandine (MU4472)

Cordierite-biotite-minor K-feldspar (MU4383)

Cummingtonite-brown/green hornblende (MU4384)

Diopside-brown/green hornblende-scapolite-K-feldspar (MU4455)

Tan hornblende * (Flood, 1971)

* The writer has observed tan hornblende in basic hornfelses adjacent to the western contact of the Walcha Road Adamellite.

(ii) Description

The development of metamorphic K-feldspar within the Walcha Road aureole is restricted to within 100 metres of the contact (\pm 10 metres). In hand specimen, the rocks from this zone take on a "gneissic" appearance and are much lighter in colour than rocks from the outer zones. In thin section there is a noticeable decrease in modal percent biotite (Table 19; Plates 29, 30 and 31) and a rough segregation of minerals into bands. This segregation of minerals has been interpreted

as being due to metamorphic differentiation. The banded appearance of rocks from this zone (Plate 19) coupled with their lighter colour (lower mafic index) make field identification rather straightforward, especially within 50-60 metres of the contact.



Plate 19: Banded appearance of hornfels from inner cordierite-K-feldspar zone, Macdonald River area.

Minerals present exhibit a preferred orientation, this fabric is interpreted as the result of the intruding adamellite. Porphyroblasts of K-feldspar, cordierite and quartz are xenoblastic but associated plagioclase ($An_{32}-An_{36}$) is usually sub-idioblastic. Cordierite, K-feldspar and quartz porphyroblasts are poikiloblastic (Plates 9, 10 and 16), the included material usually being rounded or sub-rounded (see previous chapter). There is a noticeable decrease in the number of inclusions in porphyroblasts of the cordierite-K-feldspar zone, and also a marked difference in the habit of this included material, compared to the outer zones (see Plates 11 and 25),

The cordierite-K-feldspar zone is also characterised by an abundance of quartz-tourmaline pegmatites and veins, which have been contorted and buckled subsequent to their introduction into the contact metamorphosed pelitic rocks. The buckling of these veins and pegmatites is due to further intrusion by the adamellite. An increase of tourmaline as disseminated grains throughout the rocks of this zone is also apparent.

K-feldspar is the last mineral to develop in the Walcha Road aureole (Table 16), no sillimanite being observed. The significance of the cordierite-K-feldspar zone is discussed in the following chapter.

TABLE 16

New Minerals	Time	Space
Biotite	Earliest	Outer aureole
Muscovite	↓	↓
Andalusite		
Cordierite		
Almandine	↓	↓
K-feldspar	Latest	Inner aureole

(Late stage, post magmatic muscovite replaces cordierite and K-feldspar in some areas.)

Mineral Development in the Walcha Road Aureole

(b) The Cordierite-Almandine Zone

(i) Assemblages

Biotite-cordierite-almandine-graphite

Biotite-cordierite

Biotite-green hornblende

Green hornblende-diopside

Green hornblende

(ii) Description of Pelitic Assemblages

The cordierite-almandine isograd has been accurately located at approximately 250 metres (± 20 m) from the contact. In hand specimen, the almandine bearing rocks have a purplish colour and appear to be a true hornfels, with no directed fabric. In thin section, the metamorphic foliation is quite obvious (Plate being produced by the red-brown biotite. Only in thin section can the cordierite and garnet be observed.

The slightly zoned garnet (Table 17) attains an average size of approximately 0.18mm and is less poikiloblastic than the associated cordierite (average size 0.32mm). Inclusions within the garnet consist of biotite, quartz and pyrrhotite, the latter being a minor phase. The associated iron rich cordierite (high 2V, optically negative) is highly poikiloblastic, included material being mainly quartz and pyrrhotite with minor biotite.

The formation of cordierite occurred post the S_1 cleavage, but pre the flattening, which was induced by the intruding granite. This is borne out in thin section by the biotite folia wrapping the

TABLE 17

GARNET ANALYSES

	1	2	3	4
SiO ₂	36.18	36.25	35.99	35.97
TiO ₂	0.17	0.12	0.12	-
Al ₂ O ₃	20.91	20.85	20.75	20.98
FeO*	35.03	35.24	35.43	35.56
MnO	3.40	3.40	3.66	3.60
MgO	3.06	3.04	2.72	2.75
CaO	1.25	1.10	1.22	1.13
Cr ₂ O ₃	-	-	0.11	-
Total	100.00	100.00	100.00	99.99

Number of Ions on the Basis of 24(O)

Si	5.8658	5.8810	5.8598	5.8540
Al	0.1344	0.1190	0.1402	0.1460
Al	3.8598	3.8680	3.8400	3.8778
Ti	0.0208	0.0150	0.0152	-
Fe ²⁺	-	-	-	-
Cr	-	-	0.0144	-
Mg	0.7410	0.7340	0.6612	0.6666
Fe ²⁺	4.7498	4.7798	4.8230	4.8396
Al	0.4670	0.4676	0.5050	0.4968
Ca	0.2158	0.1914	0.2132	0.1982

Mg/Mg + Fe	13.5	13.3	12.1	12.1
Almandine	76.94	77.43	77.76	78.04
Grossular	3.50	3.10	3.44	3.20
Pyrope	12.00	11.89	10.66	10.75
Spessartine	7.56	7.58	8.14	8.01

1. MU4435, probe analysis⁺ of centre of garnet.
2. MU4435, probe analysis⁺ of centre of garnet.
3. MU4435, probe analysis⁺ of rim of garnet.
4. MU4435, probe analysis⁺ of opposite rim of garnet.

+ All analyses recalculated to 100% dry

* Total iron as FeO

+ Analyst: R.H. Flood

Analyses 1-4 from one garnet

Garnet Analyses (cont.)

	5	6
SiO ₂	36.00	36.53
TiO ₂	0.18	-
Al ₂ O ₃	20.85	20.97
FeO	35.19	35.07
MnO	3.36	3.64
MgO	3.17	2.63
CaO	1.25	1.16
Cr ₂ O ₃	-	-
Total	100.00	100.00

Number of Ions on the Basis of 24(0)

Si	5.8498	-6.0000	5.9235	-6.0000
Al	0.1502		0.0764	
Al	3.8428		3.9324	
Ti	0.0218	-3.8646	-	-3.9324
Fe ³⁺	-		-	
Cr	-		-	
Mg	0.7682		0.6350	
Fe ²⁺	4.7818	-6.2304	4.7570	-5.9798
Mn	0.4622		0.5006	
Ca	0.2182		0.0872	

Mg/Mg + Fe	13.8	11.8
Almandine	76.75	79.55
Grossular	3.50	1.46
Pyrope	12.33	10.62
Spessartine	7.42	8.37

5. MU4435, probe analysis of centre of garnet.

6. MU4435, probe analysis of rim of same garnet.

cordierite porphyroblasts. Textural evidence indicates the post cordierite (post-tectonic) nature of the garnet which grows across pre-existing micro-structures and mineral phases. The tendency for the almandine garnet to nucleate close to the iron rich cordierite, can be explained by the fact that almandine garnet will enter the system in a sliding reaction involving the breakdown of iron cordierite (Hensen and Green, 1970). The biotite and cordierite associated with the almandine garnet schists are slightly more Mg rich than biotite-cordierite pairs from other zones (Figure 8) which are not associated with almandine garnet. This is due to the removal of iron from the system during the formation of the almandine garnet.



Plate 20: Biotite-Cordierite-Almandine Schist
xl04

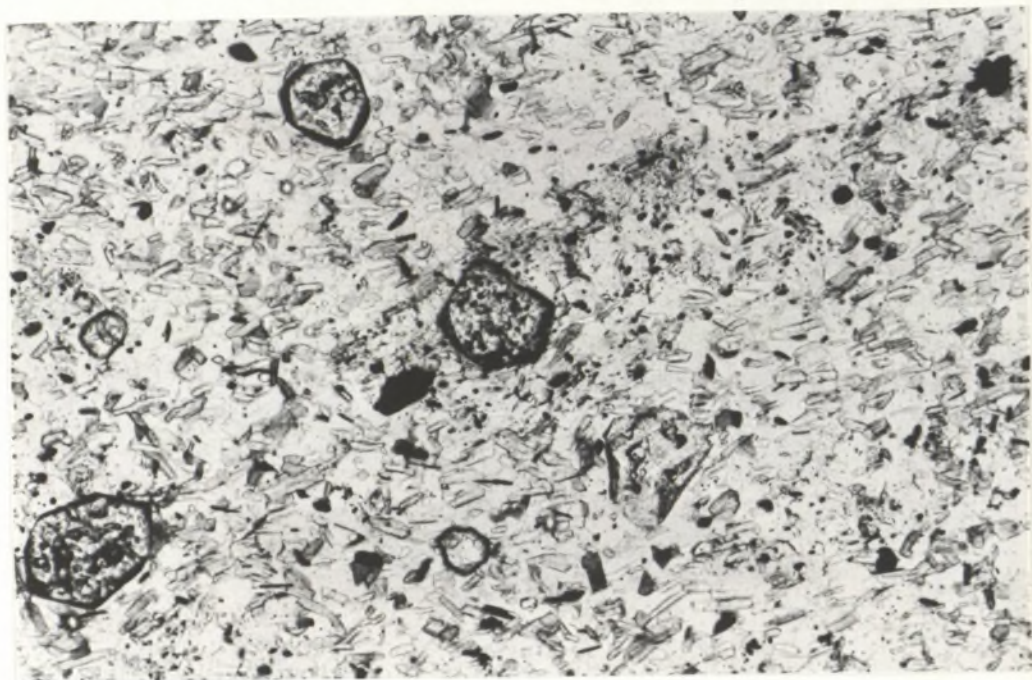


Plate 21: MU4435, Almandine garnet nucleating in
Fe rich cordierite
x 104

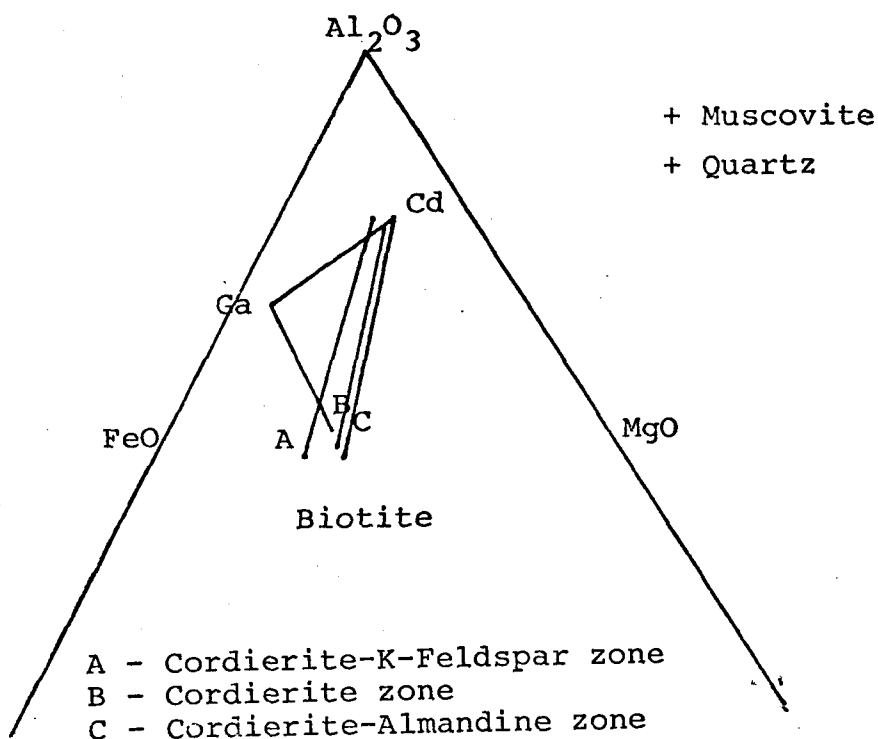


Figure 8: Mineral Compositions from Cordierite, Cordierite-Almandine and Cordierite-K-Feldspar Zones Plotted on a Thompson Projection

The role of almandine in low pressure metamorphism, once considered an anomaly, is now well documented (Chinner, 1960, 1962; Okrusch, 1971; Muller and Schneider, 1971; Seki, 1957; Stewart, 1942). Chinner explained the relative rarity of almandine in the contact metamorphic environment as a reflection of the overall tendency towards the relatively rare occurrence amongst the original pelitic sediments of rocks of appropriate

composition. He (Chinner) also states that cordierite and biotite associated with almandine garnet have higher FeO/MgO ratios than cordierite and biotite existing together without garnet. However, this is not the case in the Walcha Road area. Table 18 demonstrates that the cordierite and biotite associated with almandine have lower FeO/MgO ratios than cordierite-biotite pairs which are not associated with almandine. Rock composition is therefore not a critical factor in the formation of almandine, at least in the Walcha Road area.

Table 18

	Garnet		Cordierites		Biotites		
	A	A	B	C	A	B	C
SiO ₂	36.15	48.41	48.03	48.07	35.26	35.65	34.05
Al ₂ O ₃	20.89	33.13	32.64	33.05	18.67	19.97	20.72
TiO ₂	0.09	-	-	-	2.72	1.48	2.98
FeO*	35.25	10.05	10.58	11.81	21.92	21.50	21.91
MnO	3.51	0.28	0.27	0.23	-	-	-
MgO	2.90	7.60	7.19	6.30	8.60	7.83	5.92
CaO	1.17	-	-	-	-	0.09	-
Na ₂ O	-	0.48	0.43	0.46	-	0.17	0.28
K ₂ O	-	0.05	0.86	0.08	8.30	8.22	8.58
Cr ₂ O ₃	0.01	-	-	-	0.23	-	-
Total	99.97	100.00	100.00	100.00	95.70	94.91	94.44
FeO/MgO	6.83	0.74	0.83	1.05	1.43	1.47	2.08

* Total Iron as FeO

Garnet (A) is the average of six analyses from MU4435

A = MU4435, biotite-cordierite-almandine schist

B = MU4466, biotite-cordierite schist

C = MU4383, cordierite-biotite-K-feldspar schist

Many workers (Tilley, 1926; Miyashiro and Shido, 1973; Muller and Schneider, 1971) place an emphasis on the MnO content of the garnet and also the MnO content of garnets found at lower grades. It is suggested by some workers (Miyashiro and Shido, 1973) that garnets of the regional metamorphic episode, being essentially Mn rich, act as nucleation sites for the formation of the almandine in the aureole. Tilley (1926) has even suggested that only garnet, essentially enriched in the spessartine molecule, may be stable in the metapelitic hornfels. The common occurrence of spessartine rich garnet in the thermal aureoles of other regions is explained as a result of the wider stability field of spessartine relative to almandine (Hsu, 1968) and also that original compositions of the metamorphosed rocks were possibly more Mn rich.

At Walcha Road there are no garnets in any zone other than the cordierite-almandine zone. The almandine bearing rocks are relatively Mn poor (0.11%), however, most of this Mn is present in the garnet.

	Garnet	Biotite	Cordierite	Chlorite
Wt% MnO	3.51	<0.02	0.19	0.12

Compared to the host rock, Mn in the garnet is enriched by a factor of 32. For iron the factor is only 6.

Manganese enrichment of this order from the rocks of the Stavanger region, Norway, suggested to Muller and Schneider (1971) that garnet crystallisation may start at points of local Mn concentrations in the sediments. Stewart (1942) when discussing rocks from the Sparcraigs area, north of Aberdeen in Scotland, noted that whole rock Mn contents were very low and that the almandine garnet associated with these rocks also had relatively low Mn contents. Stewart considered that other factors had played an important part in promoting the formation of almandine garnet in this particular area. It is suggested that the rather high Mn enrichment factor in the garnet at Walcha Road is only due to the fact that there has been strong partitioning of Mn into the garnet during its formation. The garnet at Walcha Road is slightly zoned, and becomes more Mn and Fe rich toward the rim. There is also a depletion in the Mg component toward the rim.

Recent publications (Okrusch, 1971; Muller and Schneider, 1971; Hsu, 1968) have stressed the importance of oxygen fugacity (fO_2) in the formation of almandine garnet. Theoretical considerations (French, 1966) reveal the influence of graphite on the partial pressure of oxygen as related to the important parameters of metamorphism. Therefore, the buffering capacity of graphite stabilises minerals whose existence depends on low fO_2 . Almandine is one of these minerals (Hsu, 1968).

(iii) The Formation of Almandine Garnet at Walcha Road

Only graphitic rocks that occur less than approximately 250 metres from the contact contain almandine. A typical example of rocks from this zone can be found approximately 1km south of the Oxley Highway in Surveyors Creek. Here, intercalated graphitic and non graphitic rocks with similar FeO/MgO ratios contain the assemblages, biotite-cordierite-almandine-graphite and biotite-cordierite, respectively. This suggests a lowering of the PH_2O in the graphite bearing rocks with a concomitant increase in PCo_2 , allowing almandine to form. It also implies marked differences in the oxygen fugacity ($f\text{O}_2$) over areas of a few metres or less. Chinner (1960) states that graphite has control on the activity of oxygen (A_{O}). When applying Chinner's oxidation ratio, i.e.

$$\text{Oxidation Ratio} = \frac{\text{Mol } 2\text{Fe}_2\text{O}_3 \times 100}{2\text{Fe}_2\text{O}_3 + \text{FeO}}$$

to the graphite bearing almandine schists, it is noted that they have oxidation ratios (7.2-8.1) considerably lower than the associated non graphitic schists (average 18). (These ratios are still much lower than discussed by Chinner, 1960.)

The absence of magnetite and the presence of pyrrhotite and chalcopyrite suggest a low $f\text{O}_2$, possibly lower than that defined by the fayalite-magnetite + quartz buffer (Hsu, 1968).

Another feature of these almandine bearing schists is the presence of an Fe chlorite (Corundophilite-Thuringite).

Providing this chlorite is not of secondary origin, then, according to the fO_2 -T diagram of Hsu (1968) (Figure 9) this would place the almandine garnet just to the right of curve A-D (Figure 9). However, the presence of impurities (Mn, Ca, Mg) in the garnet, and the presence of co-existing mineral phases would appreciably lower the temperatures needed to form the almandine that occurs at Walcha Road.

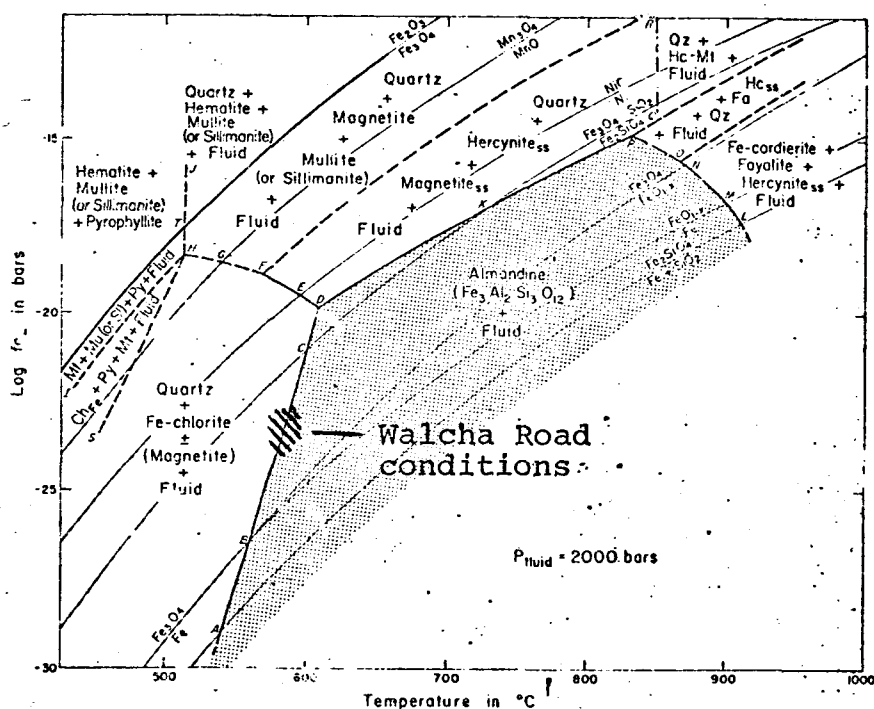


Figure 9: fO_2 -T Diagram for Almandine Bulk Composition + excess H_2O at 2000 bars fluid pressure (Hsu, 1968)

A low fO_2 , therefore, does play an important role in the formation of almandine garnet in the Walcha Road area. The fact that fO_2 is an important parameter in the form-

ation of almandine has been recognised by many workers (Hsu, 1968; Okrusch, 1971; Muller and Schneider, 1971).

The importance of a low fO_2 combined with the right T and P conditions is emphasised by an investigation of pyritic and graphitic hornfels found adjacent to the Way-Way Granite, Yarrahapinni, north of Kempsey, NSW. (A full description of rock types and contact metamorphism is given in Appendix 2.) The hornfels collected from Yarrahapinni are dominantly cordierite-biotite-graphite and higher grade cordierite-biotite-K-feldspar-graphite rocks. No garnet of any type is associated with these hornfels. The lack of magnetite and abundance of pyrite and/or pyrrhotite again suggests a low fO_2 .

The contact metamorphism at Yarrahapinni approaches a high level type situation, with the bulk of the hornfels sitting on top of an underlying granitic body. That we are looking at the top of an intrusion is further evinced by the abundant hydrothermal alteration of stable mineral phases, and the presence of minor molybdenite mineralisation, indicating a release of volatiles from the top of the granitic body.

The garnet free assemblages on top of the intrusion may simply be a reflection of a lower P_{total} during formation of the hornfels. The presence of almandine at Walcha Road suggests, therefore, a slightly higher P_{total} .

(c) The Cordierite Zone

(i) Assemblages

Biotite-cordierite-graphite (minor phengite + chlorite)
(MU4466)

Biotite-cordierite (minor muscovite + chlorite) (MU4430)

Biotite (minor muscovite + chlorite (MU4362)

Blue/green hornblende-biotite (MU4398)

Diopside-green hornblende (MU4487)

Epidote-diopside-calcite (MU4423)

(ii) Description

The cordierite bearing graphitic schists are characterised in hand specimen by their knotted appearance and dark colour. The knots (porphyroblasts) usually stand out as dark patches on weathered surfaces. The cordierite bearing non graphitic schists cannot usually be identified in hand specimen due to their more massive outcrop pattern and lack of knots.

The cordierite isograd occurs at a distance of approximately 0.8km from the contact in graphitic free schists, and can reach a distance of approximately 1.2km in graphite bearing schists. The occurrence of cordierite in graphitic schists at 1.2km from the contact can be given three explanations.

(a) Thermal conductivity: The graphitic schists "absorbed" more heat from the intrusion and possibly held this heat for longer periods than the surrounding non graphitic schists.

(b) An increase in PCo_2 , due to the presence of graphite, would lower the PH_2O . Reactions always try to maintain the correct $\text{H}_2\text{O}:\text{Co}_2$ ratio, so that any departure from this ratio will cause the reaction to proceed at a lower temperature to restore the balance.

(c) The reducing effect of the low $f\text{O}_2$ in these graphitic rocks means more FeO is available for the formation of cordierite.

The writer believes that explanations (b) and (c) adequately solve the problem. It is noted that overall $\text{FeO}/\text{Fe}_2\text{O}_3 + \text{FeO}$ ratios of graphitic schists are higher than associated non graphitic schists in the cordierite zone.

In the outer cordierite zone brown biotite is developed in both the pelitic and the psammitic layers of the graphitic and non graphitic schists. Cordierite forms spongy poikiloblasts (Plate 25) in these schists, and is easily identified in thin section. The micaceous folia wrap these cordierite porphyroblasts and as the contact is approached this wrapping effect increases in severity (Plate 22). All minerals present have a preferred orientation, this orientation being exemplified by the biotite (Plate 23).

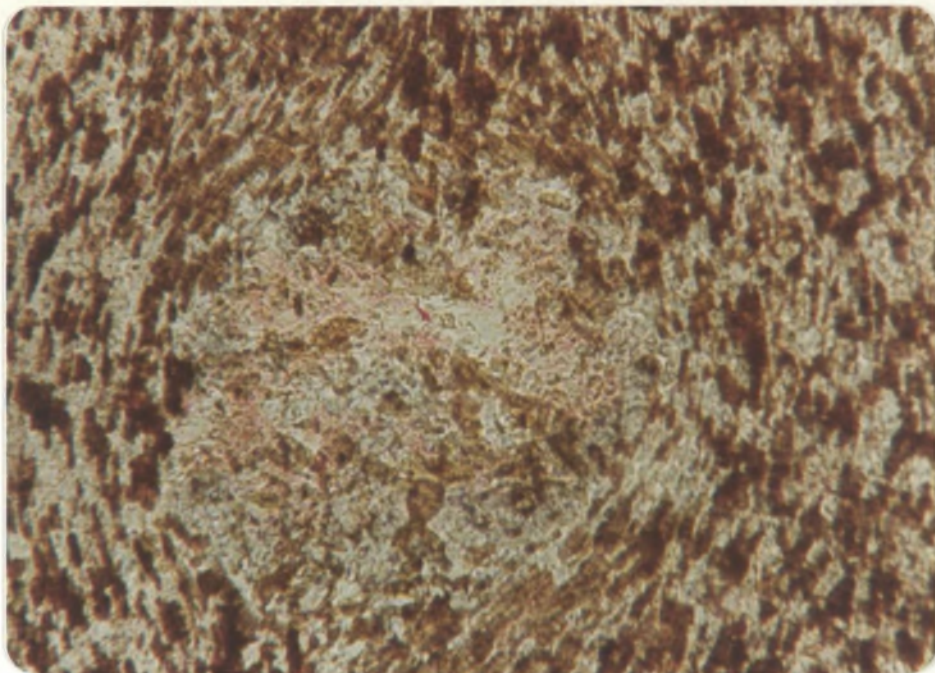


Plate 22: MU4368, Biotite folia wrapping cordierite
porphyroblast (inner cordierite zone)
x 104

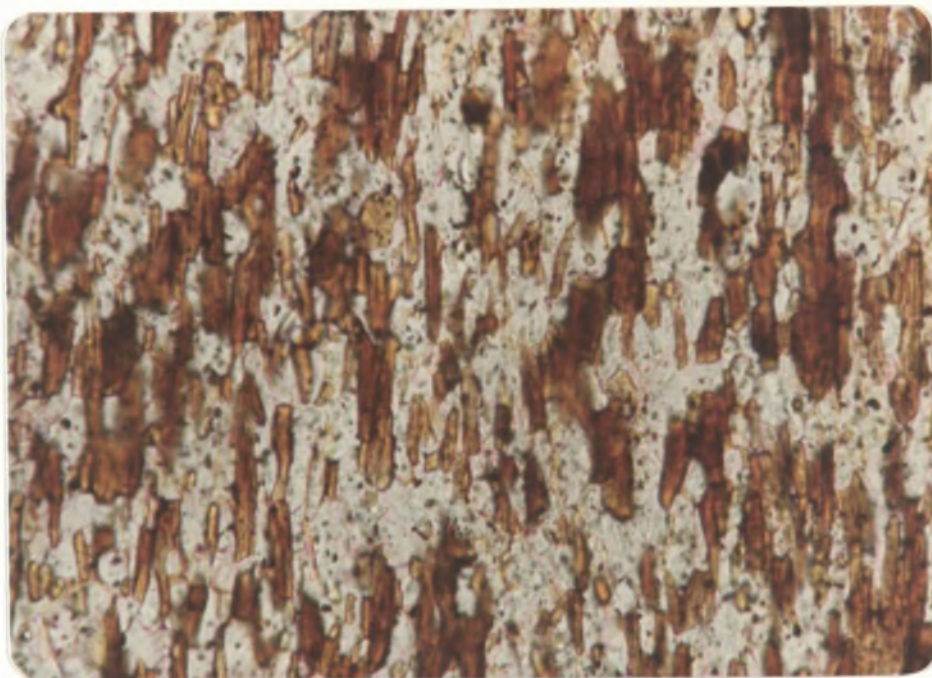


Plate 23: MU4417, Preferred orientation of biotite
from inner cordierite zone
x 260

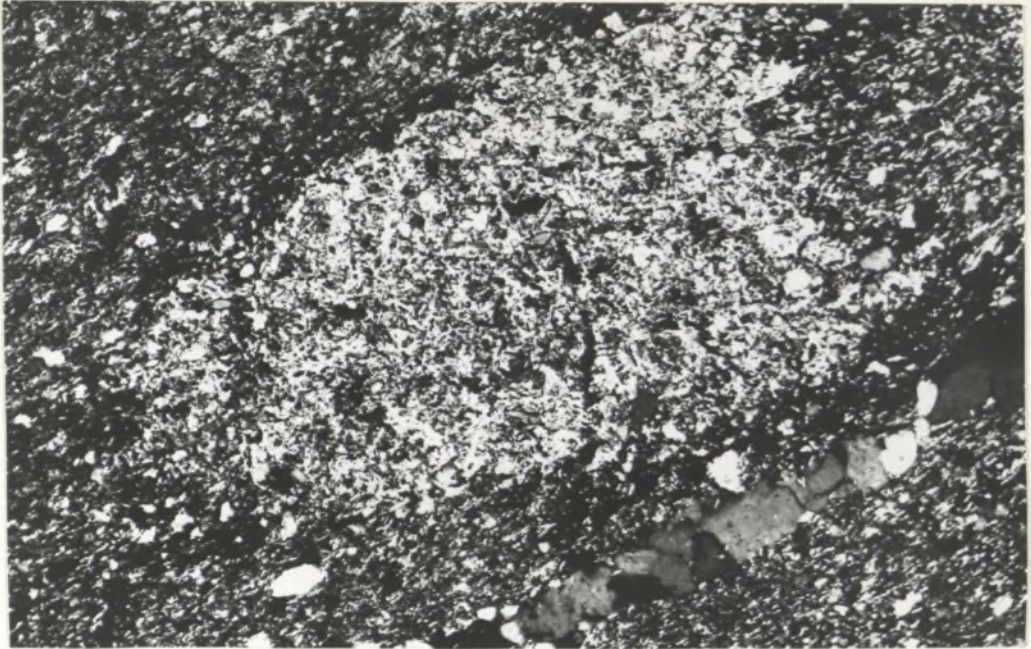


Plate 24: MU4466, Cordierite from outer cordierite
zone
x65 (crossed nicols)

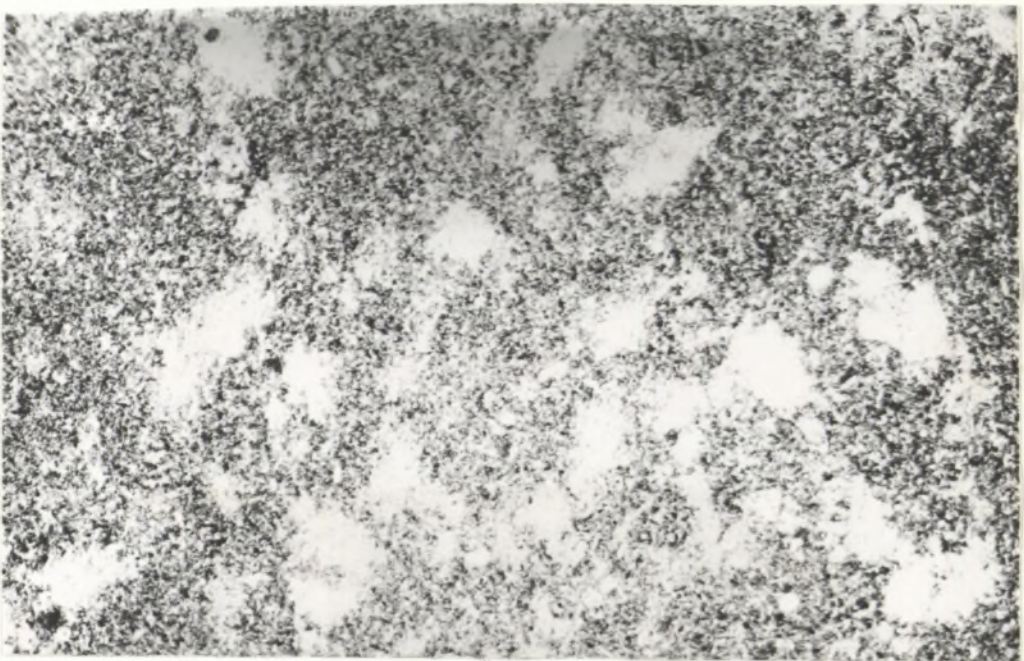


Plate 25: MU4449, Spongy nature of cordierite from the
outer cordierite zone
x 25

(d) Andalusite Zone

(i) Assemblages

Biotite-muscovite-chlorite-andalusite (MU4394)

Biotite-muscovite-chlorite-andalusite-cordierite
(MU4393)

Biotite-muscovite-chlorite (MU4392)

Blue/green hornblende-biotite (MU4534)

(ii) Description

The andalusite schists of the Walcha Road aureole are distinguished from the cordierite schists by their more "gritty" appearance in hand specimen. The schists are usually a dark colour due to the presence of carbonaceous matter. The andalusite isograd is located approximately 1.8 kilometres from the contact. In thin section the andalusite schists are identified by the high modal percent of muscovite that is present (6-12%). The andalusite forms idioblastic grains which are usually found in the coarser, more psammitic layers of the schist. In the pelitic layers there is often a development of cordierite in "knots" (see Part Two) and andalusite is seldom observed associated with these knots. The formation and breakdown of andalusite is discussed in Part Two.

(e) The Biotite Zone

(i) Assemblages

Chlorite-phengite-graphite (MU4500)

Chlorite-phengite-biotite-graphite (MU4465)

Chlorite-K-feldspar (detrital) - biotite (MU4396)

Biotite-chlorite (MU4391)

Biotite-chlorite-muscovite (MU4536)

Biotite-chlorite-muscovite-K-feldspar (detrital) (MU4397)

Blue/green amphibole-chlorite-epidote-calcite-biotite
(MU4489)

(ii) Description

The meta-pelites of the biotite zone are distinguished from meta-pelites of higher grade zones by their lack of "knots". In thin section they are very fine grained, with an S_1 surface usually present in the more graphitic rocks. The increase in metamorphic grade generally produces a darker colour, but colour variation is not a reliable indicator of grade. In the outer biotite zone, small (0.02mm) green coloured grains occur, but these quickly give way to brown coloured biotites with increase in grade. In the inner biotite zone it is not unusual to see ragged porphyroblasts of biotite, these porphyroblasts being parallel to the general schistosity. Relict plagioclase and quartz grains can be found in the coarser sediments. The quartz grains have, in most cases, straight extinction under crossed nicols, which suggests that it could have been originally volcanic quartz (Folk, 1968).

The sharp demarcation of the biotite isograd is similar to the Ardara biotite isograd, Donegal, Eire (Pitcher and Berger, 1972). It appears that the thermal gradient fell slowly throughout the distance of the aureole, and finally dropped very rapidly. From theoretical considerations (Jaeger, 1964) this would seem to imply that the initial heating was of relatively short duration, however, once set up, this sharp gradient was apparently retained for long periods.

8. DISCUSSION

The use of hornblende as an indicator of metamorphic grade (Binns, 1965) can be useful in areas containing predominantly basic hornfelses. In the Walcha Road aureole it was observed that blue-green hornblende occurred at distances of greater than 300 metres from the contact, that green hornblende occurred roughly in the area outlined by the cordierite-almandine zone (Table 20) and brown-green and tan hornblende occurred in the cordierite-K-feldspar zone. The significance of this colour change has been explained in a previous chapter. The boundary between different coloured hornblendes is sometimes vague and it is the pelitic schists that are the best indicators of grade in the Walcha Road aureole. It is considered, therefore, that appropriate experimental work would be more precise when working with pelitic assemblages.

The clear mineral zonation in the thermal schists of the Walcha Road aureole obviously reflects the temperature gradient away from the intrusion. Certain mineralogical and field observations allow an approximation of the temperatures that existed over the three kilometre wide Walcha Road aureole. The width of the aureole, the simplicity of the metamorphic zones, and the structural effects (Appendix One) that the intrusion has had on the rocks adjacent to the contact suggest that the adamellite was forcibly intruded as a single pulse of magma. The assemblages observed suggest also that the adamellite itself was intruded at a depth of 5-7 kilometres.

In attempting to estimate the temperatures across the aureole the results of Jaeger (1957) have been used. Jaeger's (op. cit.) calculations are based on the assumption that the heating of the country rock by an intrusion is due entirely to conductivity, and that heating by a transfer of volatile constituents is not applicable. Winkler (1967) adequately summarised Jaeger's (op. cit.) work, the summary concluding that at the immediate contact the temperature of the country rock is slightly greater than 60% of the intrusion temperature + T_c (where T_c equals the temperature of the country rock) and that at a distance equal to one-tenth of the thickness of the intrusion the temperature of the country rock is about 50% of the intrusion temperature + T_c .

It is estimated that the total pressure that existed in the aureole was 1.5-2.0Kb (Part 2). At this pressure the water saturated solidus for granitic liquids occurs between 700°C (2Kb) and 740°C (1Kb) (Brown and Fyfe). To determine the temperature of the country rock one should take into account the grade of metamorphism observed in the regionally metamorphosed rocks that have been intruded. Adjacent to the Walcha Road adamellite this grade of metamorphism is greenschist, suggesting temperatures of 300°C-500°C ($PH_2O = 3Kb - 8Kb$; Turner and Verhoogen, 1960). If temperatures such as these are used for the T_c value, then calculated temperatures across the aureole are too high. For example, if $T_c = 250^\circ C$, and intrusion temperature equalled 700°C, then the temperature at 2km from the contact would be 600°C. It has been, therefore, assumed that the geo-

thermal gradient had been lowered prior to the intrusion of the adamellite, and at the 5-6km depth of intrusion the T_c was 150°C .

Using an intrusion temperature of 700°C , a T_c of 150°C and an intrusion thickness of 20km, the temperature at the immediate contact of the Walcha Road adamellite would have been 605°C and at a distance of 2km from the contact the temperature would have been 500°C . By joining these two temperature plots by a straight line (on a temperature-distance curve) an estimate of the temperature across the aureole is obtained.

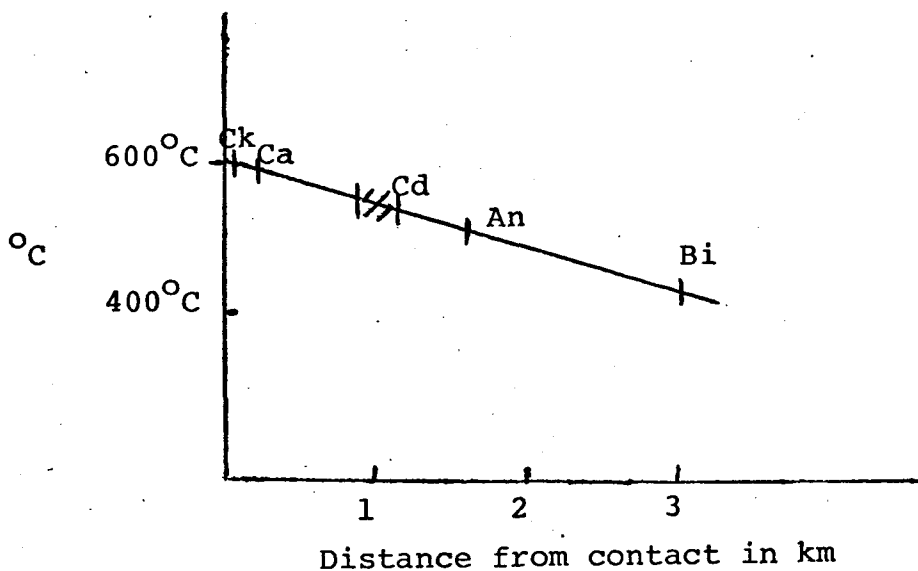


Figure 10: Deduced, maximum temperature thermal gradient for the Walcha Road aureole.

The computed temperature-distance curve (Figure 10) can then be used to calculate the temperature gradient across the aureole.

<u>Incoming Mineral</u>	<u>Temperature</u>
Biotite	$425^{\circ}\text{C} \pm 10^{\circ}\text{C}$
Andalusite	$495^{\circ}\text{C} \pm 10^{\circ}\text{C}$
Cordierite (in graphitic schists)	$530^{\circ}\text{C} \pm 10^{\circ}\text{C}$
Cordierite (in non graphitic schists)	$550^{\circ}\text{C} \pm 10^{\circ}\text{C}$
Almandine	$590^{\circ}\text{C} \pm 10^{\circ}\text{C}$
K-feldspar	$600^{\circ}\text{C} \pm 10^{\circ}\text{C}$

In the Shalimar aureole, almandine garnet occurs within one metre of the contact, cordierite within 150-200 metres of the contact and the first appearance of biotite in pelitic rocks is approximately 800 metres from the contact. It is suggested that the cordierite-K-feldspar zone is not developed adjacent to this intrusion due to its smaller size (approximately 2km in diameter), and also due to the more passive emplacement of the tonalite (which is a function of size) compared to the Walcha Road adamellite.

It was found that a straight line estimate was a surprisingly good fit for the maximum temperature thermal gradient for the Walcha Road aureole, indicating that a static cooling model with a concave temperature-distance curve was not applicable. In the Shalimar aureole, however, the reverse is true, with the concave temperature-distance curve giving the best results. This can be explained by the size of the intrusions concerned. Wide aureoles in which the temperature is held between 400°C - 500°C are to be expected near large bodies of granitic material (Turner, 1968). In the case of smaller intrusive bodies such as the Shalimar Tonalite,

the rate of heat fall off is much more rapid away from the body, and a concave temperature-distance curve would result (see Turner, 1968, Figure 1.7 page 19; Figure 1.9 page 21).

These results when compared with those deduced for the Walcha Road aureole are quite compatible. (The same parameters were used as in the Walcha Road calculations, except for intrusion thickness.)

<u>Incoming Mineral</u>	<u>Temperature</u>
Biotite	$410^{\circ}\text{C} \pm 10^{\circ}\text{C}$
Cordierite	$525^{\circ}\text{C} \pm 10^{\circ}\text{C}$
Almandine	$600^{\circ}\text{C} \pm 10^{\circ}\text{C}$

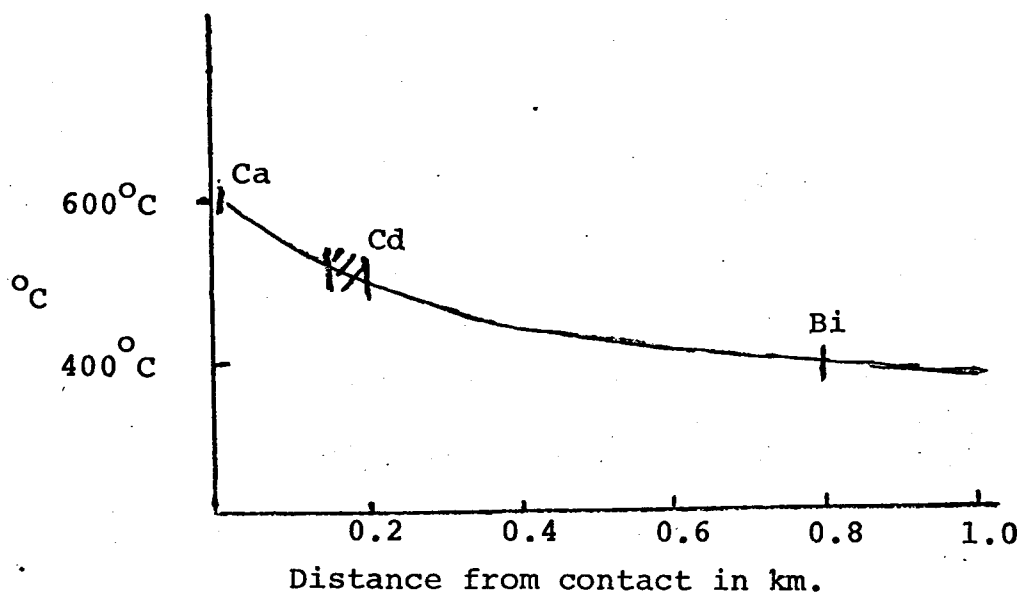


Figure 11: Deduced, maximum temperature thermal gradient for the Shalimar aureole.

The indicated temperatures of the formation of the Walcha Road and Shalimar metamorphic minerals are similar to temperatures experimentally determined by other workers:

Mineral	Temperature	Total Pressure	Source
Biotite	420°C	1-2kb	Compton (1960)
Biotite	300-400°C	2kb	Turner (1968)
Andalusite	525°C	2kb(PH ₂ O)	Winkler (1957)
Andalusite	500°C	3kb	Loomis (1972)
Cordierite	560°C	2kb(PH ₂ O)	Winkler (1957)
K-feldspar/cordierite	620°C±20°C	1.5kb	Winkler (1967)

The structures created by the forcible emplacement of the Walcha Road Adamellite are discussed in detail in Appendix One. In brief, however, the regional structures "wrap" around the pluton, and S surfaces were destroyed close to the contact. Farther from the contact a "wrapping" of porphyroblasts by the micas suggests that flattening must have occurred after the main period of growth. The Ardara aureole, Donegal, Eire, is very similar to the Walcha Road aureole. In the Ardara area regional structures have been deformed in such a way as to concordantly wrap around the Ardara pluton. The old S₁, S₂ and S₃ structures were squeezed together and reinforced by further flattening so as to nearly obliterate the early record of regional polyphase metamorphism. In the contact rocks new porphyroblasts overprinted the aligned micas which formed the reinforced schistosity, and as at Walcha Road, micas external to larger porphyroblasts still sweep around them, showing that a further flattening occurred after the main period of growth.

An important difference between the two plutons is the mineralogy of the associated contact rocks. It has been estimated by the writer (Part 2) that total pressure in the Walcha Road aureole was 1.5-2.0Kb. The "high level" Ardara Pluton according to Pitcher and Berger (1972) has undergone pressures of approximately 1Kb, which would appear incorrect when an initial study of the contact minerals present is made. The Ardara aureole contains the minerals sillimanite, kyanite and staurolite, minerals which have not been observed in the Walcha Road aureole. At the low pressures suggested by Pitcher and Berger (op. cit.) and Turner (1968, p249) it would be difficult to understand the reasons for the formation of "higher pressure" minerals in the Ardara aureole.

Pitcher and Berger (op. cit.) believe that method of emplacement has a lot to do with the formation of these particular minerals observed in the Ardara aureole. According to the experimental work of Hoschek (1969) and Hirschberg and Winkler (1968) the P/T controls of the staurolite and cordierite reactions are much the same. Pitcher and Berger (1972) however, state that the formation of cordierite is "favoured" at lower pressures. They put forward the convincing data that in the Donegal area cordierite occurs throughout each of the static aureoles in contrast to the moderately deformed Ardara aureole, which only carries this mineral in its innermost zone, and the strongly deformed rocks of the main Donegal granite in which cordierite is virtually absent; in every case, quite the reverse is true of staurolite. Compton (1960) takes a different view on the genesis of cordierite and staurolite suggesting that reaction thresholds are overstepped. He believes that cordierite grows where reaction rates

are slow, staurolite when they have been accelerated. The absence of kyanite in the Walcha Road aureole is a function of not only P/T conditions but also a function of bulk rock chemistry (Naggar, Atherton and Pitcher, 1970) for in the aureole no rocks of the required bulk rock chemistry exist.

Pitcher and Berger (op. cit.) have stressed the fact that it is especially significant whether a magma was permissively or forcibly emplaced. "During forceful intrusion, the creation of overpressures and the effect of deformation must influence not only the structural evolution of the contact rocks but the metamorphic reactions taking place within them. In permissive emplacement, on the other hand, such influences are at a minimum, and the reactions are largely controlled by temperature." (Pitcher and Berger op. cit., p327). This explanation can be used to explain the occurrence of the observed "high pressure" minerals in the high level Ardara aureole. The same explanation can also be used when trying to explain the presence of almandine in the Walcha Road aureole, but not in the Yarrahapinni aureole (Appendix Two). At Yarrahapinni no evidence of forceful intrusion can be observed and the formation of almandine has not occurred. Therefore, the nature of emplacement mechanism does influence the chemical controls of metamorphism.

9. BIBLIOGRAPHY

- Benson, W.N.: 1913, The Geology and Petrology of the Great Serpentine Belt of New South Wales. Part I. Introduction; Proc. Linn. Soc. NSW, 38, 490-517.
- Benson, W.N.: 1914a, Ibid., Part II, The Geology of the Nundle District. Ibid., 38, 569-596.
- Benson, W.N.: 1914b, Ibid., Part III, Petrology. Ibid., 38, 662-724.
- Benson, W.N.: 1915, Ibid., Part IV, The Dolerites, Spilites and Keratophyres of the Nundle District. Ibid., 40, 121-173.
- Benson, W.N.: 1917, Ibid., Part VI, A General Account of the Geology and Physiography of the Western Slopes of New England. Ibid., 42, 223-283.
- Benson, W.N.: 1918, Ibid., Appendix to Part VI. The Attunga District. Ibid., 42, 693-700.
- Binns, R.A.: 1965, Hornblendes from Some Basic Hornfelses in the New England Region, NSW. Mineral. Mag. 34, 52-65.
- Binns, R.A.: 1966, Granitic Intrusions and Regional Metamorphic Rocks of Permian Age from the Wongwibinda District, North Eastern NSW. J. Proc. Roy. Soc. NSW, Vol. 99
- Binns, R.A.: 1967, Geological Map of the Southern New England Tableland. Dept. Geol., Uni. New England.
- Browne, W.R.: 1943, The Geology of the Cooma District, NSW. Part II The Country Between Bunyan and Collinton. Journ. Proc. Roy. Soc. NSW, 77, 156-172.
- Chappell, B.W.: 1968, Volcanic Greywackes from the Upper Devonian Baldwin Formation, Tamworth-Barraba District, NSW. J. Geol. Soc. Aust., 15(1), 87-102.
- Chinner, G.A.: 1960, Pelitic Gneisses with Varying Ferrous/Ferric Ratios from Glen Clova, Angus, Scotland. Journ. Petrology 1, 1240-1266.

- Chinner, G.A.: 1962, Almandine in Thermal Aureoles.
Journ. Petrology., 3, 316-340.
- Compton, R.R.: 1960, Contact Metamorphism in Santa Rosa Range, Nevada. Bull. Geol. Soc. Am. 71, 1383-1416.
- Crawford, M.L.: 1972, Plagioclase and Other Mineral Equilibria in a Contact Metamorphic Aureole. Contr. Mineral. and Petrol., 36, 293-314.
- Deer, W.A., Howie, R.A., Zussman, J.: 1966, An Introduction to the Rock Forming Minerals. Longmans.
- Engel, A.E.J., Engel, C.G.: 1958, Progressive Metamorphism and Granitisation of the Major Paragneiss, Northwest Adirondack Mountains, New York, Pt. 1, Bull. Geol. Soc. Am., Vol. 69.
- Engel, A.E.J., Engel, C.G.: 1960, Ibid., Pt. II. Mineralogy. Bull. Geol. Soc. Am., Vol 71, 1
- Flood, R.H.: 1972, A Study on Part of the New England Batholith. Unpub. Ph.D. Thesis, Univ. New England.
- Folk, R.L.: 1968, Petrology of Sedimentary Rocks. Hemphills, University of Texas, Austin.
- French, B.M.: 1966, Some Geological Implications of Equilibrium Between Graphite and a C-H-O Gas Phase at High Temperatures and Pressures. Rev. Geophys. 4, 223-253.
- Gunthorpe, R.J.: 1970, Plutonic and Metamorphic Rocks of the Walcha-Nowendoc-Yarrowitch District, Northern NSW. Ph.D. Thesis, University of New England (unpub.)
- Guy, B.B.: 1968, Progressive and Retrogressive Metamorphism in the Tumbarumba-Geehi District, NSW. Jour. Roy. Soc. NSW, Vol. 101, 183-196.
- Hayama, Y.: 1959, Some Considerations on the Colour of Biotite and its Relation to Metamorphism. Journ. Geol. Soc. Japan, 65, 21-30.

- Hensen, B.J., Green, D.H.: 1970, Experimental Data on Co-Existing Cordierite and Garnet Under High Grade Metamorphic Conditions. Phys. Earth Planet. Interiors. 3, 431-440.
- Hoschek, G.: 1969, The Stability of Staurolite and Chloritoid and Their Significance in Metamorphism of Pelitic Rocks. Contr. Mineral. and Petrol. Vol. 22, 208-232.
- Howarth, F.R.: 1973, Some Contact Metamorphic and Manganiferous Rocks from Southern New England. Macquarie University Hons. Thesis (unpub.)
- Hsu, L.C.: 1968, Selected Phase Relationships in the System Fe-Al-Mn-Si-O-H. Journ. Petrology. Vol. 9, 40-83.
- Iiyama, T.: 1960, Recherches Sur le Role de L'eau dans la Structure et le Polymorphisme de la Cordierite. Bull. Soc. Franc. Miner. Crist. 83, 155-178.
- Jaeger, J.C.: 1957, The Temperature in the Neighbourhood of a Cooling Intrusive Sheet. Am. J. Sci., 255, 306-318.
- Jaeger, J.C.: 1964, Thermal Effects of Intrusions. Rev. Geophysics 2, 443-446.
- Joplin, G.A.: 1942, Petrological Studies of the Ordovician of NSW, 1., The Cooma Complex. Proc. Linn. Soc. NSW, 67, 156-196.
- Leitch, E.C.: 1973, Lecture delivered at Macquarie University (unpub.)
- Leitch, E.C.: 1974, The Geological Development of the Southern Part of the New England Fold Belt. Journ. Geol. Soc. Aust., Vol. 21, Pt. 2, 133-156.
- Lewington, G.L.D.: 1973, The Geology of an Area East and South East of Limbri, NSW. Hons. Thesis, Macquarie Uni. (unpub.)
- Loomis, A.A.: 1966, Contact Metamorphic Reactions and Processes in the Mt. Tallac Roof Remnant, Sierra Nevada, California. Journ. Petrol. 7, 221-245.

- Mather, J.D.: 1970, The Biotite Isograd and the Lower Greenschist Facies in the Dalradian Rocks of Scotland. Journ. Petrol., Vol. 11, Pt. 2, 253-275.
- Michel-Levy, M.C.: 1960, Sur L'alteration de la Cordierite. Bull. Soc. Franc. Min. Crist., Vol. 83, 142-143.
- Miyashiro, A., Shido, F.: 1973, Progressive Compositional Change of Garnet in Meta-Pelite. Lithos 6 13-20.
- Muller, G., Schneider, A.: 1971, Chemistry and Genesis of Garnets in Metamorphic Rocks. Contr. Mineral. and Petrol., Vol. 31, 178-200.
- Naggar, M.G., Atherton, M.P., Pitcher, W.S.: 1970, Composition of Some Aluminium Silicate Bearing Contact Rocks from County Donegal, Eire. Nature, Vol. 226, p841.
- Newton, R.C.: 1972, An Experimental Determination of the High Pressure Stability Limits of Mg. Cordierite Under Wet and Dry Conditions. Journ. of Geol., Vol. 80, 398-420.
- Okrusch, M.: 1971, Garnet-Cordierite-Biotite Equilibria in the Steinach Aureole, Bavaria. Contr. Mineral. and Petrol, Vol. 32, 1-23.
- Packham, G.H.: ed 1969, The Geology of NSW. J. Geol. Soc. Aust., Vol. 10, Pt. 1.
- Pitcher, W.S., Berger, A.R.: 1972, The Geology of Donegal - A Study of Granitic Emplacement and Unroofing. Regional Geology Series. Wiley-Interscience, Toronto.
- Pitcher, W.S., Sinha, R.C.: 1957, The Petrochemistry of the Ardara Aureole. Quart. Journ. Geol. Soc. London, Vol 113.
- Schreyer, W., Yoder, H.S.: 1964, The System Mg Cordierite H₂O and Related Rocks. Neus. Jahrb. Mineral. Abhandl., Vol. 3.
- Seki, Y.: 1957, Petrological Study of Hornfelses in the Central Part of the Median Zone of Kitakami Mountainland, Iwate Prefecture. Sci. Rep. Saitama Univ., Ser. B. 2, 307-360.

- Spry, A.: 1953, The Thermal Metamorphism of Portions of the Woolomin Group in the Armidale District, NSW, Part I, The Puddledock Area. Journ. Proc. Roy. Soc. NSW, Vol. 87.
- Spry, A.: 1955, Thermal Metamorphism of Portions of the Woolomin Group in the Armidale District, Part II The Tilbuster and Dumaresque Areas. Proc. Roy. Soc. NSW, Vol. 87, 129.
- Stewart, F.H.: 1942, Chemical Data on a Silica Poor Argillaceous Hornfels and its Constituent Minerals. Miner. Mag. p260-266.
- Suzuki, J.: 1934, Metamorphosed Calcareous Concretions in the Hornfels at the Southeastern Coast of Tokati Province, Hokkaido. J. Fac. Sci. Hokkaido Univ. Ser. 4, Vol. 2, 323-338.
- Teale, G.S.: 1972, Hornfelses From the Bendemeer District, NSW. Macquarie Univ. 3rd year field report (unpub.)
- Tilley, C.E.: 1926, On Some Mineralogical Transformations in Crystalline Schists. Mineral. Mag., 21, 34-46.
- Turner, F.J.: 1968, Metamorphic Petrology, Mineralogical and Field Aspects, New York.
- Turner, F.J., Verhoogen, J.: 1960, Igneous and Metamorphic Petrology. McGraw Hill Book Co.
- Vallance, T.G.: 1953, Studies in the Metamorphic and Plutonic Geology of the Wantabadgery-Adelong-Tumbarumba District, NSW. Proc. Linn. Soc. NSW, Vol. 78, Parts 3-4.
- Vernon, R.H.: 1961, The Geology and Petrology of the Uralla Area, NSW. J. Proc. Roy. Soc. NSW 95, 23-33.
- Vernon, R.H.: 1968, Intergranular Microstructures of High Grade Metamorphic Rocks at Broken Hill, Australia. Journ. Petrol. 9.
- Vernon, R.H.: 1972, Lectures delivered at Macquarie University (unpub.)
- Voisey, A.G.: 1959, Tectonic Evolution of North-Eastern New South Wales. Journ. Proc. Roy. Soc. NSW, Vol. 92, 191-203.
- Weisbrod, A.: 1973, The Problem of Water in Cordierite. Geophys. Lab. Carneg. Inst. Year Book.
- Winkler, H.G.F.: 1967, Petrogenesis of Metamorphic Rocks. Springer-Verlag, New York, 2nd ed.

P A R T T W O

CORDIERITE FORMING REACTIONS

IN THE AUREOLE OF THE

WALCHA ROAD ADAMELLITE

1. INTRODUCTION

The location of metamorphic zones containing different mineral assemblages in rocks of a restricted chemical composition allows a documentation of the metamorphic reactions that led to the formation of particular minerals in the zonal sequence. Mineral analyses from three of the five metamorphic zones observed at Walcha Road give an indication of the changes in mineral chemistry as metamorphic grade is increased.

The isochemical nature of the contact metamorphism was ascertained by a thorough geochemical investigation of the pelitic schists at Walcha Road. The results of this geochemical study have been recorded on the various compositional diagrams shown (Figures 12, 13, 14, and 15). The anomalous plots that can be observed approaching the Al_2O_3 apex of the compositional diagrams are the result of the samples in question having very low $\text{FeO}/\text{Fe}_2\text{O}_3 + \text{FeO}$ ratios. Samples MU4395, MU4462, MU4414 and MU4436, for example, have Fe_2O_3 values higher than associated FeO values, and all plot towards the Al_2O_3 apex of the compositional diagrams. The increase in Fe_2O_3 indicates that the rocks have undergone weathering.

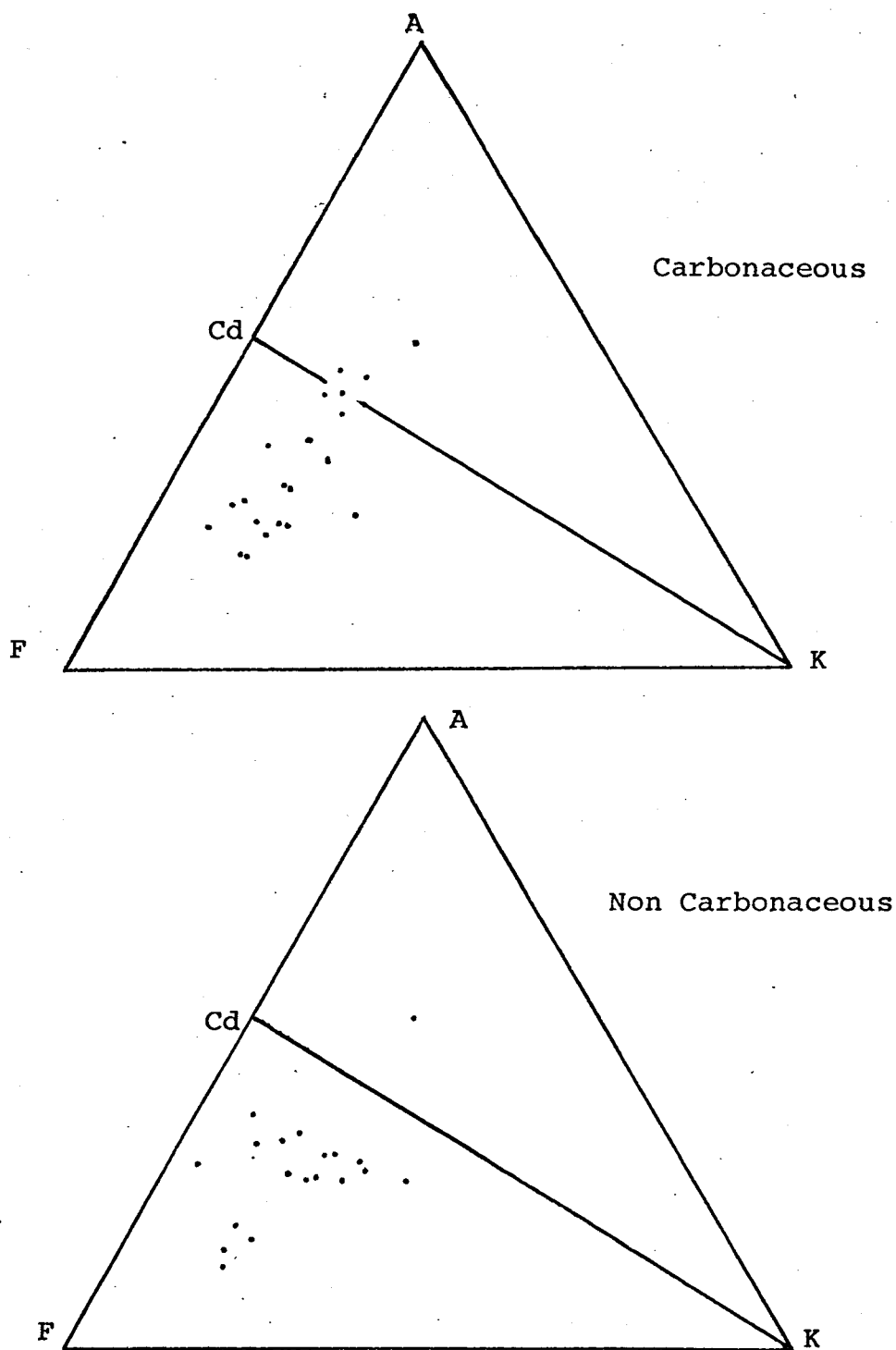


Figure 12: AFK compositional diagram for carbonaceous and non carbonaceous meta-pelites.

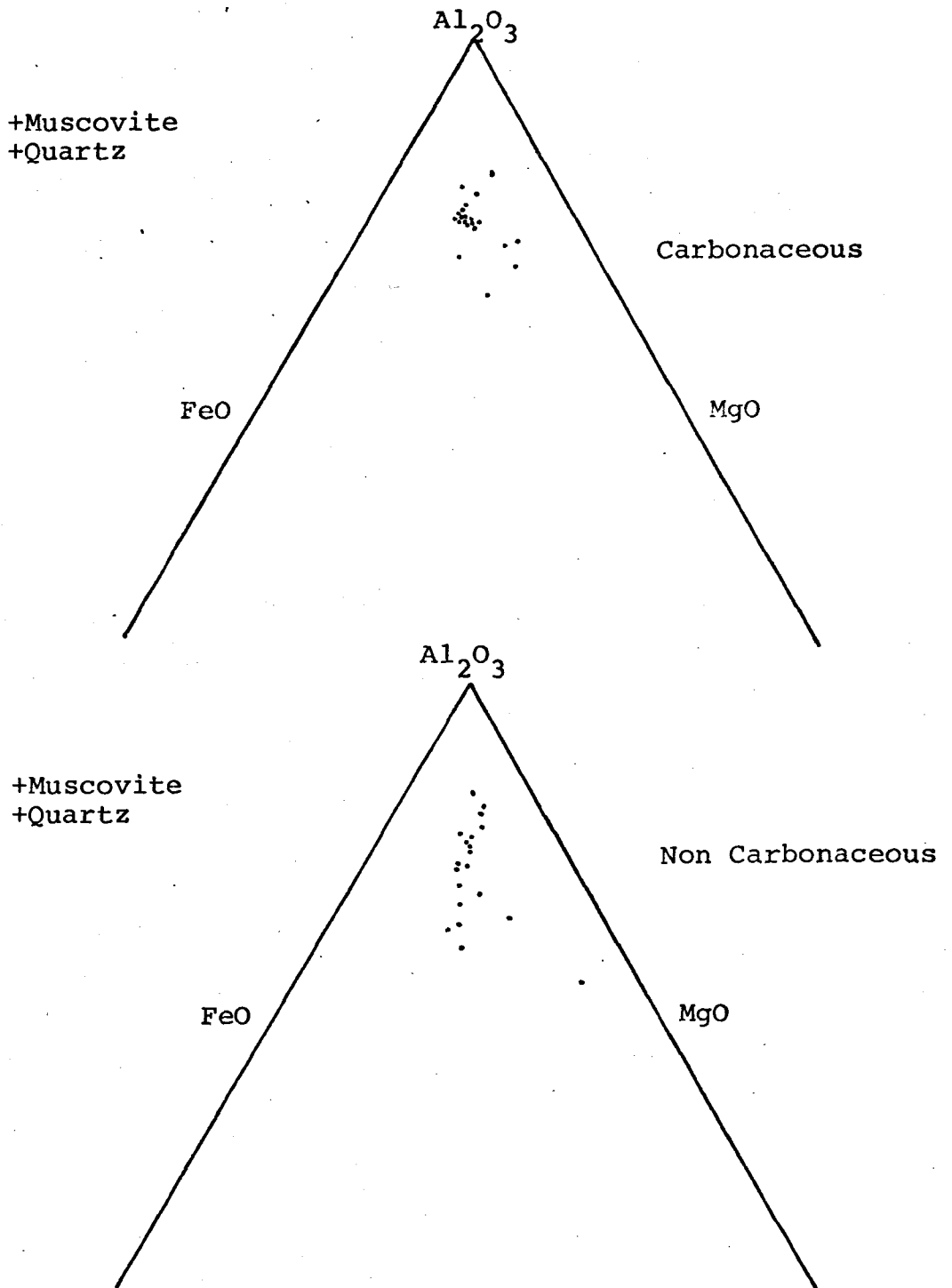


Figure 13: Carbonaceous and Non Carbonaceous meta-pelite compositions plotted on the AFM projection plane.

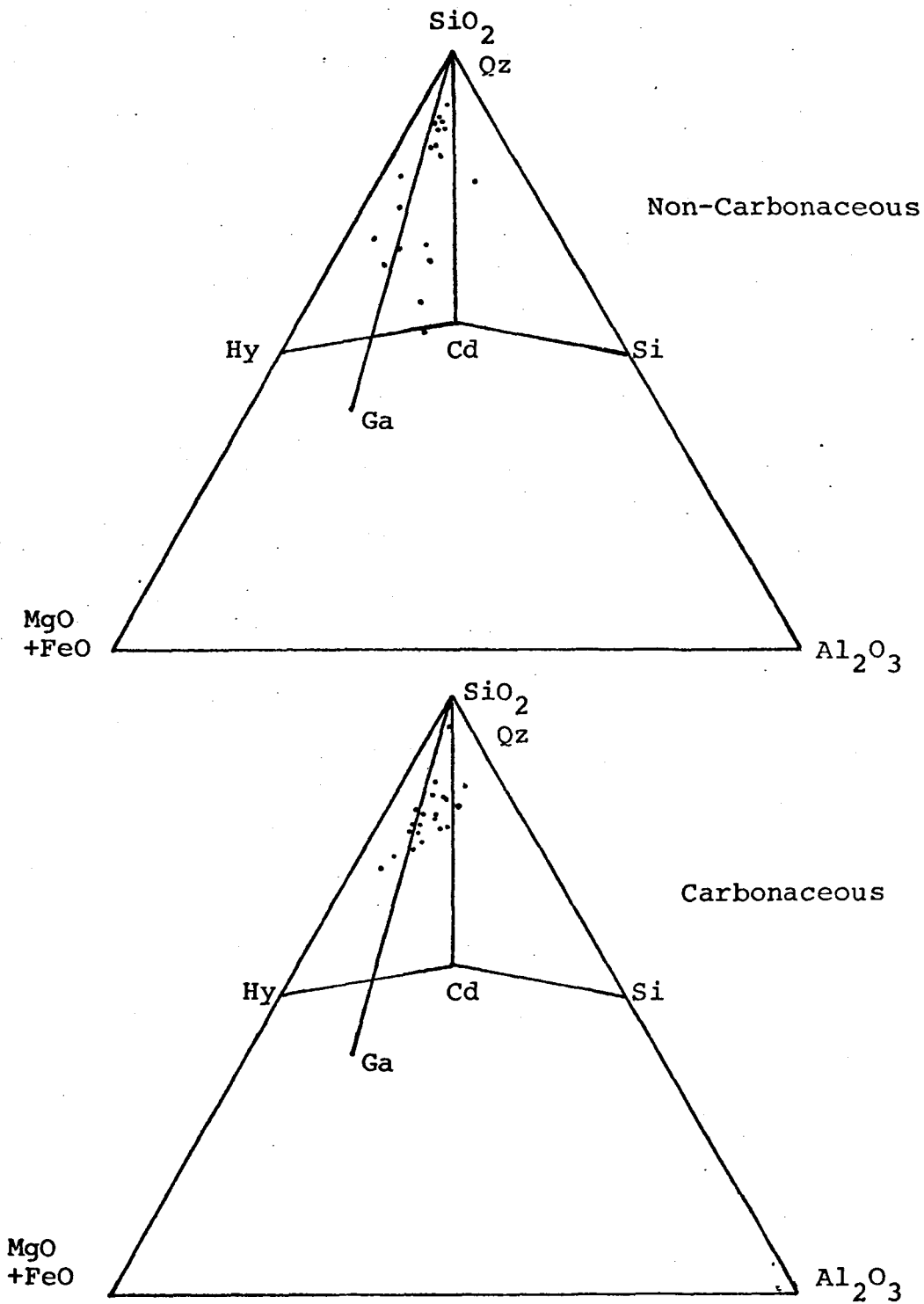


Figure 14: SiO_2 - $(\text{MgO} + \text{FeO})$ - Al_2O_3 diagram showing the positions of carbonaceous and non-carbonaceous meta-pelites.

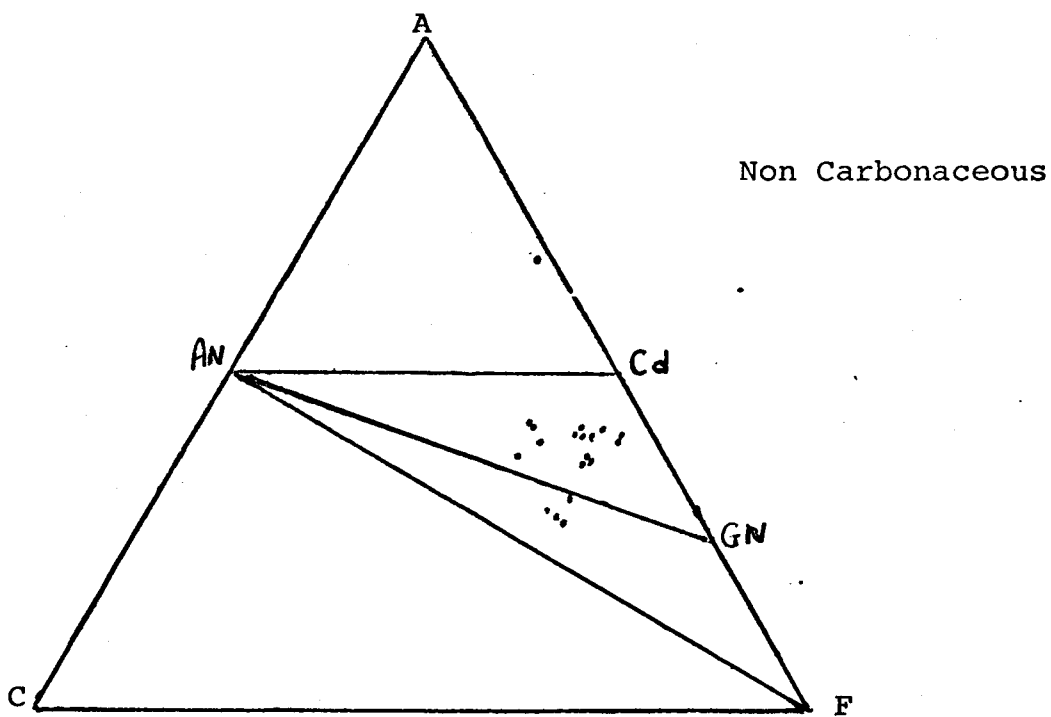
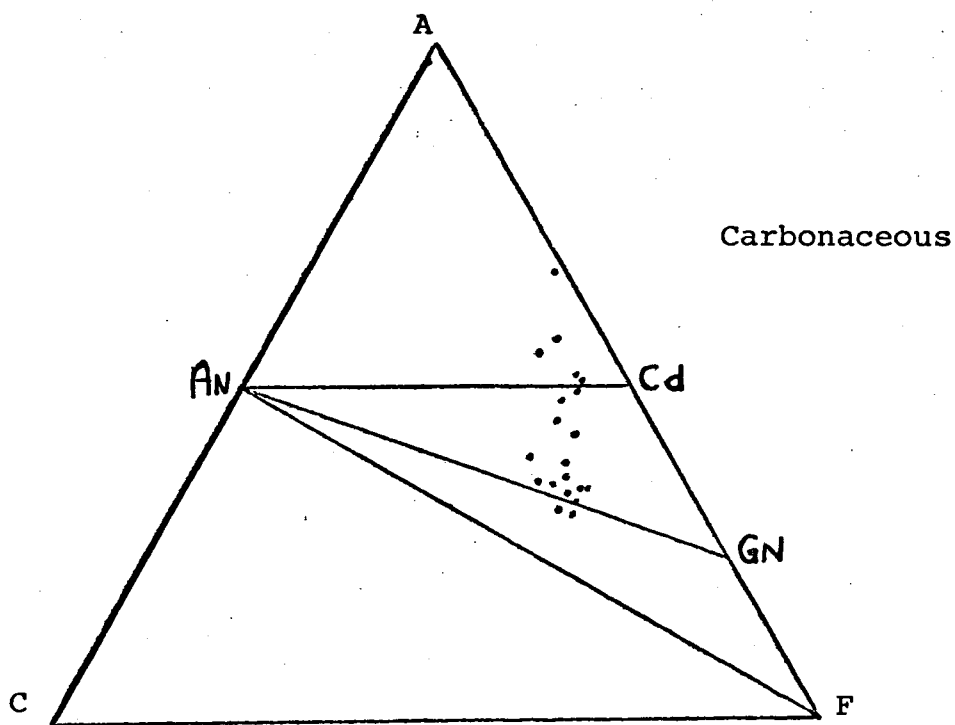


Figure 15: ACF compositional diagrams for meta-pelites from Walcha Road

2. PREVIOUS WORK

The reaction muscovite + chlorite + quartz \longrightarrow cordierite + biotite + H_2O was recognised by Schreyer and Yoder (1961) as one of the most important reactions producing cordierite in pelitic rocks. The early works of Tilley (1924) suggested that cordierite formed from the breakdown of muscovite and chlorite, and much documented evidence for a reaction of this type has been produced (Schreyer and Yoder, op. cit.; Seifert, 1969; Hess, 1969). Reactions involving the minerals muscovite, chlorite and biotite to produce cordierite have also been suggested (Winkler, 1967). It should be noted that discrepancies do exist between experimental work and field observations, and even the work of the experimentalists does present conflicting views at times. For example, the equilibrium muscovite + biotite + quartz \rightleftharpoons cordierite + K-feldspar + H_2O , according to Winkler, is located at higher temperatures than that of muscovite + quartz \rightleftharpoons K-feldspar + andalusite + H_2O , the position of which has been determined from Evans (1965) data. This clearly cannot be so. The reaction muscovite + chlorite + quartz \longrightarrow cordierite + biotite + H_2O has been observed at Walcha Road, and the temperature and pressure at which this reaction proceeds has been calculated as $530^{\circ}C$ at 2Kb. This temperature and pressure is extremely compatible with the experimental work of Seifert (op. cit.) who found that the same reaction proceeds at $525^{\circ}C \pm 10^{\circ}C$ at 2Kb.

The reaction chlorite + muscovite + quartz \longrightarrow cordierite + biotite + andalusite + H_2O occurs at $527^{\circ}C \pm 10^{\circ}C$ at 2Kb (Hirschberg and Winkler, 1968). A reaction of this sort does not occur at Walcha Road due to the instability of andalusite in the cordierite zone. The reaction that leads to the breakdown of andalusite as the cordierite zone is entered is discussed in the following chapter.

The breakdown of andalusite to form cordierite has been recognised by certain workers (Joplin, 1942; Hess, 1969). Hess (op. cit.) states that at pressures of less than 2.7Kb one of the univariant reactions that can introduce cordierite into pelitic rocks is chlorite + andalusite + quartz \longrightarrow garnet + cordierite + H_2O . At Walcha Road andalusite does breakdown to form cordierite, however, no garnet is produced during the reaction, and it is suggested that the reaction that occurs is similar to that proposed by Joplin (op. cit.), namely,

biotite + andalusite \longrightarrow cordierite + muscovite.

Another cordierite forming reaction suggested by Hess is staurolite + chlorite + quartz \longrightarrow garnet + cordierite + muscovite + H_2O . This reaction is rather interesting in that experimental work carried out (Hoschek, 1969; Hirschberg and Winkler, op. cit.) suggests that the pressure/temperature controls of the staurolite and cordierite reactions are basically the same. Pitcher and Berger (1972) believe that cordierite is favoured at lower pressures. The presence of staurolite and absence of cordierite in the outer zones of the Ronda Ultramafic aureole (Loomis, 1972) and the absence of staurolite and presence of cordierite in the inner aureole led Loomis (op. cit.) to suggest a temperature of $730^{\circ}C$ (3.5Kb) for the incoming of cordierite. The writer feels that this temperature is too high for the incoming of cordierite and believes that the relationship between cordierite and staurolite is more complicated than experimental work shows.

The breakdown of biotite in the presence of muscovite (and chlorite) to form cordierite and K-feldspar is an observed reaction at Walcha Road. The reaction $6 \text{ muscovite} + \text{biotite} + 15 \text{ quartz} \longrightarrow 3 \text{ cordierite} + 8 \text{ K-feldspar} + \text{H}_2\text{O}$ has been proposed by Winkler (op. cit.) and Okrusch (op. cit.).

Temperatures deduced for the incoming of cordierite by experimental work appear to agree with the observed reactions that occur at Walcha Road. Many more cordierite forming, and breakdown reactions have been determined by other workers (Vernon, 1972; Weisbrod, 1973; Seifert, 1974, 1970, 1973; Dahl, 1972), however, many of them cannot be applied when discussing the formation and breakdown of cordierite at the pressure/temperature conditions that existed in the Walcha Road aureole.

TABLE 19

MODAL ANALYSES OF META-PELITES
FROM THE WALCHA ROAD AREA

	MU4383	MU4471	MU4382	MU4359
Quartz	17.97	56.23	30.46	49.69
Cordierite	42.40	12.74	28.57	6.72
Biotite	17.12	14.53	16.56	7.11
Muscovite	4.65	-	12.63	-
Plagioclase	11.57	8.61	11.06	14.29
K-feldspar	2.06	7.89	-	20.21
Chlorite	3.38	trace	-	-
Andalusite	-	-	-	-
Graphite	-	-	-	-
Almandine	-	trace	-	-
Opaques	trace	-	0.57	1.58
Tourmaline	trace	trace	0.15	trace
Zircon	trace	trace	trace	trace
Rutile	-	-	-	-
Apatite	trace	trace	-	trace
	CK	CK	CK	CK

	MU4454	MU4394	MU4492	MU4361
Quartz	37.13	28.49	34.93	39.61
Cordierite	13.87	2.66	0.60	-
Biotite	18.64	24.03	20.97	18.82
Muscovite	-	11.02	14.72	17.96
Plagioclase	23.50	20.02	18.40	11.26
K-feldspar	6.83	-	-	-
Chlorite	-	3.90	4.39	4.49
Andalusite	-	4.11	4.49	5.88
Graphite	-	4.00	0.40	trace
Almandine	-	-	-	-
Tourmaline	-	trace	-	trace
Opagues	trace	1.67	0.80	1.96
Zircon	trace	trace	trace	-
Rutile	-	-	-	-
Apatite	trace	-	-	-
	CK	A	A	A

	MU4418	MU4413	MU4397	MU4435
Quartz	28.57	25.68	30.18	33.41
Cordierite	-	-	-	11.38
Biotite	18.66	21.43	22.16	18.81
Muscovite	-	-	2.48	0.62
Plagioclase	43.59	41.59	29.80	28.32
K-feldspar	3.78	3.01	6.43	-
Chlorite	4.27	5.35	6.86	2.2
Andalusite	-	-	-	-
Graphite	-	trace	trace	trace
Almandine	-	-	-	3.77
Opagues	1.13	2.90	1.73	0.80
Tourmaline	trace	trace	trace	trace
Zircon	trace	trace	trace	trace
Apatite	trace	-	-	trace
Rutile	-	-	trace	trace
	B	B	B	CA

	MU4368	MU4417
Quartz	34.37	37.81
Cordierite	6.37	6.60
Biotite	29.07	27.81
Muscovite	trace	4.50
Plagioclase	23.40	19.39
K-feldspar	-	-
Chlorite	3.77	3.89
Andalusite	-	-
Graphite	2.72	trace
Almandine	-	-
Opagues	trace	trace
Tourmaline	trace	trace
Zircon	-	trace
Apatite	trace	-
	C	C

CK = Cordierite-K-feldspar zone

CA = Cordierite-almandine zone

C = Cordierite zone

A = Andalusite zone

B = Biotite zone

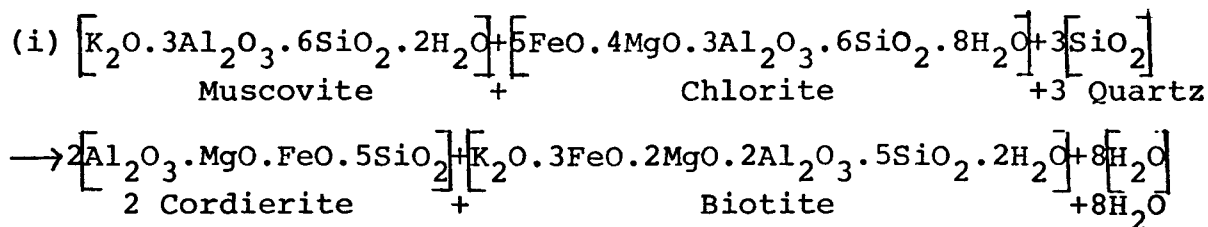
3. SUGGESTED REACTIONS

(a) Cordierite Forming Reactions in the Walcha Road Thermal Aureole

The following reactions, observed or inferred, have been proposed after a careful study of chemical and modal analyses coupled with petrographic and mineralogical observations. Only a small number of modal analyses have been determined because of the extremely fine grain size of the rocks and the presence of carbonaceous material in many samples, preventing effective staining for such minerals as plagioclase and K-feldspar.

It is in the transitional stage between the andalusite and cordierite zones that all reactants and products have been observed in thin section. The comparatively high modal percent of muscovite in the andalusite zone (Table 19) is due to the breakdown of K-feldspar and it is this muscovite, combined with chlorite that first forms cordierite in the Walcha Road aureole. As the cordierite zone is entered there is an increase in modal percent biotite and cordierite, and a subsequent decrease in the amount of muscovite and chlorite (Table 19).

The proposed reaction is:



The development of cordierite according to the above reaction leads to a zone of "knotted" schists, these knots forming due to the incipient local development

	MINERALOGICAL ZONE MINERAL	REGIONAL GREENSCHIST	BIOTITE	ANDALUSITE	CORDIERITE	CORDIERITE- ALMANDINE	CORDIERITE- K-FELDSPAR
Pelitic	Chlorite					--	
	Biotite						
	Andalusite			-----			
	Muscovite		--	-----			
	Cordierite			--			
	Almandine					-----	
	K-Feldspar						
	Detrital K-Feldspar		-----	--			
	Albite		-----	--			
	Oligoclase			-----	--		
	Andesine				--		
	Graphite						
Calcar- eous	Phengite				--		
	Diopside			-----			
	Scapolite				-----		-----
	Cummingtonite					--	-----
	Blue-green Hornblende				-----		
Mafic	Green Hornblende				-----	-----	
	Brown-green Hornblende						-----
	Tan Hornblende						-----
	Plagioclase		MU4365 An ₃₂	MU4534 An ₄₈			MU4384 An ₄₀

TABLE 20

of cordierite in the outer cordierite zone and inner andalusite zone (Plate 26).

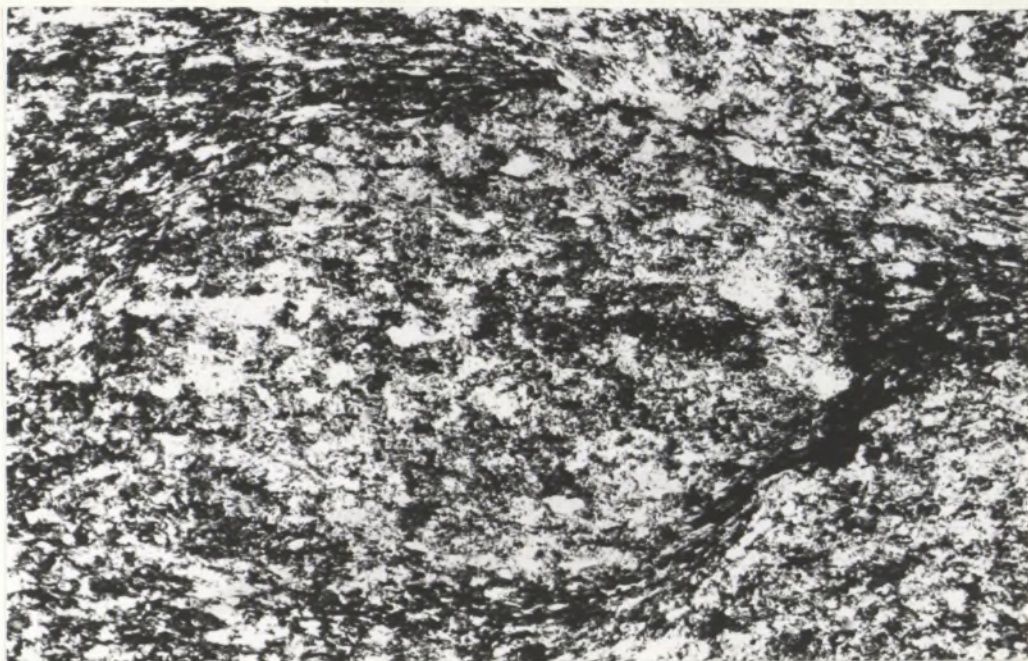
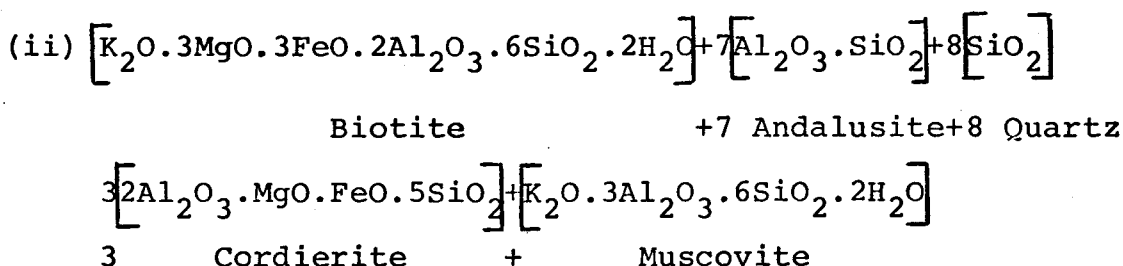


Plate 26: MU4408, incipient development of cordierite in "knots" of the inner andalusite zone
x 65

That the porphyroblasts (knots) represent cordierite that has undergone retrogression is not correct, for these knotted schists occur in a particular zone, this zone being located slightly downgrade from the actual cordierite isograd. If formed by retrogression of cordierite they would be present throughout the aureole and not in one particular zone. Cordierite that has been partly or completely retrogressed in other areas of the aureole is replaced by randomly oriented flakes of muscovite and chlorite. In the andalusite zone the orientation of the phyllosilicates is parallel to the general schistosity prevailing in the rocks, suggesting that the muscovite and chlorite are primary and are reacting to form cordierite.

At Walcha Road, andalusite does not occur in the higher temperature zones. Analysed samples (MU4492, MU4393) from the andalusite zone have similar chemical compositions to rocks from other zones and are no more corundum normative than schists from the inner zones. The formation of andalusite is brought about by the reaction of chlorite with K-feldspar, as discussed in detail in the section on biotite formation. Andalusite, therefore, forms at lower temperature conditions than cordierite. As temperature is increased andalusite reacts with biotite to form cordierite, the suggested reaction being:



This reaction accounts for the small drop in the modal percent of biotite and is partly responsible for the rise in modal percent muscovite in the inner andalusite zone.

Textural evidence for reaction (ii) was obtained from the Yarrahapinni area, north of Kempsey, NSW (Appendix 2). Here graphitic hornfels of similar chemistry to the Walcha Road thermal schists contain the assemblages

Cordierite-K-feldspar-biotite
Cordierite-biotite

Many of the cordierite porphyroblasts contain outlines of what was originally andalusite. The almost perfect

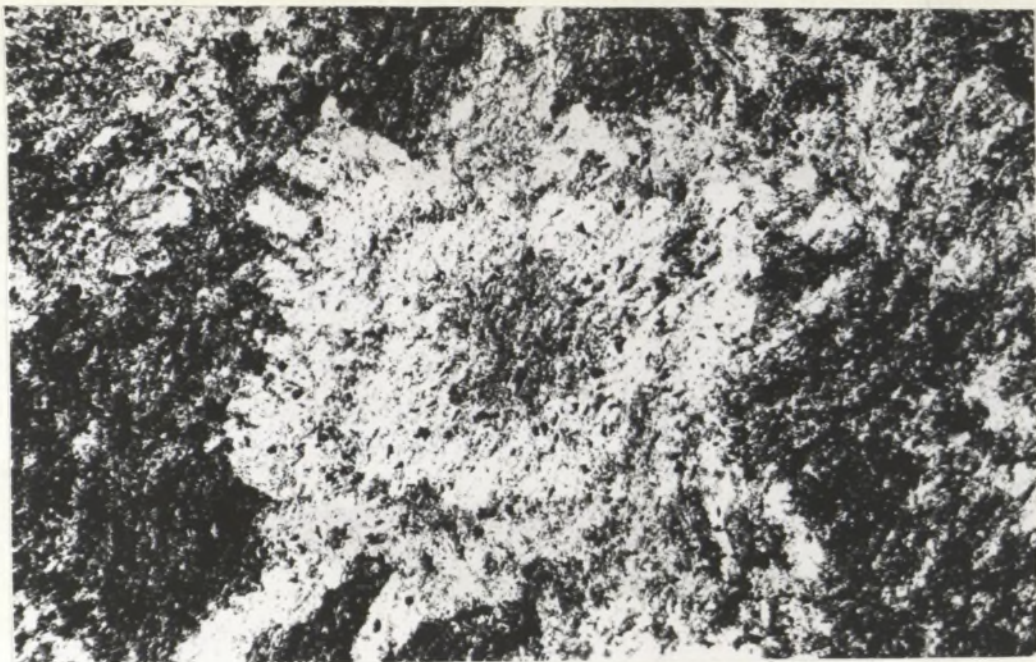


Plate 27: MU4508, Relict outline of andalusite marked by carbonaceous material. The andalusite has been entirely replaced by cordierite. Note the carbonaceous inclusions in the central section of the pre-existing andalusite.
x 65

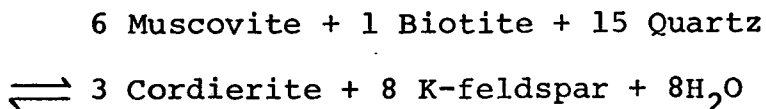


Plate 28: MU4394, Andalusite from Walcha Road. Compare grain shape with the above "ghost" outline of the original andalusite.
x 135

preservation of the idioblastic form of the pre-existing andalusite, complete with carbonaceous inclusions in the central section of the porphyroblast is shown in Plate 27. The pseudomorphing of the andalusite by cordierite takes place as temperature is increased within the aureole, the reaction at Yarrahapinni being similar to reaction (ii) that takes place at Walcha Road.

The development of K-feldspar in the cordierite-K-feldspar zone is brought about by a cordierite forming reaction that involves biotite as the major reactant. The amount of biotite present in the schists falls off rapidly as the cordierite-K-feldspar zone is approached. Plates 29, 30 and 31 show an average schist from the inner cordierite zone, the cordierite-almandine zone and the cordierite-K-feldspar zone respectively. The rocks contain similar FeO values and whole rock composition does not influence the amount of biotite present.

A reaction leading to an increase in the amount of cordierite and an introduction of K-feldspar must agree with certain mineralogical and modal observations. The minor amounts of chlorite and muscovite found in the inner zones apparently combines with the abundant biotite to form cordierite, K-feldspar and water. The reaction put forward by Winkler (1967, p74) namely,



could not be applied in the Walcha Road area due to the paucity of muscovite.

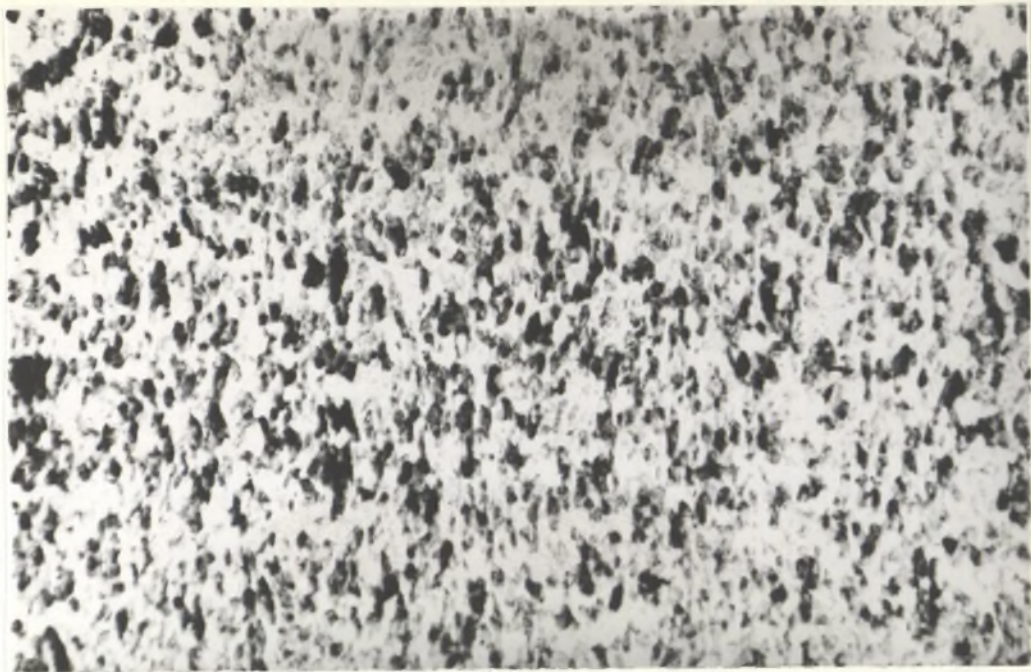


Plate 29: MU4368, Inner cordierite zone
x 104



Plate 30: MU4438, Cordierite-almandine zone
x 104

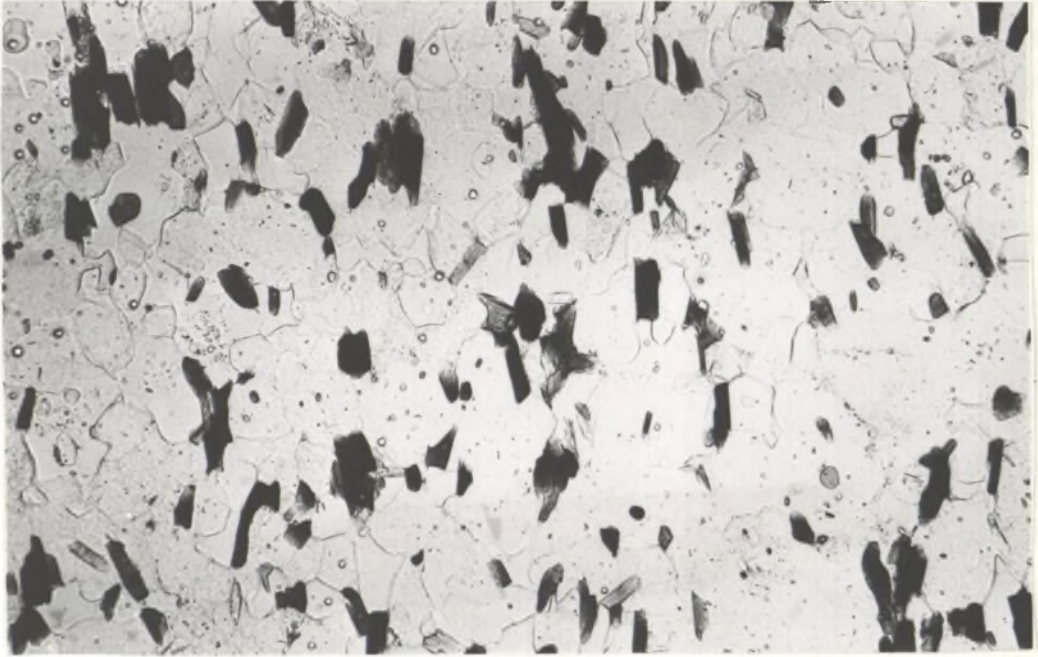


Plate 31: MU4354, Cordierite-K-feldspar zone
x 104

TABLE 21

C.I.P.W. NORMS OF PELITIC ROCKS

Specimen No.	MU4438	MU4404	MU4400	MU4395
Quartz	39.66	31.42	51.48	40.78
Orthoclase	20.44	18.08	19.91	16.19
Albite	18.35	19.11	6.85	17.68
Anorthite	5.45	7.64	4.39	5.07
Corundum	4.39	7.11	4.94	7.79
Hypersthene	9.65	9.61	8.50	5.09
Magnetite	1.35	1.96	1.16	3.80
Ilmenite	1.08	1.46	0.85	1.41
Apatite	0.30	0.44	0.19	0.21
Total	100.68	96.83	98.27	98.02
Plag. An	22.89	28.55	39.04	22.28
Specimen No.	MU4368	MU4491	MU4393	MU4466
Quartz	31.89	32.70	30.88	34.75
Orthoclase	15.42	4.37	21.68	11.52
Albite	19.71	18.18	18.95	23.43
Anorthite	13.25	17.06	6.28	7.24
Corundum	3.64	5.00	7.06	6.60
Hypersthene	10.96	12.81	7.90	10.20
Magnetite	1.99	3.31	2.46	1.94
Ilmenite	1.37	1.92	1.37	1.44
Apatite	0.35	0.52	0.39	0.37
Total	98.57	95.86	96.98	97.49
Plag. An.	40.21	48.41	24.89	23.60

C.I.P.W. Norms of Pelitic Rocks (cont.)

Specimen No.	MU4403	MU4450	MU4417	MU4465
Quartz	25.33	12.49	20.81	23.52
Orthoclase	18.26	15.54	19.67	16.31
Albite	25.37	36.88	30.02	32.14
Anorthite	8.98	11.31	8.56	9.47
Corundum	5.71	4.03	3.10	3.31
Hypersthene	11.37	14.93	13.69	10.42
Magnetite	1.10	0.78	0.97	1.29
Ilmenite	1.42	1.65	1.25	1.44
Apatite	0.44	0.58	0.32	0.37
Total	97.99	98.19	98.40	98.27
Plag. An.	26.13	23.47	22.18	22.76

Specimen No.	MU4413	MU4383	MU4356	MU4382	MU4431
Quartz	20.12	18.41	14.76	11.50	42.81
Orthoclase	14.18	16.54	35.27	32.97	22.57
Albite	33.15	15.14	19.45	13.45	6.85
Anorthite	12.71	6.87	9.95	3.91	9.33
Corundum	2.07	14.49	6.58	12.51	4.95
Hypersthene	11.89	23.35	9.73	19.96	10.03
Magnetite	1.36	1.49	0.68	1.39	1.28
Ilmenite	1.67	1.99	1.92	1.90	1.16
Apatite	0.42	0.32	0.97	0.37	0.28
Total	97.58	98.35	99.32	97.96	99.26
Plag. An.	27.71	31.22	33.85	22.55	57.67

C.I.P.W. Norms of Pelitic Rocks (cont.)

Specimen No.	MU4418	MU4409	MU4435	MU4366
Quartz	16.87	24.02	29.53	40.12
Orthoclase	16.25	13.23	10.58	21.74
Albite	37.04	29.18	24.44	13.79
Anorthite	10.20	11.17	12.22	3.89
Corundum	2.77	5.20	4.49	6.85
Hypersthene	11.57	12.89	14.83	6.23
Magnetite	1.32	1.65	0.81	4.32
Ilmenite	1.44	1.63	1.50	1.18
Apatite	0.46	0.65	0.49	0.49
Total	97.93	99.63	98.88	98.61
Plag. An.	21.59	27.68	33.33	21.99

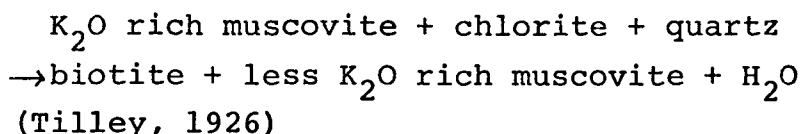
(b) The Genesis of Biotite in the Walcha Road Area

Insufficient data are available to precisely evaluate the biotite forming reactions, however, using modal and petrographic observations, coupled with the known composition of some of the mineral phases, two biotite forming reactions can be inferred.

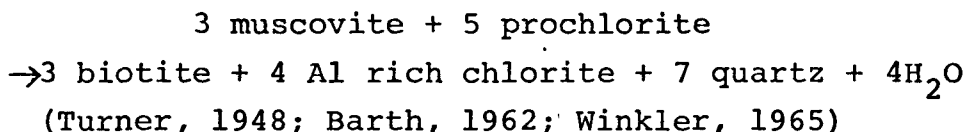
(i) Previously Proposed Reactions

Mather (1970) adequately summarised biotite forming reactions that had been proposed prior to 1970. Since the publication of Mather's (op. cit.) paper, Brown (1971) and Ramsay (1973) have suggested further reactions. A discussion of previous reactions ensues.

Many of the reactions which have been proposed, such as:



and a reaction of the type:

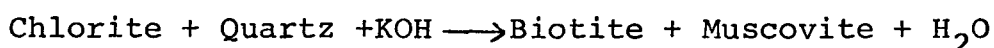


can not be applied in the Walcha Road area for muscovite has not been observed in the low grade regional metamorphics. Mather (op. cit.) suggests that a reaction of the type:



suggested by Ernst (1963) is not valid for it implies that phengite is the stable white mica of the chlorite zone and muscovite the stable white mica of the biotite bearing biotite zone rocks. He states that phengite is stable in the Dalradian biotite zone rocks. At Walcha Road the phengite-chlorite pair are stable in fine grained graphitic schists (MU4466) well into the cordierite zone.

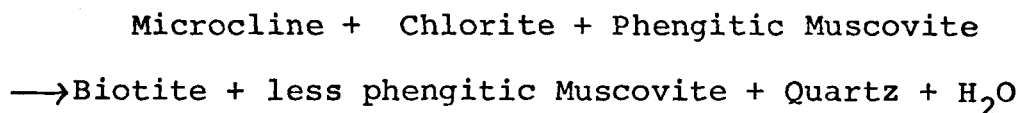
McNamara (1966) believed that there was sufficient K_2O within lower greenschist rocks, present as intergranular potassium bearing solutions, for a reaction of the sort:



However, evidence used by McNamara (op. cit.) rests on the misidentification of oxidised chlorite as biotite (Mather, op. cit.).

Ramsay (op. cit.) suggested that biotite originated by reaction of chlorite, muscovite and ilmenite producing rutile, K-feldspar and quartz as subordinate reaction products. This is not the case at Walcha Road for there is no muscovite at the lowest grades, and (detrital) K-feldspar was being consumed in the biotite zone, no K-feldspar being generated as a reaction product.

Mather (op. cit.) suggested the reaction:



for Dalradian sediments of the Aberfoyle area. On phase diagrams, however, (Ibid, pp269-270) he shows that

phengite has not been consumed in the reaction at the biotite isograd. In other words, according to Brown (op. cit.), he indicates that biotite is first produced by reaction between chlorite and microcline, and at higher grades, by breakdown of chlorite and phengite.

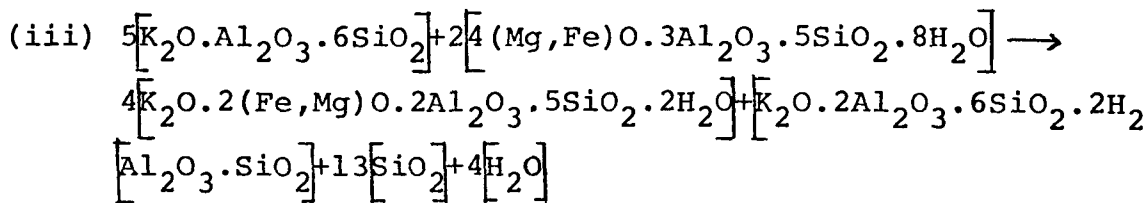
(ii) Possible Biotite Forming Reactions in the Walcha Road Contact Schists

The interpretation by Brown (op. cit.) of Mather's (op. cit.) work is suggested for the contact schists of the Walcha Road area. At Walcha Road, biotite is first produced in pelitic rocks by the breakdown of K-feldspar. The reaction involved being similar to the reaction proposed by Brown (op. cit.) i.e.

K-feldspar + chlorite \longrightarrow biotite + muscovite

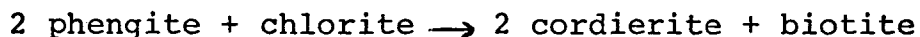
The assemblage chlorite-biotite-K-feldspar can be stable in the lower biotite zone (Albee 1968, p333) and this is observed at Walcha Road. With increasing temperature the remaining K-feldspar becomes unstable in the presence of chlorite and the following reaction marks the beginning of the andalusite zone:

5 K-feldspar + 2 chlorite \longrightarrow
4 biotite + muscovite + andalusite + 13 quartz + 4H₂O



The formation of biotite in the finer graphitic schists occurs at a higher grade by the breakdown of phengite

and chlorite (Mather op. cit.). As temperature increases phengite and chlorite become unstable and the following reaction marks the beginning of the cordierite zone in the fine grained graphitic schists.



Biotite occurs at a higher grade in these graphitic schists and cordierite forms at lower grades in the same schists.

North of the Shalimar Tonalite, biotite is first recorded in MU4489, which contains the assemblage:

green hornblende(?) - plagioclase - chlorite - calcite - biotite

However, closer to the contact (MU4500) pelitic rocks containing the chlorite-phengite pair are biotite free. The reasons for this have been explained in part one, but the point being that an entirely different type of reaction has produced biotite in rocks that are devoid of white mica and/or K-feldspar

4. DISCUSSION

An investigation of the metamorphic zones and metamorphic reactions has facilitated reasonable estimations of the temperature gradient across the aureole of the Walcha Road Adamellite. The computed temperature suggested for the immediate contact (605°C) and the total pressure suggested (1.5-2.0Kb) for the aureole region places the inner zone of the Walcha Road aureole in the lower subdivision of Winkler's (1967) cordierite-K-feldspar hornfels facies.

At the pressure conditions envisaged for the Walcha Road aureole, orthopyroxene would form at temperatures between 730°C and 760°C (Winkler, 1967, p73), these temperatures being higher than the actual estimated intrusion temperature. (No orthopyroxene is found in xenolithic material, further evidencing that the suggested intrusion temperature was close to 700°C .)

The use of assemblages containing cordierite and garnet as indicators of metamorphic grade is well documented (Wynne-Edwards and Hay, 1963; Currie, 1971, 1974; Hensen and Green, 1971, 1973; Hutcheon, Froese and Gordon, 1973). At Walcha Road almandine garnet associated with cordierite occurs within 250 metres of the contact (see chapter seven, part one), and it is from the outer cordierite-almandine zone that analyses of cordierite and garnet are available (Tables 11 and 17). Using these analyses and the data of Hensen and Green (1972, Figure 3, p155) the pressure and temperature conditions that existed 250 metres from the contact of the adamellite were 600°C , 4.5Kb. According to observed mineralogy and to the estimated temperature

gradient of the aureole a temperature and pressure of 600°C and 4.5Kb is too high for the Walcha Road aureole. Impurities in the garnet would allow it to be stable at lower pressures, however, the lower pressure would still not be in the 1.5Kb-2.0Kb range. Similar high pressures are obtained when using the data of Currie (op. cit.) and Hutcheon, Froese and Gordon (op. cit.).

The absence of sillimanite in the highest temperature (605°C) zone of the Walcha Road aureole implies that the total pressure suggested (1.5-2.0Kb) is approximately correct.

Explanation for Figure 16:

- (a) Muscovite + quartz \longrightarrow K-feldspar + Al_2SiO_5 + H_2O
(Winkler, 1967)
Muscovite + quartz \longrightarrow sanidine + sillimanite + H_2O
(Day, 1973)
- (b) Chlorite + muscovite \longrightarrow staurolite + biotite + H_2O
(Hoschek, 1967)
- (c) Aluminium silicate curves and triple point location
(Holdaway, 1971)
- (d) Chlorite + muscovite \longrightarrow cordierite + biotite + Al_2SiO_5
(Hirschberg and Winkler, 1968)
- (e) Chlorite + andalusite \longrightarrow cordierite + corundum
(Seifert, 1973)
- (f) Minimum melting curve (Luth et. al., 1964)

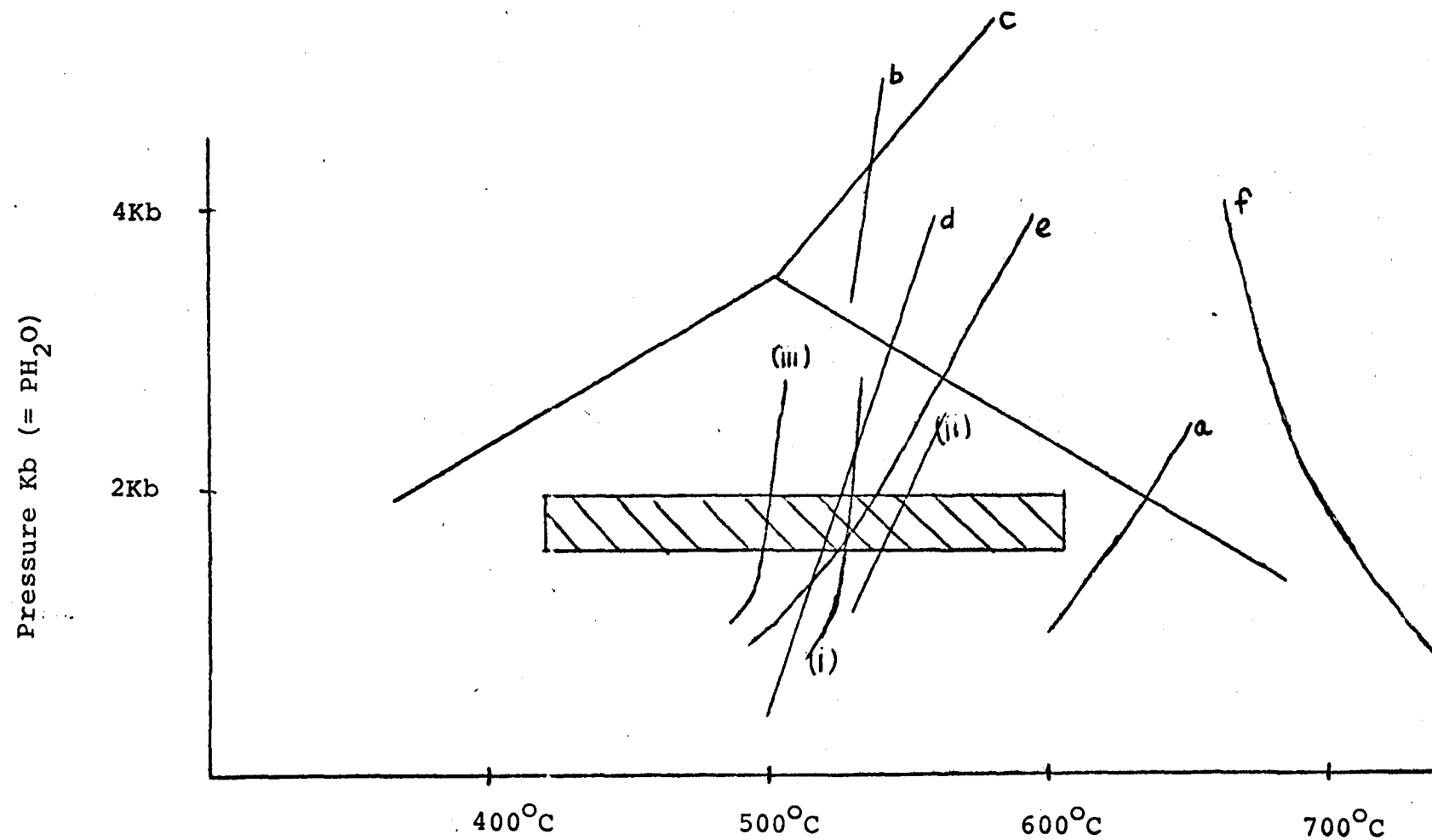


Figure 16: Shaded area represents PT conditions that existed in the Walcha Road aureole.

- (i) Muscovite + chlorite + 3 quartz \longrightarrow 2 cordierite +
biotite + $8\text{H}_2\text{O}$
- (ii) Biotite + 7 andalusite + 8 quartz \longrightarrow 3 cordierite +
muscovite
- (iii) 5 K-feldspar + 2 chlorite \longrightarrow 4 biotite + muscovite +
andalusite + 13 quartz + $4\text{H}_2\text{O}$

5. BIBLIOGRAPHY

- Albee, A.L.: 1968, Metamorphic Zones in Northern Vermont. In: Zen, White, Hadley and Thompson, ed., Studies of Appalachian Geology. New York: Interscience.
- Barth, T.W.F.: 1962, Theoretical Petrology. 2nd Ed. New York., John Wiley.
- Brown, E.H.: 1971, Phase Relations of Biotite and Stilpnomelane in the Greenschist Facies. Contr. Mineral. and Petrol. 31, 275-299.
- Currie, K.L.: 1971, The Reaction 3 Cordierite = 2 Garnet + 4 Sillimanite + 5 Quartz in the Opinicon Lake Region, Ontario. Contr. Mineral. and Petrol. 33, 215-226.
- Currie, K.L.: 1974, A Note on the Calibration of the Garnet-Cordierite Geothermometer and Geobarometer. Contr. Mineral. and Petrol. 44, 35-44.
- Dahl, O.: 1972, Some Aspects on the Evolution of Fleck Gneisses in the Vastervik Area. Geologiska Foreningen i Stockholm Forhandlingar. Vol. 94 Pt. 1.
- Day, H.N.: 1973, The High Temperature Stability of Muscovite Plus Quartz. Am. Mineralogist. Vol. 58, 255-262.
- Ernst, W.G.: 1963, Significance of Phengitic Micas from Low Grade Schists. Am. Mineralogist. Vol. 48, 1357-1373.
- Evans, B.W.: 1964, Application of a Reaction Rate Method to the Breakdown Equilibria of Muscovite and Muscovite + Quartz. Am. Journ. Sc., 263, 647-667.
- Fyfe, W.S.: 1967, Stability of the Al_2SiO_5 Polymorphs. Chem. Geol., Vol. 2 67-76.
- Hensen, B.J., and Green, D.H.: 1973, Experimental Study of the Stability of Cordierite and Garnet in Pelitic Compositions at High P and T. Pt. III. Synthesis of Experimental Data and Geological Applications. Contr. Mineral and Petrol. 38, 151-166.

- Hess, P.C.: 1969, The Metamorphic Paragenesis of Cordierite in Pelitic Rocks. Contr. Mineral. and Petrol. 24, 191-207.
- Hirschberg, A., Winkler, H.G.F.: 1968, Stabilitätsbeziehungen zwischen Chlorit, Cordierite und Almandin bei der Metamorphose. Contr. Mineral. and Petrol. 18, 17-42.
- Holdaway, M.J.: 1971, Stability of Andalusite and the Aluminium Silicate Phase Diagram. Am. Jour. Sc., Vol. 271, 97-131.
- Hoschek, G.: 1967, Untersuchungen zum Stabilitätsbereich von Chloritoid und Staurolith. Contr. Mineral. and Petrol. Vol. 14, 123-162.
- Hoschek, G.: 1969, The Stability of Staurolite and Chloritoid and their Significance in Metamorphism of Pelitic Rocks. Contr. Mineral. and Petrol. Vol. 22, 208-232.
- Hutcheon, I., Froese, E., Gordon, T.M.: 1974, The Assemblage Quartz-Sillimanite-Garnet-Cordierite as an Indicator of Metamorphic Conditions in the Daly Bay Complex, N.W.T. Contr. Mineral and Petrol. Vol. 44, 29-34.
- Joplin, G.A.: 1942, Petrological Studies in the Ordovician of New South Wales. I The Cooma Complex. Proc. Linn. Soc. NSW 67, 156-196.
- Loomis, T.P.: 1972, Contact Metamorphism of Pelitic Rock by the Ronda Ultramafic Intrusion, Southern Spain. Geol. Soc. Am. Bull., Vol. 83, 2449-2474.
- Luth, W.C., Jahns, R.H., Tuttle, O.F.: 1964, The Granite System at Pressures of 4-10Kb. Journ. Geophys. Research. 69, 759-773.
- Mather, J.D.: 1970, The Biotite Isograd and the Lower Greenschist Facies in the Dalradian Rocks of Scotland. Journ. Petrol., Vol. 11 Pt. 2, 253-275.
- McNamara, M.J.: 1966, Chlorite-Biotite Equilibrium Reactions in a Carbonate Free System. Journ. Petrol., Vol. 7, No. 3, 404-414.

- Okrusch, M.: 1969, Die Gneishornfelse um Steinach in der Oberpfalz - Eine Phasenpetrologische Analyse. Contr. Mineral. and Petrol., Vol. 22, 32-72.
- Pitcher, W.S., Berger, A.R.: 1972, The Geology of Donegal - A Study of Granite Emplacement and Unroofing. Regional Geology Series. Wiley-Interscience, Toronto.
- Ramsay, C.R.: 1973, The Origin of Biotite in Archean Meta Sediments Near Yellowknife, N.W.T., Canada. Contr. Mineral. and Petrol. Vol. 42, 433-454.
- Schreyer, W., Yoder, H.S.: 1961, Breakdown Reactions of Cordierite. Carneg. Inst. Wash. Year Book. 60 151-152.
- Seifert, F.: 1969, Compatibility Relations of the Aluminium Silicates in the Systems $\text{MgO-Al}_2\text{O}_3\text{-SiO}_2\text{-H}_2\text{O}$ and $\text{K}_2\text{O-MgO-Al}_2\text{O}_3\text{-SiO}_2\text{-H}_2\text{O}$ at High Pressures. Am. Jour. Sc., Vol. 267, 371-388.
- Seifert, F.: 1970, Low Temperature Compatibility Relations of Cordierite on Haplopelites of the System $\text{K}_2\text{O-MgO-Al}_2\text{O}_3\text{-SiO}_2\text{-H}_2\text{O}$. Journ. Petrol., Vol 11, 73-99.
- Seifert, F.: 1973, Stability of the Assemblage Cordierite-Corundum in the System $\text{MgO-Al}_2\text{O}_3\text{-SiO}_2\text{-H}_2\text{O}$. Contr. Mineral. and Petrol., Vol. 41, 171-178.
- Seifert, F.: 1974, Stability of Sapphirine: A Study of the Aluminous Part of the System $\text{MgO-Al}_2\text{O}_3\text{-SiO}_2\text{-H}_2\text{O}$. Journ. Geol. Vol. 82, 173-204.
- Tilley, C.E.: 1924, Contact Metamorphism in the Comrie Area of the Perthshire Highlands. Quart. Journ. Geol. Soc., Vol. 80, 22-71.
- Turner, F.J.: 1948, Evolution of Metamorphic Rocks. Mem. Geol. Soc. of Am., No. 30.
- Vernon, R.H.: 1972, Reactions Involving Hydration of Cordierite and Hypersthene. Contr. Mineral. and Petrol. 35, 125-137.
- Weisbrod, A.: 1973, Cordierite-Garnet Equilibrium in the System Fe-Mn-Al-Si-O-H. Carnegie Inst. Wash. Year Book.

Winkler, H.G.F.: 1957, Experimentelle Gesteinsmetamorphose,
I. Geochim et Cosmochim. Acta. Vol. 13, 42-69.

Winkler, H.G.F.: 1967, Petrogenesis of Metamorphic Rocks.
Springer-Verlag., New York. 2nd ed.

Wynne-Edwards, H.R., Hay, P.W.: 1963, Co-Existing
Cordierite and Garnet in Regionally Metamorphosed
Rocks from the Westport Area, Ontario. Can.
Mineralogist. 7, 453-478.

P A R T T H R E E

APPENDICES

APPENDIX ONE

STRUCTURAL ASPECTS AT WALCHA ROAD

(a) Introduction

The nature of the rocks, the poor outcrop and the recrystallisation of the rocks in the inner zones of the Walcha Road aureole make structural mapping difficult. Mesoscopic structures (folds and cleavages) are rarely observed in outcrop.

Recognition of S_1 (slaty cleavage) and S_2 (crenulation cleavage) in thin section indicates that the area has been multiply deformed. S_1 is represented by a preferred orientation of the phyllosilicates and quartz, the cleavage surface being parallel or subparallel to S_0 (bedding). S_2 structures range from incipient crenulations to distinct cleavage traces defined by thin zones of carbonaceous material. The S_2 surfaces are always oblique to the S_1 fabric. S_1 and S_2 can only be identified in thin section and are well developed in the fine grained graphitic schists (Plate 32). In the coarser grained schists a crude S_1 surface is present and no S_2 surface has been observed. A flattening induced by the intruding adamellite has locally caused the cleavage traces to wrap around the porphyroblasts.

In the cordierite-K-feldspar zone complete recrystallisation of the rocks has destroyed the S_1 and S_2 structures. A "gneissic" or "migmatitic" metamorphic foliation (see plates in this section) defined by



Plate 32: MU4404, Crenulation cleavage developed in
pelitic layer of schist.
x 65



Plate 33: MU4361, Ptygmatic quartz vein caused by
flattening.
x 25 (crossed nicols)

alternating micaceous and quartzo-feldspathic layers has developed in this zone. The foliation appears concordant with the granite contact. It is steeply dipping and generally has the same strike as the contact.

The S_1 surface is parallel or subparallel to S_0 (bedding) in all thin sections observed. This feature, coupled with the fact that no fold hinges were seen in the field suggests that the area has undergone tight isoclinal folding (F_1), with locally developed F_2 folds (defined by the crenulation cleavage).

The Walcha Road Adamellite is cut by a NNW/ESE trending fault which displaces the adamellite by 0.8km to the west. This fault was added after a study of aerial photographs and a subsequent study of the strikes of bedding close to the adamellite in this area. The displacement of isograds shown on the map is only inferred as most of this area is covered by Miocene laterite and associated soil cover.

(b) Structures Associated with the Intrusion of the Adamellite

Flood (1971) and Lewington (1973) noted a change in the regional N-S trend in the vicinity of the adamellite. As the contact is approached the foliation (bedding) becomes subparallel to the contact. Within 10 metres of the contact the rocks are sheared to such an extent that only disconnected fold hinges are visible. The development of a gneissic foliation at the contact suggests metamorphic differentiation accompanied by mobilisation of mineral components (discussed in chapter

seven of Part One). Small (5-20cm) folds occur in this foliation close to the contact (not observed at distances greater than 30 metres). The folds always have "S" vergence and plunge at approximately 80° in a general northerly direction (always parallel to the contact).

The writer considers that the "gneissic" foliation, and the small folds are genetically related to the intrusion of the adamellite. The clear spatial relationship, in that both foliation and small folds are only developed up to 30 metres from the contact, and description of similar structures elsewhere (Ramberg, 1970; Dearman, 1968) tend to suggest a cause and effect relationship.

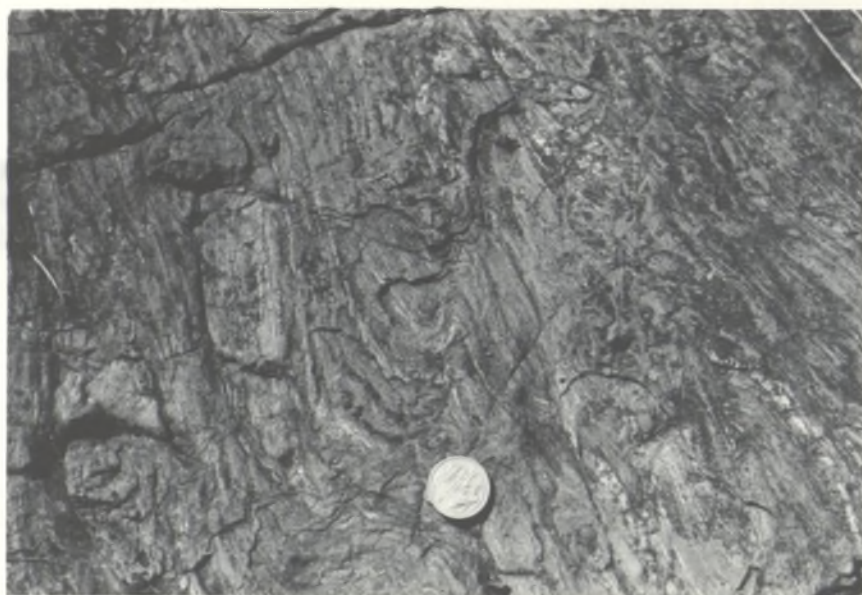


Plate 34; "S" vergence of fold from location three (Figure 17)

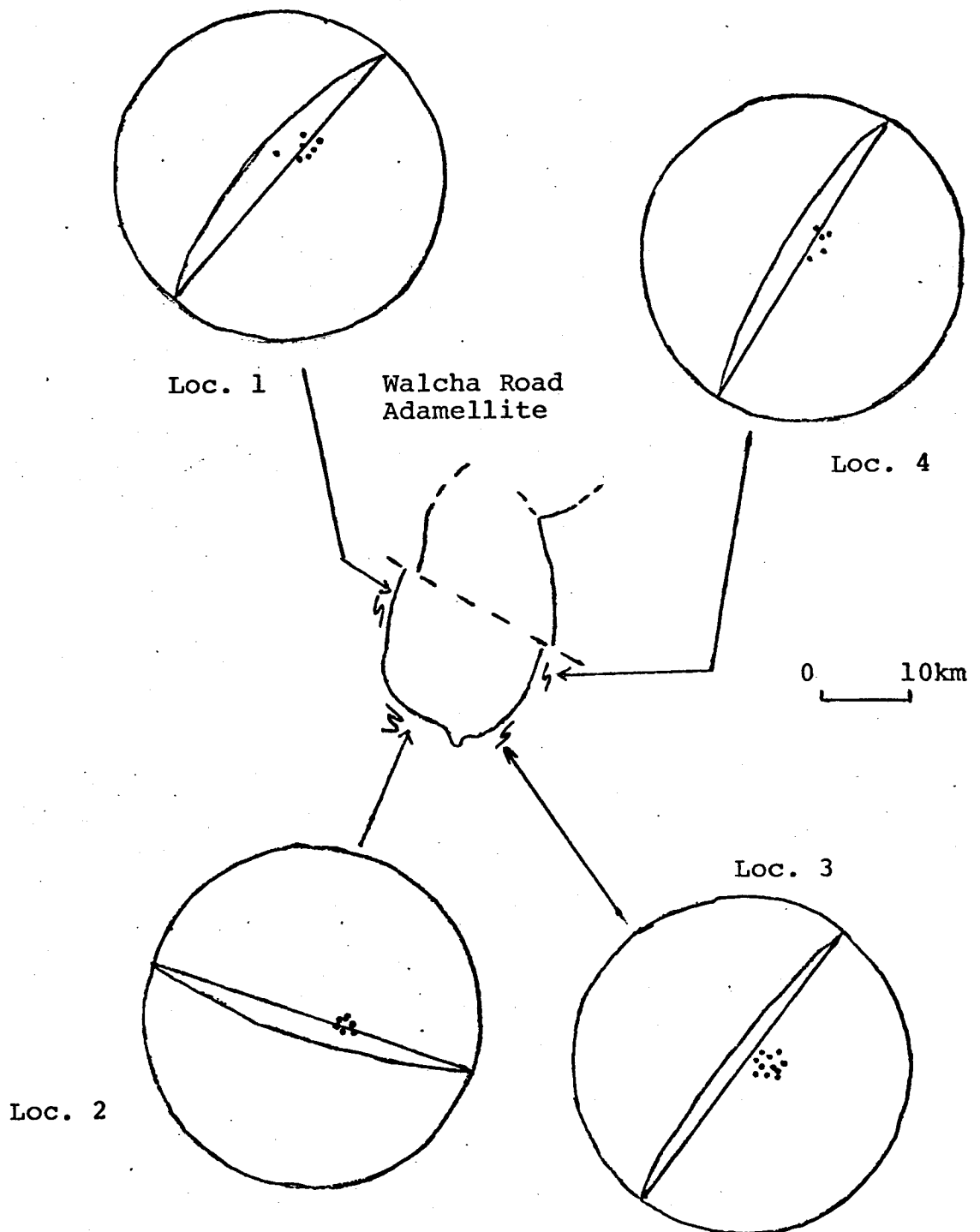


Figure 17: Orientation diagram of fold axes



Plate 35: "M" vergence of fold from location two
(Figure 17)



Plate 36: "M" vergence of fold from location four
(Figure 17)



Plate 37: "S" vergence of folds from location three
(Figure 17)

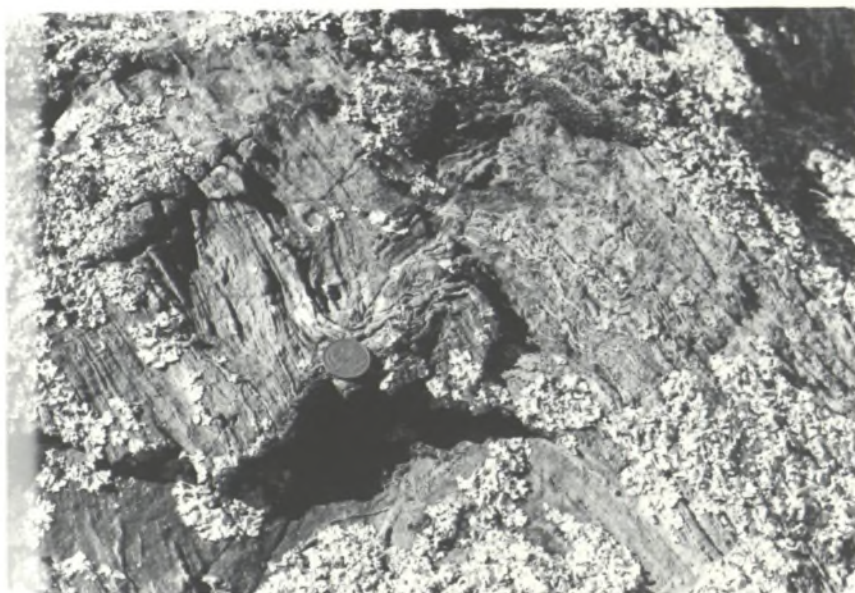


Plate 38: Small fold ("S" vergence) from location one
(Figure 17)

APPENDIX TWO

THE YARRAHAPINNI AREA

(a) Introduction

The Yarrahapinni area lies 185km due east of Walcha Road, 32km north-northeast of Kempsey and 10km south of Macksville in New South Wales. The fine grained (Permian) carbonaceous rocks are intruded by fine and medium grained hornblende-biotite adamellites (Way-Way Granite) of Permian age. Associated with the carbonaceous sediments are minor acid volcanics,

Rare sedimentary structures (symmetrical ripple marks) in the graphitic sediments suggest that shallow water conditions prevailed.

The regional metamorphism has been investigated by Leitch (in prep.) and the Way-Way intrusives are currently being studied by R. Webber (Macquarie University). No other previous work has been carried out in the area. The hornfels-adamellite boundaries were mapped by Webber (op. cit.) and these boundaries, with minor modifications by the writer, have been used in the preparation of a metamorphic map of the area (Appendix 10b).

(b) Structure

The Yarrahapinni area has been multiply deformed, with evidence for four stages of deformation present in the hornfelses. Bedding (S_0) relationships are

TABLE 22

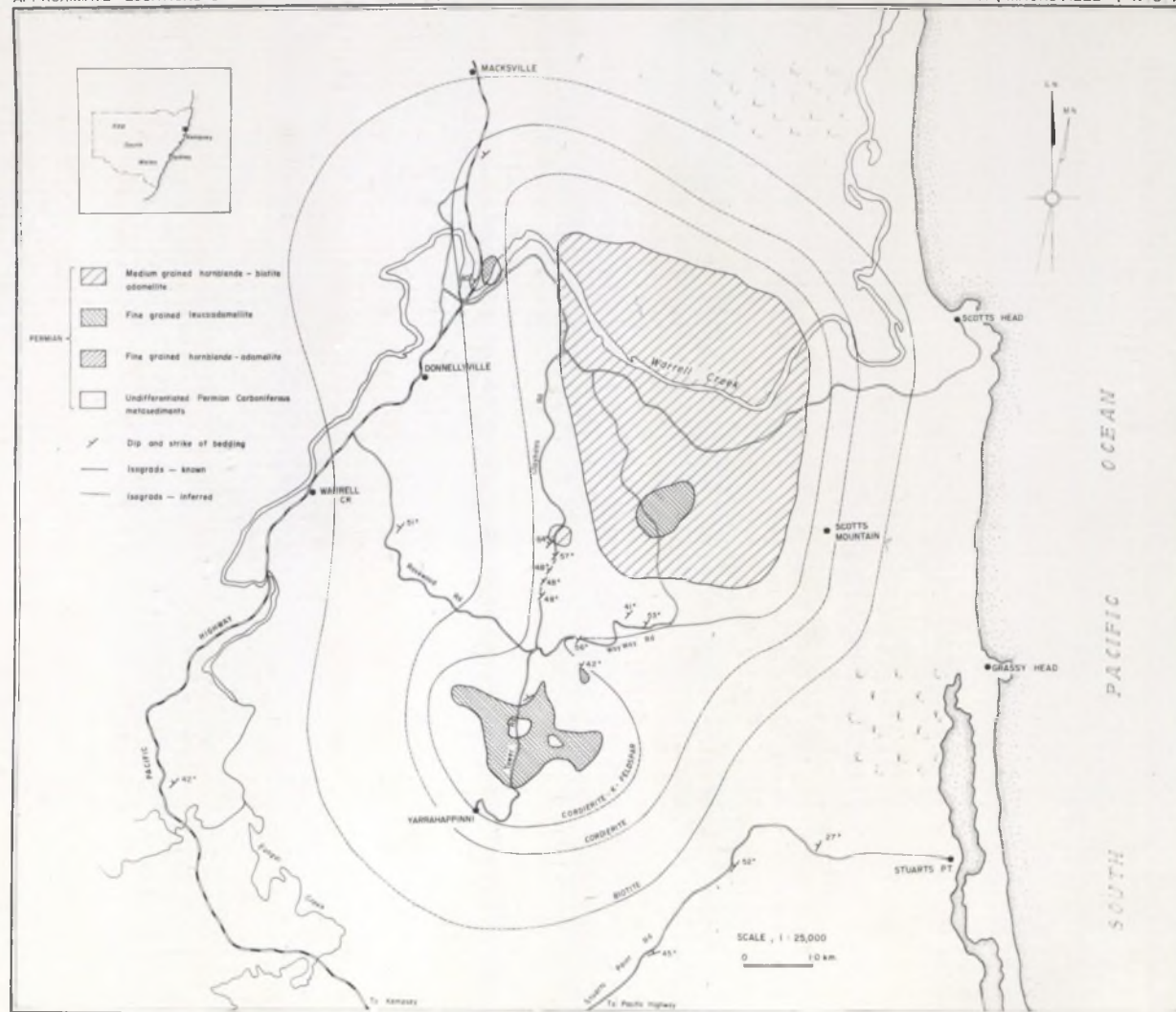
CHEMICAL ANALYSES OF CARBONACEOUS
META-PELITES FROM YARRAHAPINNI, NSW

	MU4507	MU4503	MU4528	
SiO ₂	67.08	66.89	65.53	
TiO ₂	0.79	0.85	0.84	
Al ₂ O ₃	15.61	17.66	14.41	
Fe ₂ O ₃	0.20	0.68	0.87	
FeO	5.44	4.36	3.96	
MnO	0.03	0.06	0.06	
MgO	2.22	2.25	1.89	
CaO	0.92	0.69	1.51	
K ₂ O	3.07	3.25	2.49	
Na ₂ O	2.15	2.22	3.81	
P ₂ O ₅	0.12	0.10	0.22	
Total	97.63	99.01	95.59	
	CK	CK	R	
MgO/MgO + FeO	42.13	47.90	45.98	
	MU4529	MU4527	MU4530	MU4526
SiO ₂	73.05	68.31	74.21	69.67
TiO ₂	0.56	0.76	0.65	0.81
Al ₂ O ₃	12.95	17.27	13.47	16.38
Fe ₂ O ₃	0.09	2.64	0.39	2.43
FeO	2.29	0.69	2.83	0.44
MnO	0.04	0.01	0.05	0.01
MgO	1.17	0.82	1.44	1.15
CaO	1.49	0.01	0.63	0.01
K ₂ O	3.86	3.14	2.97	2.95
Na ₂ O	3.23	2.00	1.98	1.58
P ₂ O ₅	0.14	0.09	0.07	0.15
Total	98.87	95.73	98.69	95.48
	B	R	C	R
MgO/MgO + FeO	47.62	67.89	47.54	82.37

Analyst: G.S. Teale

CK = Cordierite-K-feldspar zone
C = Cordierite zone
B = Biotite zone
R = Regional

Fig. 18.



only recognisable where rhyolitic (?) flows occur intercalated with the graphitic sediments. The S_1 surface is represented by a preferred orientation of the graphitic material, and is sub parallel to S_0 , when S_0 can be recognised. S_2 can only be observed in thin section and occurs as distinct cleavage traces defined by thin zones of graphitic material, occurring in cordierite porphyroblasts (Plate 39). The formation of the cordierite has preserved the microscopic S_2 crenulation within the porphyroblast, with complete destruction of the S_2 surface in the recrystallised matrix.



Plate 39: MU4504, Crenulation (S_2) preserved in cordierite porphyroblast. Note second generation cordierite (formed during the cordierite-K-feldspar producing reaction) x 65 (crossed nicols)

The S_3 crenulation surface can be recognised in hand specimen. In thin section it is observed that the S_3 surface occurs pre the formation of the cordierite porphyroblasts. The S_4 surface, however, has occurred post the formation of the cordierite porphyroblasts and in thin section it can be easily distinguished from the S_3 cleavage surface. The S_4 surface deforms the cordierite porphyroblasts, and this deformation or "drag" effect is shown in Plate 40.



Plate 40: MU4508, S_4 crenulation cleavage. Note the "drag" effect on the porphyroblasts
x 65

(c) General Geology

The outstanding feature of the Yarrahapinni area is the wide metamorphic aureole associated with the adamellite

intrusions. The extension of the aureole is in the dip direction (N-W) and it can be assumed that the intrusive bodies also dip in the same direction. The extension is also due to the nature of the intruded sediments. A similar widening of the cordierite zone at Walcha Road was due to the presence of dispersed graphitic material also. This has been discussed in Part One.

A release of H_2O and possibly K_2O from the top of the intrusion has converted the hornfelses in some sections of the area to rocks containing the assemblage.

Muscovite-biotite-chlorite-graphite. This release of volatiles was presumably responsible for the minor molybdenite mineralisation that is present.

Chemical analyses of hornfelses from the area illustrate the similarity of chemistry between the Walcha Road schists and the hornfelses from the Yarrahapinni area (Table 22). It is noted that when analyses of Yarrahapinni rocks are plotted on various compositional diagrams (Figures 19 and 20) their locations on those diagrams are similar to plots of analyses of Walcha Road schists. Two Yarrahapinni analyses, however, plot well away from the expected locality. These two rocks (MU4527, MU4526) are pelites from the regionally metamorphosed rocks outside the aureole and contain extremely low $FeO/Fe_2O_3 + FeO$ ratios, this low ratio being responsible for their location close to the Al apex of the AFK and AFM projections.

(d) Metamorphic Zones

(i) Cordierite-K-Feldspar Zone

Rocks from the cordierite-K-feldspar zone cannot be distinguished from rocks of the cordierite zone in hand specimen. Meta-pelites from both zones have a similar spotted appearance, the spots representing cordierite porphyroblasts. In thin section the K-feldspar is easily identified after staining with sodium cobaltinitrite. The metamorphic K-feldspar forms small xenoblastic grains and is associated with quartz and plagioclase in the granoblastic groundmass. The cordierite porphyroblasts are always highly poikiloblastic, and are much larger than associated mineral phases (up to 1mm). Mineral assemblages observed in the cordierite-K-feldspar zone are:

Red-brown biotite-cordierite-K-feldspar

Biotite-cordierite.

(ii) Cordierite Zone

The extent of the cordierite zone is shown in Figure 18. The cordierite bearing rocks of this zone occur as dark spotted hornfelses. Stable mineral assemblages developed in the meta-pelites of this zone are:

Biotite-chlorite-muscovite

Biotite-cordierite-chlorite

Biotite-cordierite-muscovite



Plate 41: MU4503, Cordierite from the cordierite zone
x 104

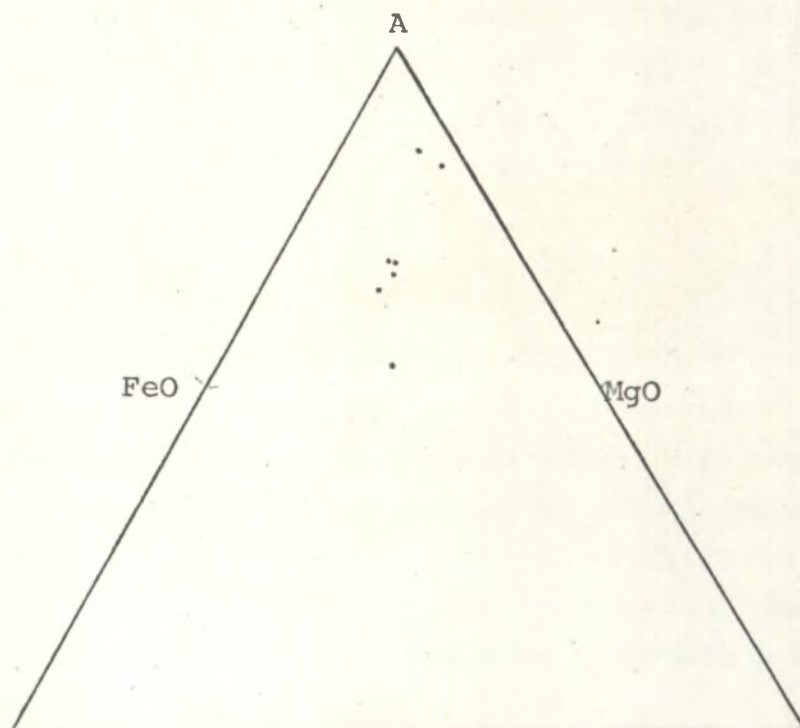
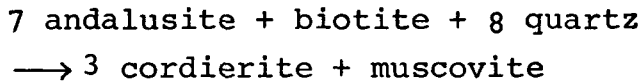


Figure 19: Carbonaceous meta-pelites plotted on AMF
projection plane

Cordierite is highly poikiloblastic, included material being mainly graphite. Cordierite has formed in most cases by the reaction:



This reaction has been discussed in Part Two.

(iii) Biotite Zone

Biotite zone hornfelses are distinguished in hand specimen from higher grade hornfelses by the absence of "knots" and from lower grade rocks by a more massive outcrop pattern. In this zone, biotite, chlorite and white mica (minor) can be observed in thin section, these minerals having no real preferred orientation (Plate 42). The biotite occurs as small (0.02mm) grains with poorly developed (001) faces. There is an increase in the size of the biotite as metamorphic grade increases.

(e) Discussion

The Yarrahapinni rocks were used in this study to help delineate cordierite forming reactions. The rocks have similar $\text{MgO}/\text{MgO} + \text{FeO}$ ratios as the Walcha Road meta-pelites, are 1-9% corundum normative, which is again similar to the Walcha Road meta-pelites and both areas have undergone similar temperature conditions during contact metamorphism.

The textural evidence for the andalusite cordierite reaction used in part two, was observed at Yarrahapinni. The study of the Yarrahapinni hornfelses helped a great deal in providing an understanding of the metamorphic zones and metamorphic reactions that occur in the Walcha Road area. The Yarrahapinni study itself is also of value as biotite, cordierite and cordierite-K-feldspar isograds have been located in an aureole which was previously unknown.

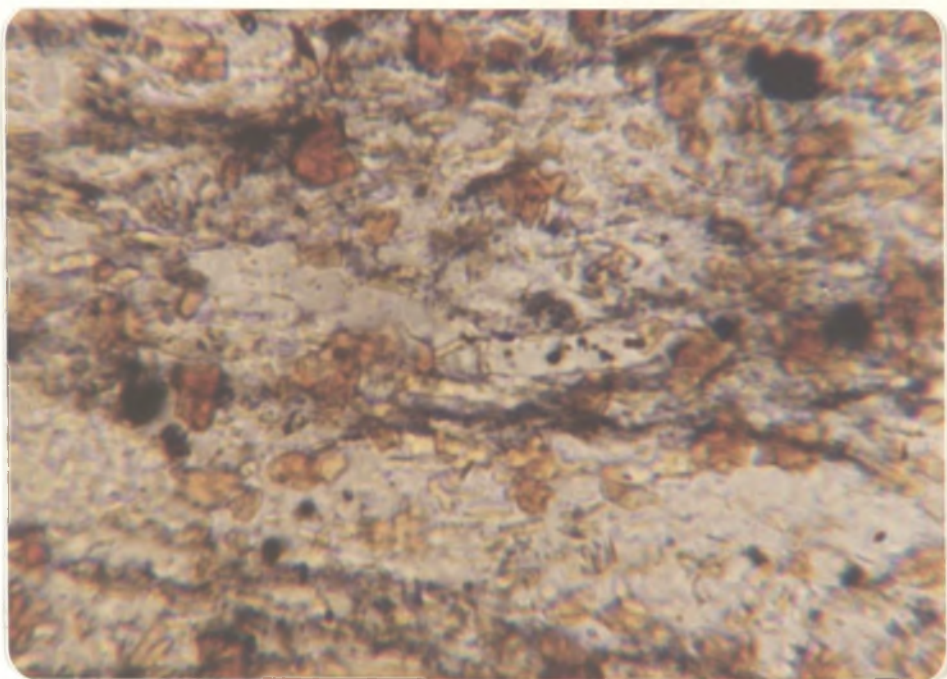


Plate 42: MU4529, Biotite and chlorite from the
biotite zone.
x 415

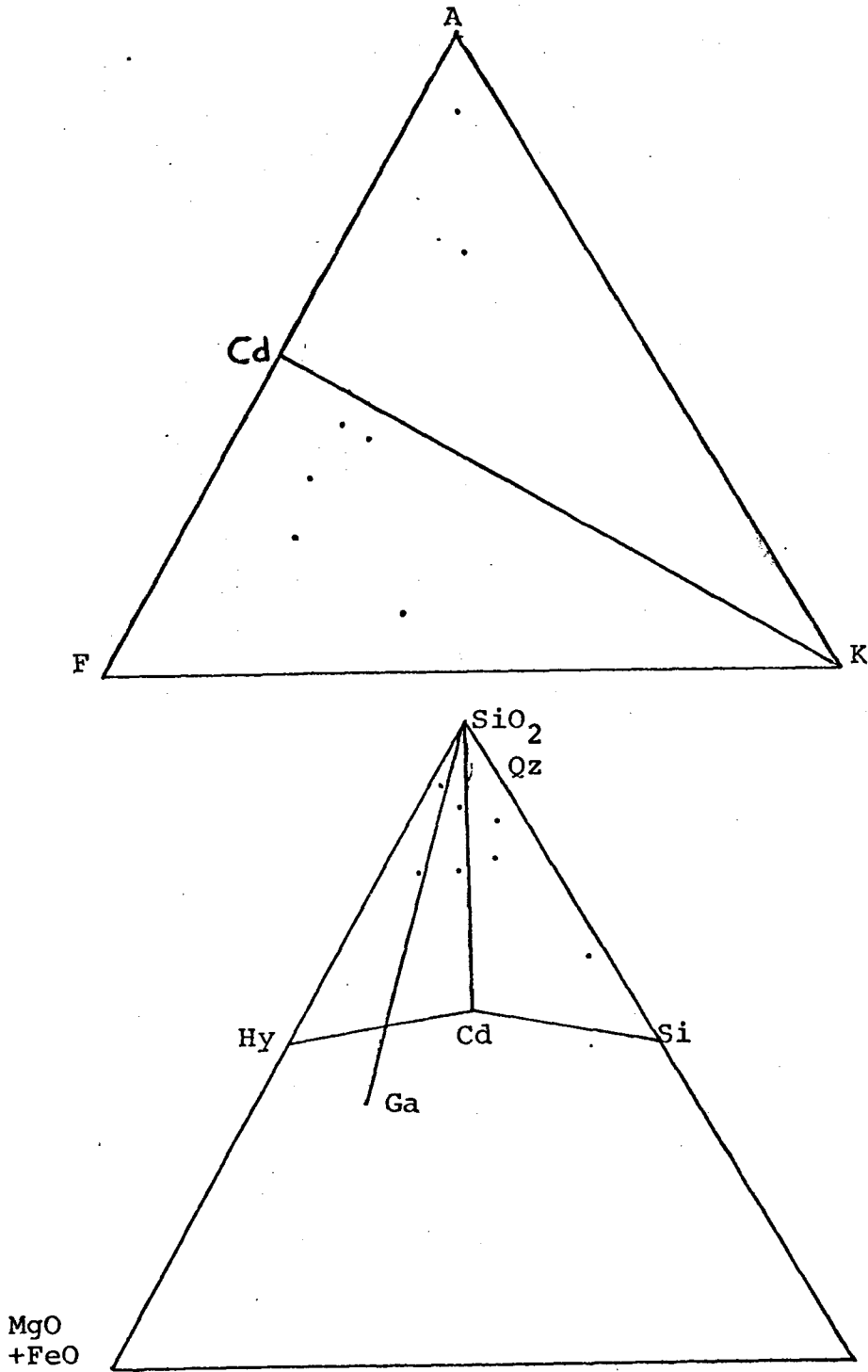


Figure 20: AFK (top) and SiO₂ - (MgO+FeO) - Al₂O₃ diagrams showing positions of carbonaceous meta-pelites from Yarrahapinni.

TABLE 23

C.I.P.W. NORMS OF CARBONACEOUS
META-PELITES FROM YARRAHAPINNI, NSW

Specimen No.	MU4507	MU4529	MU4530	MU4503
Quartz	33.99	33.47	46.27	34.20
Orthoclase	18.14	22.81	17.55	19.20
Albite	18.18	27.32	16.75	18.78
Anorthite	3.78	6.48	2.67	2.77
Corundum	7.37	1.09	6.02	9.48
Hypersthene	14.10	6.19	7.48	11.75
Magnetite	0.29	0.13	0.57	0.99
Ilmenite	1.50	1.06	1.23	1.61
Apatite	0.28	0.32	0.16	0.23
Total	97.63	98.87	98.69	99.01
Plag. An.	17.21	19.16	13.74	12.85

TABLE 24

TRACE ELEMENT ANALYSES OF META-PELITES
FROM YARRAHAPINNI, NSW
(IN PPM)

	MU4503	MU4530	MU4507	MU4529
Y	31.82	26.09	27.71	26.54
Sr	104.14	93.50	84.70	167.01
Zr	186.06	243.34	171.55	211.72
U	2.36	1.32	1.95	2.96
Rb	96.06	110.56	103.41	81.33
Th	10.04	9.38	9.86	6.91
Pb	10.20	9.57	15.88	35.51
Ga	15.35	13.13	14.33	12.25

Analyses in ppm

Analyst: G.S. Teale

APPENDIX THREE

ANALYTICAL PROCEDURE

X-ray fluorescent spectrometry and wet chemical techniques were used in major and trace element rock analyses. The major oxides SiO_2 , TiO_2 , Al_2O_3 , MnO , MgO , CaO , Total Fe as Fe_2O_3 , K_2O and P_2O_5 were determined by x-ray fluorescent spectrometry in the manner outlined by Norrish and Chappell (1967). Na_2O was also analysed by XRF (to compare with wet chemical techniques) using pressed powder pellets, following the method discussed by Norrish and Hutton (1969). The equipment used was a Siemens S.R.S. spectrometer, with a 4 KW generator and standard counting rack. A Cr anode tube was used in the determination of the major oxides, a Au anode tube for Zn, Cu, Ni, Cr, Mn, V and Ti trace elements. Mass absorptions for trace elements were calculated from bulk rock analyses.

Standards for Major and Trace element analyses were the U.S. Geological Survey rock standards; W-1, GSP-1, G-2, and BCR-1.

Trace element calibration was made on artificial standards prepared from crushed glossy quartz, 5 wt % cellulose binder and pure (Analar and Spec. Pure) chemical compounds.

Na_2O determinations by the XRF method did not meet the desired standards of accuracy and, therefore, Na_2O was again determined by using flame photometric techniques (Evans Electroselenium Ltd. flame photometer, model 866150) with closely spaced standards. Li_2SO_4 was used to suppress inter-element interference.

FeO was determined using the Na metavanadate titration method of Wilson (1955). Extremely accurate results were obtained using this method (U.S. Geological Survey BCR-1; FeO, 8.91%; Fe₂O₃, 3.68%: results obtained; FeO 8.81%, Fe₂O₃, 3.67%). Selected samples were re-analysed to check the consistency of the method.

Individual mineral analyses were obtained using an electron probe. The probe data was obtained from an instrument manufactured by Technisch Physische Dienst (T.P.D.), Deft, Netherlands. It is fitted with an Ortec Si (Li) detector of resolution 165 ev at 5.89 Kev, and a Northern Scientific (N.S.) 710 multichannel analyser. The following analytical conditions were used: accelerating voltage 15 KV, beam current 3nA, beam diameter 50-100 , counting period 100 sec. and a total counting rate of approximately 4000 cps.

A Siemens x-ray diffractometer was used for mineral identification. CuK α radiation and a Ni filter were used for all samples.

Optical studies were carried out on Leitz binocular normal stage microscopes. Universal stage methods were not used.

Successful staining for alkali feldspar (Sodium Cobalt-initrite) and plagioclase and cordierite (Amaranth) was carried out using the technique discussed by Norman (1974).

References

1. Borg, I.Y. and Smith, D.K., 1969 Calculated X-Ray Powder Patterns for Silicate Minerals. Geol. Soc. Am. Mem., 122

2. Norrish, K. and Chappell, B.W., 1967 X-Ray Fluorescence Spectrography; in, Physical Methods in Determinative Mineralogy, 161-214, ed. J. Zussman, Academic Press, London.
3. Norrish, K. and Hutton, J.T., 1969 An Accurate X-Ray Spectrographic Method for the Analysis of a Wide Range of Geological Samples. Geochim. et Cosmochim. Acta, Vol. 33, No. 4, pp431-453.
4. Norman II, M.B., 1974 Improved Techniques for Selective Staining of Feldspar and Other Minerals Using Amaranth. Jour. Res. U.S. Geol. Survey, Vol. 2, No. 1, pp 73-79.
5. Wilson, A.D., 1955 A New Method for the Determination of Ferrous Ion in Rocks and Minerals. Bull. Geol. Surv., Gt. Brit., 9, pp 56-58.

APPENDIX FOUR

MAPPING AND SAMPLING TECHNIQUES

Sampling and mapping was carried out using NSW standard 2 inches to 1 mile topographic maps (sheet names: Walcha Road, Kentucky, Aberbaldie (provisional)) and aerial photographs (Lands Department, Nundle 1458 and Bendemeer 1676 and 1659 series). Dr. R.H. Flood provided excellent photographic enlargements of aerial photographs south of the Oxley Highway onto which sample locations were plotted. North of the Oxley Highway sample locations were plotted onto the standard aerial photographs. The large scale map (Appendix 10a) was compiled using all of the above sources.

South of the Oxley Highway there were no sampling difficulties, as outcrop in the many creeks is usually excellent. It was found, however, that high potassium bearing rocks away from the contact, being more micaceous, weathered more easily than associated silica rich rocks. North of the Oxley Highway minor Tertiary basalt and extensive soil cover did create minor difficulties in the collection of samples. In the ten traverses undertaken an attempt was made to collect a fresh sample every one hundred metres (or less).

In the Yarrahapinni area, the isograd map was compiled using the Macksville and Eungai 1:25,000 topographic sheets (Lands Department). Outcrop is usually good, except for the regionally metamorphosed sediments outside the aureole.

APPENDIX FIVE

TRACE ELEMENT ANALYSES FOR META-PELITES
ADJACENT TO THE WALCHA ROAD ADAMELLITE

	MU4354	MU4462	MU4404	MU4383
Y	29.41	31.14	25.87	31.29
Sr	168.07	135.38	216.56	94.88
Zr	290.04	167.73	163.18	152.93
U	2.30	9.29	2.62	1.62
Rb	121.40	115.07	91.19	72.97
Th	8.66	9.34	7.09	12.48
Pb	10.02	11.89	12.73	7.83
Ga	18.80	19.03	15.24	19.73
Zn	586.02	320.67	747.02	1085.47
Cu	44.00	181.18	303.89	54.12
Ni	36.40	10.88	149.31	424.56
Mn	1250.00	838.59	984.93	2177.78
Cr	5.68	89.87	100.21	314.76
V	60.06	263.57	233.05	365.78
Ti	8069.20	9338.80	9255.50	15255.39

	MU4353	MU4397	MU4368	MU4435
Y	22.60	24.02	30.54	20.58
Sr	105.17	262.09	274.48	279.96
Zr	111.51	173.38	152.68	97.76
U	2.26	1.32	1.72	.67
Rb	101.20	92.33	58.68	42.92
Th	9.89	7.59	5.02	3.02
Pb	16.38	9.96	13.14	10.59
Ga	9.83	7.23	13.13	12.57
Zn	631.38	594.36	712.89	775.49
Cu	19.74	110.10	141.86	377.43
Ni	138.63	84.01	70.90	71.89
Mn	834.13	1133.00	996.51	1335.55
Cr	96.53	49.54	49.71	63.94
V	136.00	168.58	211.92	283.30
Ti	6989.27	8402.19	9599.47	10842.98

Appendix Five (cont.)

	MU4437	MU4439	MU4374	MU4400
Y	17.99	18.40	28.21	16.11
Sr	137.64	380.63	84.14	334.62
Zr	93.82	86.60	228.54	104.71
U	1.48	0.94	1.45	1.92
Rb	61.23	58.42	85.40	97.22
Th	6.89	2.10	11.08	5.60
Pb	10.79	5.24	6.83	9.68
Ga	6.11	15.60	16.34	12.61

	MU4431	MU4382	MU4438	MU4356
Y	25.59	34.10	26.54	64.93
Sr	110.11	142.08	119.67	299.99
Zr	140.69	159.53	104.59	301.13
U	1.18	1.76	0.97	2.99
Rb	136.33	99.16	91.71	136.04
Th	7.48	16.52	6.43	8.51
Pb	10.46	23.39	9.54	19.39
Ga	14.08	19.97	13.10	19.66

	MU4413	MU4366	MU4409	MU4395
Y	20.58	32.45	25.17	31.44
Sr	311.80	118.03	360.91	219.52
Zr	160.46	162.48	189.25	187.69
U	2.11	1.15	1.26	3.34
Rb	60.32	108.82	69.76	91.49
Th	6.53	7.94	6.40	8.02
Pb	12.98	10.66	13.31	12.64
Ga	13.14	15.32	15.00	17.02

Appendix Five (cont.)

	MU4418	MU4465	MU4450	MU4466
Y	22.50	27.12	20.96	28.31
Sr	249.50	254.95	388.50	229.49
Zr	113.48	199.98	119.25	210.94
U	1.75	2.45	1.92	2.13
Rb	66.71	108.78	51.38	54.37
Th	4.54	8.96	2.35	8.61
Pb	14.43	23.04	11.90	11.10
Ga	15.78	14.95	15.91	15.45

	MU4417	MU4403	MU4491	MU4393
Y	22.47	23.72	22.25	32.03
Sr	423.48	217.57	578.58	190.97
Zr	107.91	165.70	104.99	197.68
U	1.96	1.97	1.20	3.55
Rb	79.17	87.55	20.88	114.29
Th	5.91	8.00	3.62	9.93
Pb	13.83	15.14	9.47	15.09
Ga	14.25	15.81	14.10	16.32

Analyses in ppm

Analyst: G.S. Teale

APPENDIX SIX

Location of Samples
Walcha Road Area

Sample No.	Major Mineralogy	Location *
MU4353 +	Cordierite-biotite-K-feldspar	A3458, 65690
MU4354 +	Cordierite-biotite-K-feldspar	A3456, 65690
MU4355	Cordierite-biotite-K-feldspar	A3454, 65690
MU4356 +	Cordierite-biotite-K-feldspar	A3453, 65690
MU4357	Cordierite-biotite-K-feldspar	WR4020, 6400
MU4358 +	Cordierite-biotite-K-feldspar	A3455, 65687
MU4359 +	Cordierite-K-feldspar-biotite	A3456, 65687
MU4360	Biotite-cordierite	A3457, 65686
MU4361	Biotite-Muscovite-chlorite-andalusite	A3459, 65685
MU4362	Biotite	A3461, 65685
MU4363	Diopside-fibrous blue green amphibole-calcite	A3462, 65685
MU4364	Biotite-chlorite-muscovite	A3463, 65680
MU4365	Blue-green amphibole-biotite	A3464, 65679
MU4366 +	Biotite-chlorite-muscovite	A3469, 65678
MU4367	Diopside-green amphibole	WR4125, 6440
MU4368 +	Cordierite-biotite-graphite	WR4125, 6425
MU4369	Biotite-cordierite-graphite	WR4124, 6424
MU4370 +	Diopside-grossular-calcite	WR4138, 6412
MU4371	Biotite-green amphibole	WR4208, 6425
MU4372	Biotite-fibrous radiating colourless amphibole	WR4200, 6440

+ Analysed sample

* Locations taken from Department of Lands 1:31680 topographic sheets

Only thin sectioned samples are mentioned

WR = Walcha Road sheet

B = Balala sheet

K = Kentucky sheet

A = Aberbaldie sheet (Provisional 1:25,000 sheet)

Sample No.	Major Mineralogy	Location *
MU4373	Green amphibole-biotite	WR4180, 6440
MU4374	Biotite-chlorite-graphite	WR4175, 6450
MU4375	Green amphibole	WR4168, 6425
MU4376	Biotite-chlorite-muscovite	WR4178, 6430
MU4377	Green amphibole	WR4252, 6540
MU4378	Biotite-fibrous radiating colourless amphibole	WR4248, 6545
MU4379	Biotite-green amphibole	WR4236, 6552
MU4380	Diopside-green amphibole	WR4225, 6560
MU4381	Diopside-green amphibole	WR4223, 6561
MU4382 +	Cordierite-biotite	WR4218, 6562
MU4383 +	Cordierite-biotite	WR4215, 6564
MU4384	Cummingtonite-green-brown amphibole-biotite	WR4216, 6565
MU4385	Blue-green amphibole	WR4258, 6530
MU4386	Acicular colourless amphibole-biotite	WR4292, 6512
MU4387	Acicular, radiating colourless amphibole	WR4310, 6512
MU4388	Biotite-blue-green amphibole	WR4325, 6518
MU4389	Biotite-chlorite-muscovite- graphite	WR4352, 6520
MU4390	Biotite-graphite-chlorite- muscovite	WR4368, 6500
MU4391	Biotite-graphite	WR4380, 6502
MU4392	Biotite-chlorite-muscovite- graphite	WR4400, 6505
MU4393 +	Biotite-muscovite-chlorite- cordierite-andalusite	WR4540, 6778
MU4394	Biotite-muscovite-andalusite- chlorite-cordierite	WR4538, 6770
MU4395 +	Biotite-chlorite-muscovite- graphite	WR4565, 6760
MU4396	Biotite-chlorite-muscovite- graphite	WR4566, 6758
MU4397 +	Biotite-chlorite-muscovite graphite	WR4575, 6775

Sample No.	Major Mineralogy	Location *
MU4398	Biotite-green amphibole	WR4360, 6660
MU4399 +	Biotite-muscovite-cordierite chlorite	WR4371, 6667
MU4400 +	Biotite-cordierite-chlorite- muscovite	WR4372, 6667
MU4401	Biotite-actinolite	WR4373, 6662
MU4402	Cordierite-biotite	WR4374, 6660
MU4403 +	Biotite-muscovite-chlorite- graphite	WR4376, 6658
MU4404	Biotite-cordierite-graphite	WR4380, 6652
MU4405 +	Biotite-Cordierite-graphite	WR4378, 6655
MU4406	Green amphibole-biotite	WR4388, 6650
MU4407	Biotite-graphite	WR4420, 6635
MU4408 +	Biotite-chlorite-muscovite- graphite	WR4428, 6638
MU4409 +	Cordierite-biotite-graphite	WR4441, 6625
MU4410	Biotite-graphite-muscovite- chlorite	WR4450, 6630
MU4411	Acicular radiating colourless amphibole-biotite	WR4458, 6628
MU4412	Biotite-chlorite-muscovite	WR4466, 6625
MU4413 +	Biotite-chlorite	WR4475, 6625
MU4414 +	Muscovite-chlorite-biotite- andalusite	WR4275, 6620
MU4415	Biotite	WR4445, 6810
MU4416	Diopside-epidote-green amphibole	WR4450, 6810
MU4417 +	Biotite-muscovite	WR4470, 6810
MU4418 +	Biotite-chlorite-graphite	WR4467, 6800
MU4419	Biotite-blue-green amphibole	WR4425, 6775
MU4420	Diopside-green amphibole	WR4408, 6762
MU4421	Biotite-acicular colourless amphibole	WR4393, 6770
MU4422	Biotite-blue-green amphibole	WR4490, 6820
MU4423 +	Epidote-diopside-grossular	WR4479, 6818
MU4424	Blue-green amphibole-biotite	A3477, 65692
MU4425	Biotite-sericite	A3482, 65669

Sample No.	Major Mineralogy	Location *
MU4426	Biotite-sericite-chlorite-graphite	A3495, 65663
MU4427	Chlorite-sericite	WR4485, 6775
MU4428	Chlorite-sericite	WR4480, 6775
MU4429		
MU4430	Cordierite-muscovite-biotite	WR4638, 7450
MU4431 +	Cordierite-biotite	WR4610, 7470
MU4432	Green amphibole	WR4615, 7340
MU4433	Diopside-green amphibole	WR4373, 6663
MU4434 +	Biotite-sericite-chlorite	A3480, 6568
MU4435 +	Cordierite-almandine-biotite-graphite	WR4325, 6660
MU4436 +	Green amphibole-biotite	WR5045, 7830
MU4437 +	Cordierite-biotite	WR4325, 6662
MU4438 +	Muscovite-biotite-chlorite	WR4325, 6664
MU4439	Biotite-green amphibole	WR4262, 6641
MU4440	Biotite-diopside-scapolite	WR4264, 6641
MU4441	Green amphibole	WR4343, 6660
MU4442	Muscovite-chlorite-biotite-cordierite	WR4365, 6664
MU4443	Green amphibole	K4840, 7930
MU4444	Biotite-green amphibole	WR5062, 7810
MU4445	Biotite-acicular colourless amphibole	WR4620, 7450
MU4446 +	Muscovite-biotite (quartz porphyry)	WR4621, 7440
MU4447		
MU4448	Biotite-green amphibole	K5015, 8224
MU4449	Biotite-cordierite	K5030, 8190
MU4450 +	Cordierite-almandine-biotite	K5048, 8180
MU4451	Blue-green amphibole-chlorite-epidote	K5025, 8340
MU4452	Blue-green amphibole-chlorite	K5055, 8460
MU4453	Blue-green amphibole-epidote-chlorite	K5066, 8475

Sample No.	Major Mineralogy	Location *
MU4454	Biotite-K-feldspar-cordierite	WR4220, 6570
MU4455	Diopside-brown green hornblende- scapolite-grossular	WR4225, 6575
MU4456	Biotite-chlorite-sericite	K4850, 8325
MU4457	Biotite-almandine	K4680, 9350
MU4458	Biotite-hypersthene	K4700, 9060
MU4459	Biotite-muscovite-chlorite	WR4850, 6790
MU4460	Biotite-chlorite-sericite(?)	WR4840, 7775
MU4461	Biotite-chlorite-muscovite- graphite	WR4860, 7775
MU4462 +	Biotite-chlorite-muscovite	WR4780, 7728
MU4463	Biotite-chlorite-muscovite(?)	WR4760, 7724
MU4464 +	Biotite-chlorite-muscovite(?)	WR4758, 7720
MU4465 +	Biotite-chlorite-phengite(?) - graphite	WR4680, 7700
MU4466 +	Cordierite-biotite-chlorite- phengite-graphite	WR4678, 7700
MU4467	Biotite-chlorite-muscovite	WR4668, 7720
MU4468	Blue-green amphibole-biotite	WR4660, 7725
MU4469	Biotite-green amphibole	WR4645, 7725
MU4470	Graphite-magnetite(?)	K4970, 8160
MU4471 +	Biotite-cordierite-K-feldspar	WR4320, 6718
MU4472 +	Biotite-cordierite-K-feldspar	WR4318, 6720
MU4473	Brown hornblende-biotite- K-feldspar	WR4328, 6731
MU4474 +	Cordierite-K-feldspar-biotite	WR4620, 7725
MU4475	Biotite-acicular colourless amphibole	WR4440, 6820
MU4476 +	Biotite-green amphibole	WR4450, 6822
MU4477	Biotite-chlorite	K5240, 9320
MU4478	Biotite	K5200, 9320
MU4479	Biotite	K5190, 9320
MU4480	Biotite-feldspar	K5180, 9318
MU4481 +	Biotite-graphite	K5175, 9330
MU4482	Biotite-green amphibole	K5150, 9338

Sample No.	Major Mineralogy	Location *
MU4483	Biotite-brown-green amphibole	WR4609, 7428
MU4484	Cordierite-biotite-K-feldspar	WR4250, 6600
MU4485	Cummingtonite-biotite	WR4250, 6620
MU4486 +	Muscovite-biotite	WR4628, 7380
MU4487	Diopside-green amphibole- calcite	WR4650, 7450
MU4488	Chlorite-sericite-graphite	A3508, 65651
MU4489	Biotite-chlorite-epidote- calcite	K5025, 8328
MU4490 +	Chlorite-sericite-graphite	A3522, 65674
MU4491 +	Chlorite-sericite(?) -epidote	A3510, 65651
MU4492 +	Biotite-muscovite-cordierite- andalusite	WR4550, 6750
MU4493 +	Biotite-chlorite	B5060, 1862
MU4494	Biotite-chlorite-muscovite	B5068, 1865
MU4495	Biotite-green amphibole	B5075, 1873
MU4496	Biotite-acicular colourless amphibole	B5090, 1875
MU4497	Biotite-chlorite	B5100, 1876
MU4498	Biotite-green amphibole	B5110, 1878
MU4499	Biotite-sphene-blue-green amphibole	B5125, 1885
MU4500	Chlorite-sericite-graphite	K5020, 8280
MU4501 +	Biotite-muscovite-chlorite	B5115, 1880
MU4502	Biotite-cordierite-K-feldspar	WR4262, 6620
MU4532	Biotite-cordierite-K-feldspar	WR4268, 6620
MU4534	Green amphibole-biotite	A3462, 65688
MU4535	Biotite-graphite -chlorite- muscovite	A3466, 65680
MU4536	Biotite-graphite	A3467, 65678
MU4537	Cordierite-biotite-muscovite	WR4600, 7350
MU4538	Biotite	WR4540, 6751
MU4539	Acicular, radiating colourless amphibole - biotite	WR4175, 6450
MU4502A +	Pelites from the cordierite zone, Bathurst granite	
MU4501A +		
MU4500A +		

Sample No.	Major Mineralogy	Location *
MU4503 +	Cordierite-biotite-graphite-K-feldspar	E9500, 9425
MU4504	Cordierite-biotite-graphite-K-feldspar	E9391, 9352
MU4505	Cordierite-biotite-graphite-K-feldspar	E9387, 9342
MU4506	Cordierite-graphite-K-feldspar	E9380, 9338
MU4507 +	Cordierite-biotite-graphite-K-feldspar	E9378, 9336
MU4508	Cordierite-biotite-graphite-K-feldspar	E9378, 9330
MU4509	Cordierite-biotite-graphite	E9376, 9328
MU4510	Plagioclase-hornblende-K-feldspar	E9375, 9300
MU4511	Cordierite-graphite-biotite-muscovite	E9350, 9300
MU4512	Cordierite-graphite-biotite	E9360, 9295
MU4513	Biotite-muscovite-graphite-cordierite(?)	E9300, 9330
MU4514	Cordierite-biotite-graphite	E9475, 9360
MU4515	Cordierite-K-feldspar-graphite	E9300, 9260
MU4516	Biotite-muscovite-graphite-cordierite	E9282, 9240
MU4517	Graphite-chlorite-muscovite	E9321, 9383
MU4518	Hornblende-biotite	E9338, 9461
MU4519	Cordierite-K-feldspar-biotite-graphite	E9346, 9522
MU4520	Cordierite-muscovite-biotite	E9376, 9360
MU4521	Cordierite-biotite-graphite	E9449, 9370
MU4522	Cordierite-biotite-graphite	E9350, 9280
MU4523	Cordierite-graphite-muscovite	E9340, 9300
MU4524	Plagioclase-K-feldspar-chlorite	E9338, 9302

E = Eungai sheet

M = Macksville sheet

Sample No.	Major Mineralogy	Location *
MU4525	Biotite-muscovite-graphite	M9230, 0080
MU4526 +	Sericite-chlorite-graphite	E8755, 9121
MU4527 +	Sericite-chlorite-graphite	E9030, 9720
MU4528 +	Sericite-chlorite-graphite	E9980, 9800
MU4529 +	Biotite-graphite	E9062, 9680
MU4530 +	Cordierite-K-feldspar-biotite-graphite	E9282, 9110
MU4531A	Cordierite-K-feldspar-biotite-graphite	E9231, 9088
MU4533	Cordierite-biotite-graphite	M9240, 9946

APPENDIX SEVEN

CALCULATION OF COMPOSITIONAL DIAGRAM VALUES

AFM

$$A = \frac{[Al_2O_3] - 3[K_2O]}{[Al_2O_3] - 3[K_2O] + [MgO] + [FeO]}$$

$$M = \frac{[MgO]}{[MgO] + [FeO]}$$

For parageneses devoid of muscovite and containing K-feldspar, the value of A was accordingly calculated as:

$$A = \frac{[Al_2O_3] - [K_2O]}{[Al_2O_3] - [K_2O] + [MgO] + [FeO]}$$

(see Barker, 1961)

AKF

$$A = [Al_2O_3] + [Fe_2O_3] - ([Na_2O] + [K_2O] + [CaO])$$

$$K = [K_2O]$$

$$F = [FeO] + [MgO] + [MnO]$$

ACF

$$A = [\text{Al}_2\text{O}_3] + [\text{Fe}_2\text{O}_3] - ([\text{Na}_2\text{O}] + [\text{K}_2\text{O}])$$

$$C = [\text{CaO}] - 3.3 [\text{P}_2\text{O}_5]$$

$$F = [\text{MgO}] + [\text{FeO}] + [\text{MnO}]$$

$$\underline{\text{SiO}_2 - (\text{MgO} + \text{FeO}) - \text{Al}_2\text{O}_3}$$

$$\text{SiO}_2 = \text{SiO}_2 - 6(\text{K}_2\text{O} + \text{Na}_2\text{O}) - 2\text{CaO}$$

$$\text{Al}_2\text{O}_3 = \text{Al}_2\text{O}_3 - (\text{K}_2\text{O} + \text{Na}_2\text{O} + \text{CaO})$$

$$(\text{MgO} + \text{FeO}) = \text{MgO} + \text{FeO}$$

In all diagrams used, the chemical analyses of rocks were corrected for accessories, then appropriate weight percentages were converted to molecular proportions. The molecular proportions were then used to calculate the required values (these values being recalculated to equal 100%).

APPENDIX EIGHT

CHEMICAL ANALYSES OF SEDIMENTS
ADJACENT TO THE BATHURST GRANITE
AND THE URALLA GRANODIORITE

	MU4502A	MU4501A	MU4500A
SiO ₂	73.43	73.20	69.64
TiO ₂	0.66	0.64	0.10
Al ₂ O ₃	13.23	12.78	17.06
Fe ₂ O ₃	1.10	0.63	0.68
FeO	4.30	4.07	0.92
MnO	0.17	0.32	0.04
MgO	2.95	2.32	1.51
CaO	0.50	0.83	0.04
K ₂ O	4.04	3.20	6.32
Na ₂ O	0.31	0.25	1.30
P ₂ O ₅	0.13	0.12	0.02
Total	100.82	98.36	97.63

C

C

C

MgO/MgO + FeO

	MU4493	MU4531A
SiO ₂	64.79	63.45
TiO ₂	0.63	0.75
Al ₂ O ₃	16.06	17.20
Fe ₂ O ₃	1.06	0.77
FeO	3.43	4.57
MnO	0.10	0.12
MgO	1.75	2.06
CaO	2.19	2.65
K ₂ O	6.63	4.51
Na ₂ O	2.43	4.03
P ₂ O ₅	0.15	0.16
Total	99.22	100.27

B

B

MgO/MgO + FeO

Analyst: G.S. Teale

C = Cordierite zone (Bathurst)
B = Biotite zone (Uralla)

APPENDIX NINE

POLISHED SECTIONS: MINERALOGY AND LOCATION

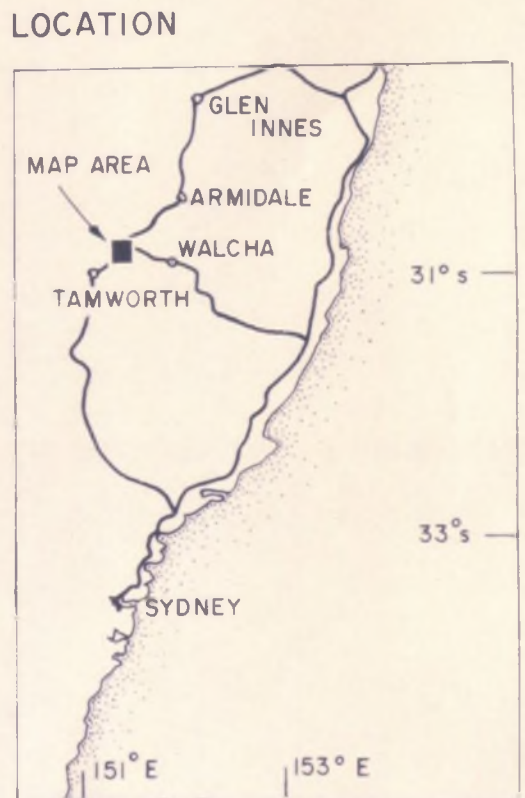
Sample	Opaque Mineralogy	Location *
MU4355	Ilmenite	A3454, 65690
MU4358	Ilmenite	A3455, 65687
MU4435	Pyrrhotite-chalcopyrite-graphite-ilmenite	WR4325, 6660
MU4383	Ilmenite	WR4215, 6564
MU4393	Pyrrhotite-graphite	WR4540, 6778
MU4397	Pyrrhotite-ilmenite-graphite	WR4575, 6775
MU4408	Pyrrhotite-ilmenite-graphite	WR4428, 6638
MU4450	Ilmenite (?)	K5048, 8180
MU4466	Graphite-pyrrhotite-ilmenite	WR4678, 7700
MU4507	Pyrrhotite-chalcopyrite-pyrite-graphite-ilmenite	E9378, 9336
MU4530	Pyrrhotite-graphite-ilmenite	E9282, 9110
MU4529	Graphite-pyrrhotite	E9062, 9680
MU4528	Pyrite-graphite-ilmenite(?)	E9980, 9800

* Locations explanation same as for thin section locations (previous appendix)

11. BIBLIOGRAPHY

- Dearman, W.R.: 1966, Tectonics and Granite Emplacement on the North-West Margin of Dartmoor, Devonshire., Trans. Rog. Geol. Soc. Cornwall., Vol. 20 pt. 1.
- Leitch, E.C.: 1973, Lecture delivered at Macquarie University (unpub.).
- Ramberg, H.: 1970, Model Studies in Relation to Intrusion of Plutonic Bodies, in Newell and Rast, "Mechanisms of Igneous Intrusion", Seel House Press.

METAMORPHIC ZONING ADJACENT TO THE EASTERN CONTACT OF THE WALCHA ROAD ADAMELLITE - NEW ENGLAND AREA - N.S.W



- Tertiary { Basalt
- Permian { Walcha Road Adamellite
- Minor Granitic Stocks
- Shalimar Tonalite
- Terrible Vale porphyritic microtonalite
- Quartz porphyry

- Carboniferous? { Carbonaceous Pelites - Sandon beds
- Ordovician - Devonian? { Basic dyke
- Carbonaceous Pelites - Woolomin beds
- Undifferentiated Sediments, (Woolomin and Sandon beds)

APPROXIMATE LOCATIONS OF CORDIERITE-K-FELDSPAR, CORDIERITE AND BIOTITE ISOGRADS , WAY WAY GRANITE AREA , MACKSVILLE , N.S.W



